

Copyright
by
Corey A. Theriot
2008

The Dissertation Committee for Corey Allen Theriot Certifies that this is the approved version of the following dissertation:

Replication-Associated Base Excision Repair Of Oxidized Bases In The Mammalian Genome

Committee:

Sankar Mitra, Ph.D., Supervisor

John Papaconstantinou, Ph.D.

Alan Tomkinson, Ph.D.

Cornelis Elferink, Ph.D.

Isvan Boldogh, Ph.D.

Tapas Hazra, Ph.D.

Dean, Graduate School

**Replication-Associated Base Excision Repair of Oxidized Bases In The
Mammalian Genome**

by

Corey Allen Theriot

Dissertation

Presented to the Faculty of the Graduate School of

The University of Texas Medical Branch

in Partial Fulfillment

of the Requirements

for the Degree of

Doctor of Philosophy

The University of Texas Medical Branch

December, 2008

This dissertation is lovingly dedicated to the memory of my
grandfather, Thomas Raymond Theriot
and
god-father, Joseph Fredman Theriot.

Acknowledgements

I would like thank all those whose support, friendship and kindness have allowed me to complete this work and have added to the fullness of my graduate education. First and foremost I must acknowledge Dr. Sankar Mitra for being such a patient and gracious mentor. His guidance is the primary reason I am the scientist that I am today. I must also acknowledge all the members of my advisory committee including Dr. Istvan Boldogh, Dr. Alan Tomkinson, Dr. Cornelis Elferink and especially Dr. John Papaconstantinou who served as the chair of the committee and an infinite source of inspiration. I also want to specifically acknowledge Dr. Tapas Hazra who is also a committee member but more importantly directly oversaw much of the work I have presented here.

I want to thank the entire Mitra lab for all of their support throughout my graduate education. Scientifically, I want to recognize Dr. Hong Dou who initiated and performed some of the experiments detailing the stimulation of NEIL1 by PCNA. As well as Dr. Muralidhar Hegde who I have worked closely with characterizing the interaction of NEIL1 with many of the replication-associated proteins.

I would also like to thank the Biochemistry and Molecular Biology Graduate Program, in particular Dr. Lillian Chan and Debora Botting, for all the support they have provided me while working on my graduate studies at UTMB.

I must also recognize the work and assistance of other labs that provided reagents and data through collaborative efforts. The lab of Dr. Yoshihiro Matsumoto provided the untagged human PCNA expression construct. The lab of Dr. Gou-Min Li provided both the RFC and Pol δ baculovirus subunit constructs. The lab of Dr. A-Lien Lu provided the 9-1-1 protein and 9-1-1 antibodies while Dr. Xin Guan from the lab performed the GST pull-down experiments and some of the NEIL1 activity assays.

Finally, I have to express my sincere thanks to my entire family for giving me their love and support. Without the example of hard work and dedication provided by my parents, grandparents, aunts and uncles for me to follow I would never have been able to be as successful as I am today. Thank you all very much.

Replication-Associated Base Excision Repair Of Oxidized Bases In The Mammalian Genome

Publication No. _____

Corey Allen Theriot, Ph.D.

The University of Texas Medical Branch, 2008

Supervising Professor: Sankar Mitra

Reactive oxygen species (ROS), the most pervasive endogenous and radiation-induced genotoxic agents induce strand breaks and a plethora of base lesions in DNA that (except double-strand breaks) are repaired via the DNA base excision repair (BER) pathway. Four mammalian DNA glycosylases, namely, OGG1 and NTH1 in the Nth family, and NEIL1 and NEIL2 in the Nei family, with overlapping substrate range initiate BER by excising oxidized base lesions and cleaving the DNA strand. NEIL1 prefers oxidized pyrimidines or ring-opened purines as substrates and is upregulated at the mRNA and protein level during S-phase. NEIL1 also demonstrates the unique ability to excise base lesions from forked or single-stranded DNA substrates that mimic intermediates generated during DNA replication. This suggests a direct linkage of NEIL1's repair activity to genome replication. In addition, inactivating mutations in the NEIL1 gene have been epidemiologically linked with gastric cancer, NEIL1-downregulation induces a mutator phenotype and NEIL1 KO mice display symptoms of the human metabolic syndrome such as obesity, dyslipidemia, and fatty liver disease.

These observations lead us to develop the working hypothesis that NEIL1 is involved in a preferential repair pathway for oxidized base damage in the replicating genome where repair of both template strands is equally important because an unrepaired base lesion in either strand could induce mutations. Thus, specific involvement of NEIL1 with the DNA replication machinery may be required to effectively and efficiently accomplish this. In support of our hypothesis, we have identified several new NEIL1 interacting proteins that are components of the DNA replication machinery, including Replication Protein A (RPA), Proliferating Cell Nuclear Antigen (PCNA), Flap Endonuclease 1 (FEN1), DNA Polymerase δ , Replication Factor C (RFC), and DNA Ligase I as well as the stress responsive Rad9-Rad1-Hus1 (9-1-1) DNA sliding clamp. We mapped the overlapping binding sites for all of these interacting protein partners to a small disordered region near the unconserved C-terminus of NEIL1 that is dispensable for its enzymatic activity. In support of the biological significance of these interactions, we showed that the DNA polymerase processivity factor and sliding clamp, PCNA, stimulates NEIL1's activity on various DNA substrates including forked and single-stranded DNA. We also investigated NEIL1's association with the DNA damage activated alternative sliding clamp 9-1-1 and showed direct interaction as well as stimulation of NEIL1 activity in a similar fashion as PCNA. In contrast, the RPA complex inhibits NEIL1's activity when the damage is in the single-stranded region of a DNA primer-template structure, inhibition that is relieved in the presence of PCNA. These results suggest that PCNA and RPA, along with other proteins, collaborate to regulate a replication-associated repair pathway in mammalian cells that not only maintains efficient and proper replication but also repair of oxidative DNA damage to prevent mutagenesis and maintain genomic integrity.

Table of Contents

Acknowledgements	v
Table of Contents	ix
List of Tables.....	xiii
List of Figures	xiv
List of Abbreviations.....	xvii
CHAPTER I	1
Introduction	1
DNA Damage	1
ROS and generation of free radicals	2
Oxidative stress	4
Oxidative DNA damage	4
Other DNA base lesions	6
Genome Stability.....	8
Checkpoint responses.....	9
Maintaining genomic integrity.....	10
Direct reversal	11
Excision repair (BER/MMR/NER)	11
Double strand break repair (NHEJ/HR).....	12
Translesion synthesis (TLS).....	14
Base Excision Repair	15
<i>E. coli</i> BER is a simple process.....	15
Recognition and cleavage of modified bases	16
Oxidized base specific DNA glycosylases.....	17
APE- vs. PNK-dependant BER.....	19
BER in mammalian systems	19
NEIL1.....	22

Reaction mechanism and structural features	22
Substrate specificity	25
Unique activity on non-duplex DNA	25
Phenotype of NEIL1-deficiency.....	27
DNA replication in eukaryotic cells.....	28
The replication fork.....	28
Proliferating cell nuclear antigen (PCNA) is a DNA sliding clamp ...	30
Relication protein A (RPA) protects single-stranded DNA	31
Replication-associated repair of oxidized bases.....	34
CHAPTER II	36
NEIL1 Associates With Proteins Of The Replisome	36
Introduction	36
Materials and Methods.....	37
Results	41
In vivo association of NEIL1 with proteins of DNA replication	41
Direct physical association of NEIL1 with DNA polymerase δ , RFC and DNA ligase I.....	43
Surface Plasmon Resonance (SPR) analysis of WT NEIL1 and NEIL1 1-311 binding affinities.....	46
Analysis of the NEIL1 C-terminal domain	49
Discussion	52
CHAPTER III	54
Functional Interaction Of NEIL1 With PCNA	54
Introduction	54
Materials and Methods.....	55
Results	60
NEIL1 association with PCNA in vivo.....	60
Mapping the interaction domain of NEIL1	62
PCNA stimulates NEIL1 in a DNA structure-specific manner..	66
Effect of PCNA on NEIL1's affinity for bubble DNA	68

Mammalian two-hybrid analysis for in vivo NEIL1-PCNA interaction.....	72
NEIL1 interacts with the interdomain connector loop of human PCNA	74
G127A mutation in the interdomain connector loop of human PCNA diminishes stimulation of NEIL1	75
DISCUSSION	77
CHAPTER IV	80
NEIL1 Interacts With The Checkpoint Activated 9-1-1 Clamp Complex.....	80
Introduction	80
Materials and Methods	82
Results	87
The human 9-1-1 complex interacts with NEIL1.....	87
Mapping the 9-1-1 interacting domain within NEIL1	89
Colocalization between NEIL1 and 9-1-1.....	91
NEIL1 activity is enhanced by Hus1, Rad1, Rad9 and the 9-1-1 complex.....	92
Discussion	95
CHAPTER V	97
Regulation of NEIL1 activity at the Replication Fork	97
Introduction	97
Materials and Methods	99
Results	102
Association of NEIL1 with RPA in vivo	102
Mapping the RPA interaction to the NEIL1 C-terminus	104
Binding affinity analysis	108
RPA regulates NEIL1 activity with DNA structure specificity	110
RPA single-stranded DNA binding polarity effect on NEIL1 inhibition.	114
EMSA analysis of RPA binding	116
NEIL1 forms a ternary complex with RPA-coated DNA	118

PCNA relieves RPA inhibition of NEIL1 activity.....	120
Discussion	122
CHAPTER VI	124
Summary and Conclusions.....	124
References	131
Vita	141
Publications.....	142

List of Tables

Table 1.1: Comparative properties of human DNA glycosylases responsible for removal of oxidative base damage.	18
Table 1.2: Comparative activities on various DNA substrates of human DNA glycosylases NEIL1, NEIL2, OGG1 and NTH1.....	26
Table 2.1: Sequence of primers used for generation of NEIL1-FLAG expression plasmid.	38
Table 2.2: Binding constants of Pol β and FEN1 interaction with WT NEIL1 and NEIL1 1-311.	48
Table 3.1: Sequences of 5-OHU containing oligodeoxynucleotides.	64
Table 3.2: Conserved KA-containing sequences in mammalian Pol δ and human NEIL1.....	74
Table 4.1: Sequences of primers used for 9-1-1 PCR reactions.....	83
Table 4.2: Sequences of thymine glycol containing oligodeoxynucleotides.	86
Table 5.1: Sequences of 5-OHU containing oligodeoxynucleotide substrates. .	111

List of Figures

FIGURE 1.1: STRUCTURE OF THE PURINES AND PYRIMIDINES FOUND IN DNA. ...	1
FIGURE 1.2: ROS AND THE FENTON REACTION.	3
FIGURE 1.3: COMMON OXIDATIVE DNA BASE LESIONS.	6
FIGURE 1.4: EXAMPLES OF OTHER DNA BASE LESIONS.	8
FIGURE 1.5: CLASSIFICATION OF DNA REPAIR MECHANISMS.	10
FIGURE 1.6: MINIMAL STEPS IN DNA BASE EXCISION REPAIR.	16
FIGURE 1.7: MAMMALIAN BER SUBPATHWAYS.	21
FIGURE 1.8: NEIL1–DNA MODEL.	24
FIGURE 1.9: CORE COMPONENTS OF THE EUKARYOTIC DNA REPLICATION COMPLEX.	30
FIGURE 1.10: STRUCTURAL ORGANIZATION OF HUMAN RPA.	33
FIGURE 2.1: NEIL1 ASSOCIATES WITH REPLICATION PROTEINS.	42
FIGURE 2.2: MAPPING NEIL1’S INTERACTION WITH POL δ , RFC AND LIGASE I.	44
FIGURE 2.3: FAR WESTERN ANALYSIS USING WT NEIL1 AND NEIL1 (1-311).	46
FIGURE 2.4: SPR ANALYSIS OF NEIL1 AND NEIL1 1-311 INTERACTIONS.	48
FIGURE 2.5: SCHEMATIC OF THE INTERACTION DOMAIN OF NEIL1.	49
FIGURE 2.6: NEIL1 C-TERMINAL DOMAIN IS PREDICTED TO BE DISORDERED. ...	51
FIGURE 3.1: NEIL1 INTERACTS WITH PCNA THROUGH ITS UNCONSERVED C-TERMINAL DOMAIN.	61
FIGURE 3.2: EFFECT OF PCNA ON NEIL1 AND NEIL2 FOR 5-OHU EXCISION FROM VARIOUS DNA STRUCTURES.	65

FIGURE 3.3: PCNA DOSE-DEPENDENT STIMULATION OF NEIL1 ACTIVITY AND SINGLE-TURNOVER KINETICS.	67
FIGURE 3.4: EFFECT OF PCNA ON NEIL1'S DNA BINDING.....	69
FIGURE 3.5: SURFACE PLASMON RESONANCE ANALYSIS OF NEIL1 DNA BINDING.	71
FIGURE 3.6: MAMMALIAN TWO-HYBRID ASSAY OF NEIL1-PCNA INTERACTION.	73
FIGURE 3.7: REDUCED STIMULATION OF NEIL1 WITH PCNA G127A MUTANT.	76
FIGURE 4.1: PHYSICAL INTERACTION BETWEEN NEIL1 AND THE 9-1-1 COMPLEX.	88
FIGURE 4.2: DETERMINATION OF REGIONS WITHIN NEIL1 INVOLVED IN BINDING TO THE 9-1-1 COMPLEX.	90
FIGURE 4.3: CO-LOCALIZATION OF NEIL1 WITH RAD9 FOLLOWING OXIDATIVE STRESS.	91
FIGURE 4.4: NEIL1 ACTIVITY WAS STIMULATED BY HUS1, RAD1, RAD9 AND THE 9-1-1 COMPLEX.	93
FIGURE 4.5: QUANTITATIVE ANALYSES OF NEIL1 STIMULATION.....	94
FIGURE 5.1: OXIDATIVE STRESS INCREASES THE LEVELS OF RPA, PCNA AND FEN1 FOUND IN THE NEIL1-FLAG IP.	103
FIGURE 5.2: MAPPING THE RPA-INTERACTING INTERFACE ON NEIL1.....	105
FIGURE 5.3: IN VITRO CO-ELUTION OF RPA AND NEIL1.	107
FIGURE 5.4: INTRINSIC FLUORESCENCE ANALYSIS OF RPA TITRATED WITH NEIL1 INTERACTION DOMAIN.	109
FIGURE 5.5: EFFECT OF RPA ON NEIL1 EXCISION OF 5-OHU FROM VARIOUS DNA STRUCTURES.	112

FIGURE 5.6: EFFECT OF RPA ON NEIL1 5-OHU CLEAVAGE ACTIVITY.....	113
FIGURE 5.7: INHIBITION OF NEIL1 ACTIVITY ON 3' VS. 5' PRIMER-TEMPLATE SUBSTRATES.....	115
FIGURE 5.8: EFFECT OF SINGLE-STRANDED DNA LENGTH IN PRIMER-TEMPLATE SUBSTRATES ON RPA BINDING.....	117
FIGURE 5.9: NEIL1 FORMS A TERNEIRY COMPLEX WITH RPA-COATED DNA.....	119
FIGURE 5.10: NEIL1 OVERCOMES RPA INHIBITION IN THE PRESENCE OF PCNA.....	121
FIGURE 6.1: SCHEMATIC OF THE OVERLAPPING INTERACTION INTERFACE IN THE NEIL1 C-TERMINUS.	127
FIGURE 6.2: A MODEL FOR THE ROLE OF NEIL1 IN REPLICATION-ASSOCIATED REPAIR.	129

List of Abbreviations

5-OHU – 5-hydroxyuracil
8-oxoG – 8-oxoguanine
9-1-1 – Rad9, Rad1, and Hus1 heterotrimeric complex
AP sites – apurinic/aprimidinic (abasic) sites
APE1 – AP endonuclease 1
ATM – ataxia telangiectasia mutated kinase
ATR – ATM and Rad3-related kinase
BER – DNA base excision repair
CDK – cyclin-dependent kinases
DHU – dihydrouracil
DNA – deoxyribonucleic acid
DNA-PKcs – catalytic subunit of DNA protein kinase
EMSA – electrophoretic mobility shift analysis
Fapy – formamidopyrimidines
Fapy-A – 4,6-diamino-5-formamidopyrimidine
Fapy-G – 2,6-diamino-4-hydroxy-5-formamidopyrimidine
FEN1 – flap endonuclease 1
HR – homologous recombination
H₂O₂ – hydrogen peroxide
IP – immunoprecipitation/immunoprecipitate
MGMT – methylguanine methyltransferase
MMR – DNA mismatch repair
NEIL – Nei-Like family of DNA glycosylases
NER – nucleotide excision repair
NFDM – nonfat dried milk
NHEJ – non-homologous end joining
NTH1 – Nth homologue 1
OGG1 – 8-oxoguanine DNA glycosylase
PBS – Phosphate buffered saline
PCNA – proliferating cell nuclear antigen
PNK – polynucleotide kinase
Pol – polymerase
RAR – replication associated repair
RFC – replication factor C
RNA – ribonucleic acid
ROS – reactive oxygen species
RPA – replication protein A
SOD – superoxide dismutase
TBS – Tris-HCL buffered saline
TCR – transcription coupled repair
Tg – thymine glycol
XRCC – X-ray cross complementary gene

CHAPTER I

Introduction

DNA DAMAGE

Deoxyribonucleic acid (DNA) is an uninterrupted polymeric chain comprised of four different monomeric deoxyribonucleotides, purines adenine (A) and guanine (G) and the pyrimidines cytosine (C) and thymidine (T) that are connected by phosphodiester linkages (Figure 1.1). The genetic make up of all living organisms is contained within the specific sequence of these DNA bases in what is called the genome. The absolute importance of genetic information for growth and reproduction has made the maintenance and dissemination of that information a requirement for all living organisms.

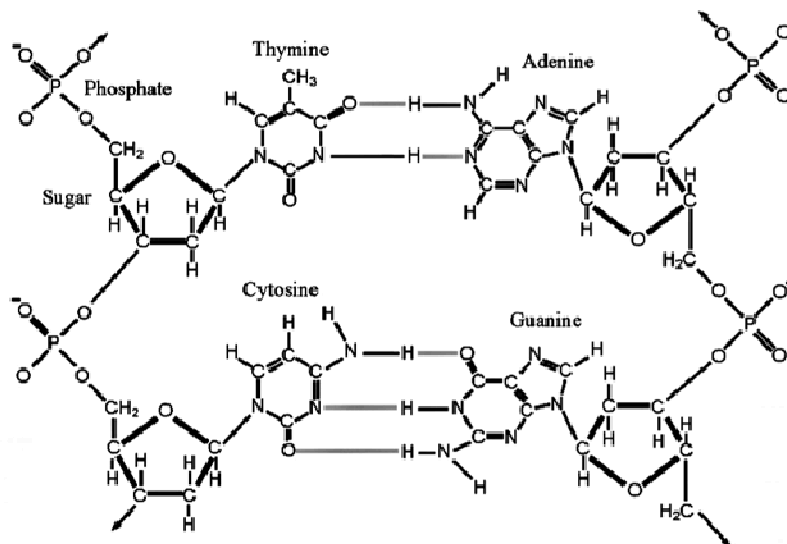


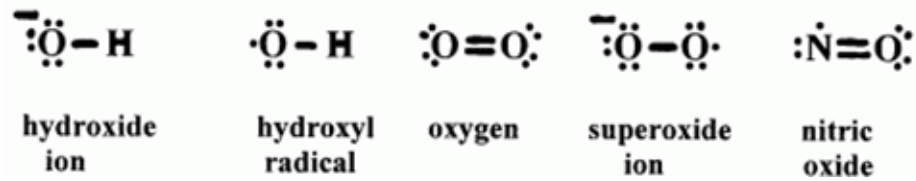
FIGURE 1.1: STRUCTURE OF THE PURINES AND PYRIMIDINES FOUND IN DNA. Schematic of a short duplex DNA oligonucleotide. Thymine hydrogen bonds with adenine while cytosine hydrogen bonds with guanine of opposite strands in an antiparallel fashion.

Although first depicted as a very stable molecule due to base stacking in the duplex held and H-bonds between complementary pairing of A with T or G with C, DNA has been shown to have inherent structural instability and the ability to adopt multiple conformations (Arnott *et al.* 1983). In addition, DNA is chemically and physically altered by a number of processes some of which can lead to harmful changes (Lindahl 1993). DNA damage is any such change to the structure or sequence of the DNA molecule leading to genomic instability or loss of genomic integrity. DNA damage occurs endogenously due to spontaneous base loss at a low but significant rate (Lindahl 1993). DNA is also insulted by a plethora of harmful agents including those produced during cellular growth and maintenance or because of exposure to exogenous agents like radiation. In addition, there are numerous compounds generated in the environment or are synthetic xenobiotics that are of concern. Many of these are also genotoxic agents capable of inducing harmful changes to the DNA structure leading to deleterious effects.

ROS and generation of free radicals

Reactive oxygen species (ROS) include hydrogen peroxide, the superoxide anion and the hydroxyl radical (Figure 1.2A). During oxidative phosphorylation, the transfer of a single electron to molecular oxygen creates the superoxide anion ($O_2^{\bullet-}$), which is converted by superoxide dismutase (SOD) into hydrogen peroxide (H_2O_2). Hydrogen peroxide is a moderately strong oxidant, but in the presence of ferrous or cuprous ions, via the Fenton reaction, it can generate the hydroxyl radical ($\bullet OH$), the most reactive ROS (Figure 1.2B). Reactive nitrogen species are also included among the pro-oxidant species (Laroux *et al.* 2001). Most notable is the nitric oxide radical (NO^{\bullet}) generated by nitric oxide synthase during certain signaling mechanisms (Figure 1.2A) (Parkins *et al.* 1995). Nitric oxide readily reacts with superoxide to produce a combined reactive species called peroxynitrite ($NO_3^{\bullet-}$), which is itself a powerful oxidant (Lavrovsky *et al.* 2000).

A. Reactive oxygen species:



B. Fenton chemistry:



Haber-Weiss reaction -



FIGURE 1.2: ROS AND THE FENTON REACTION. A. Common ROS found in the cell. Note: Nitric oxide is technically a reactive nitrogen species. B. Fenton chemistry occurs in the presence of iron. Haber-Weiss reaction also generates $\text{OH}\cdot$ without requiring Fe^{2+} or Cu^+ .

ROS are common by-products of cellular respiration and metabolism from aerobic organisms generating energy from the mitochondrial electron transport chain, as part of the inflammatory response, as well as through detoxification reactions carried out by the cytochrome P-450 system (Bondy and Naderi 1994; Gottlieb 2003). ROS may also readily be generated by environmental agents such as ultraviolet light, ionizing radiation and various redox chemicals such as those found in cigarette smoke (Shih and Hu 1996; Chuang and Hu 2006). Regardless of the source, ROS and other free radicals are capable of inducing damage, sometime irreversible, to all biomolecules including lipids, carbohydrates, amino acids, and nucleic acids.

Oxidative stress

Oxidative stress associated with the loss of cellular homeostasis occurs when ROS production exceeds the capacity of the natural antioxidant defense mechanisms causing a shift in the redox state of the cell and subsequent oxidative damage to biomolecules. The antioxidant defense system in most cells is comprised of two components: antioxidant enzymes and antioxidant compounds. The antioxidant enzymes include superoxide dismutase, catalase, glutathione peroxidase and others (Valko *et al.* 2006). The antioxidant compounds include vitamins A, C and E as well as redox chemicals glutathione and thioredoxin (Giugliano 2000; Willcox *et al.* 2004). Together, these components encompass the body's natural defense against all free radicals including both endogenous ROS and those generated by external environmental factors. Oxidative stress is believed to contribute to the general decline in functions associated with many human pathophysiologies including Alzheimer disease (Bozner *et al.* 1997; Multhaup *et al.* 1997), Parkinson disease (Mukherjee and Adams 1997; Radunovic *et al.* 1997), atherosclerosis (Alexander 1998; Fiorillo *et al.* 1998), ischemia/reperfusion neuronal degeneration (Milam *et al.* 1998), rheumatoid arthritis (Miyata *et al.* 1998), cancer (DeWeese *et al.* 1998; Meyer *et al.* 1998), as well as the aging syndrome (Beckman and Ames 1998; Stadtman and Berlett 1998).

Oxidative DNA damage

A large variety of DNA lesions occur spontaneously or are induced by ROS, especially during oxidative stress. Oxidative attack by the hydroxyl radical alone produces multiple modifications in DNA including base and sugar lesions, strand breaks and DNA-protein cross-links. The most common modifications are oxidatively damaged bases with a smaller level of DNA strand cleavage, both single- and double-stranded breaks containing 3'sugar fragments or free phosphate. Oxidative DNA damage also

includes oxidized apurinic/apyrimidinic (abasic, AP) sites after loss of the DNA base (Laval 1996).

ROS generate a plethora of oxidatively modified DNA bases (Figure 1.3) each leading to different outcomes, most frequently mutagenesis. An example is 5-hydroxyuracil (5-OHU) which is an oxidation product of cytosine that will base pair with both G and A (Figure 1.3). Another abundant and mutagenic lesion induced by ROS is 8-oxoguanine (8-oxoG, Figure 1.3), a commonly used cellular marker of oxidative stress and an example of the mutagenic capabilities of unrepaired oxidative DNA damage derived from G. 8-oxoG's mutagenic property is a result of base mispairing with A afforded by the syn conformation of 8-oxoG. If mismatches with A occurs during DNA replication the result is a G:C → T:A transversion mutation (Grollman and Moriya 1993). Such G:C → T:A transversion mutations have been observed in many activated oncogenes supporting the mutagenic role of 8-oxoG. It is also possible for 8-oxoG to mispair with G leading to a mutation of the G:C → C:G type. Other common oxidative lesions are the oxidized ring-opened purines named formamindopyrimidines (Fapys, Figure 1.3). Fapys are generated abundantly by exposure to ionizing radiation as well as ROS and have been shown to be noncoding lesions or blocking lesions during DNA replication and transcription (O'Connor *et al.* 1988; Graziewicz *et al.* 2000). Oxidative base damage is arguably the most insidious type of DNA damage because of constant production of ROS through energy production even without outside insult.

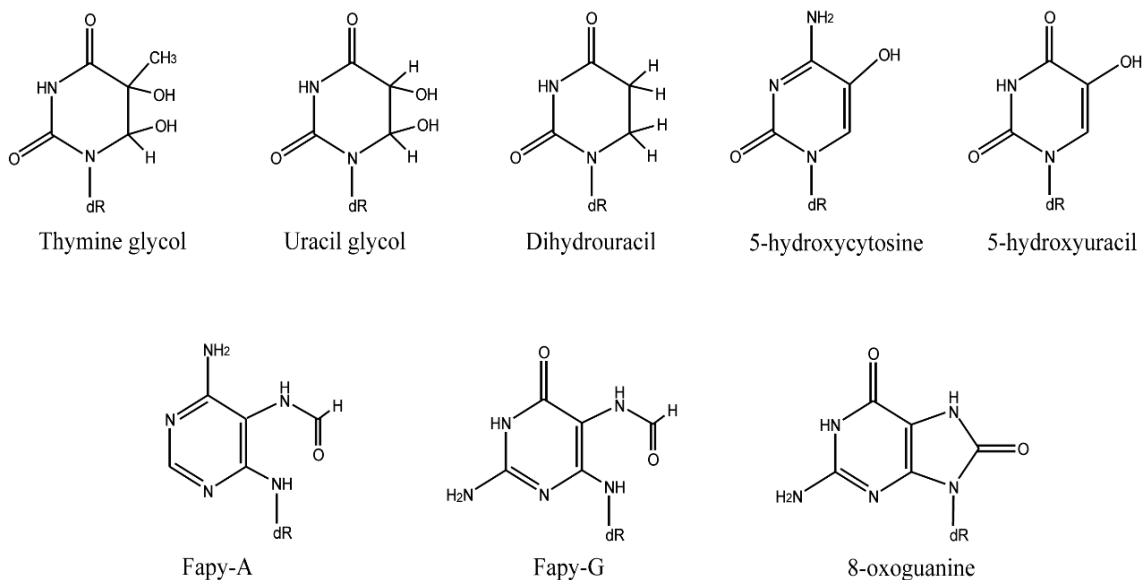


FIGURE 1.3: COMMON OXIDATIVE DNA BASE LESIONS. Important base lesions resulting from ROS attack of normal DNA bases. All must be repaired via a DNA repair pathway in order to prevent possible mutations as a result of their misreplication.

Other DNA base lesions

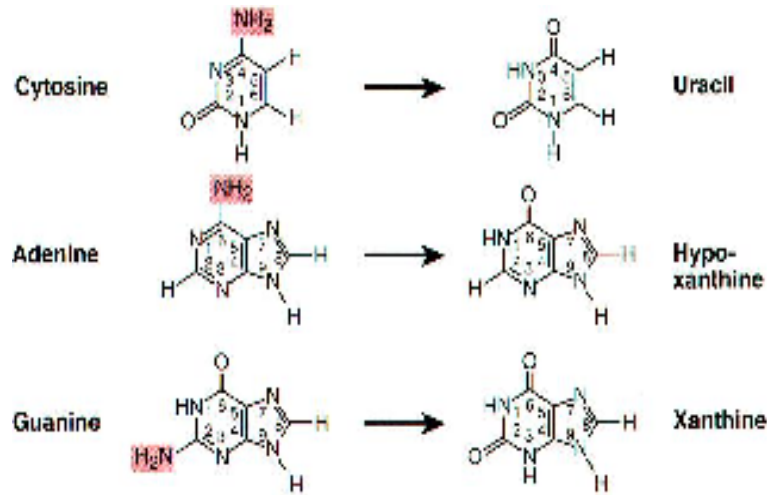
Several forms of DNA damage in addition to ROS-induced lesions are generated by deamination, hydrolysis and alkylation (mostly methylation). Deamination of the exocyclic amino group present in A, G and C can occur spontaneously in pH- and temperature-dependent reaction (Figure 1.4A). Cytosine deamination generates uracil that is present only in RNA which pairs with A rather than G (Figure 1.4A) (Duncan and Miller 1980). The G:C → A:T mutations that would occur due to cytosine deamination warrants prompt removal of uracil from DNA. Spontaneous hydrolysis of DNA purines and pyrimidines occur at a significant rate leaving abasic (AP) sites as a result. It is estimated that purines are lost at a rate of 10,000 per cell generation while depyrimidination occurs roughly 1/20 of that (Lindahl and Karlstrom 1973; Lindahl

1979). This leads to non-coding sequences in the DNA that must be corrected if genome stability is to be maintained.

Alkylating agents are common mutagens due to their electrophilic nature and affinity for the nucleophilic nitrogen and oxygens in DNA bases and phosphate. These agents may either be monofunctional, containing a single reactive group, or bifunctional, having two reactive groups which generates intra and interstrand crosslinks in DNA. The ring nitrogens of adenine (N^3) and guanine (N^7) are the most common sites for alkylating adducts. A common consequence of DNA base alkylation is spontaneous depurination/depyrimidination because the alkylation weakens the N-glycosylic bond leading to subsequent hydrolysis (Loeb and Preston 1986).

The many synthetic xenobiotics and environmental agents of today's world as well as endogenous generation of free radicals in addition to spontaneous chemical reactions have shown that the primary structure of DNA is in fact very dynamic. It was quite unexpected to the scientific community that DNA did not maintain an extremely stable structure to protect the fidelity required of such an informationally critical molecule. DNA damage is now understood to be inevitable and must be dealt with for maintaining genetic integrity and successful propagation of species.

A. Examples of deamination:



B. Example of alkylation:

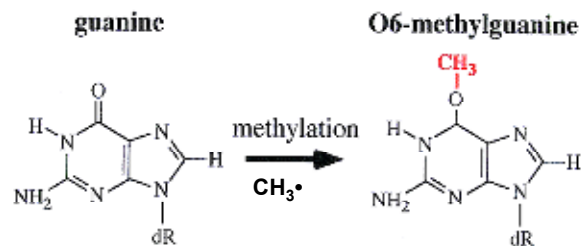


FIGURE 1.4: EXAMPLES OF OTHER DNA BASE LESIONS. A. Deamination products of cytosine, adenine and guanine. B. Alkylation product resulting from O⁶-methylation in guanine.

GENOME STABILITY

DNA replication, as well as transcription, could be blocked by the presence of damage. Alternatively, misreplication of bases could occur when DNA lesions are left unrepaired leading to cytotoxicity or even cell death. Additionally, the progeny cells that inherit these wrong bases will carry mutations from which the original DNA sequence can not be recovered. Because of these deleterious consequences, DNA damage is

countered in cells by DNA repair, which is a universal and evolutionarily conserved process that serves to protect the genetic integrity of living organisms. The genomes of eukaryotes encode cell cycle checkpoint and DNA repair proteins that continuously monitor chromosomes recognizing and repairing damaged DNA. All forms of DNA damage can lead to detrimental biological consequences in organisms, including cell death, mutations and transformation of cells towards malignancy. Therefore, DNA repair is regarded as one of the most essential events for the maintenance of all forms of life.

Checkpoint responses

Cellular replication involves a complex cycle of events to take place in an extremely ordered fashion. The cell cycle is broken down into four distinct phases: G1 phase, S phase, G2 phase and M phase. The S phase is unique in that this is when DNA synthesis occurs making a copy of the entire genome for the progeny cell. It is in this time that the cell is most closely regulated by cyclins and cyclin-dependent kinases (CDKs) that determine the cell's progress through the cell cycle.

Upon DNA damage, cell cycle checkpoints are activated. Checkpoint activation pauses the cell cycle giving time to repair the damage before continuing to cell division. DNA damage checkpoints occur at the G1/S and G2/M boundaries and throughout the S phase. Checkpoint activation is primarily controlled by two kinases, Ataxia-telangiectasia mutated kinase (ATM) and Rad3-related kinase (ATR). ATM responds to DNA double-strand breaks and disruptions in chromatin structure (Bakkenist and Kastan 2003), whereas ATR is primarily activated by UV light and stalled replication forks through the recognition of elongated RPA-DNA filaments by Rad17 and ATRIP (Zou and Elledge 2003; Zou *et al.* 2003). These kinases are effectors that phosphorylate downstream targets in a signal transduction cascade eventually leading to temporary cell cycle arrest. This gives the cell time to activate the proper repair pathways correlating to

the specific type of damage in order to make the necessary repairs before continuation of the cell cycle. If repairs are not made or the damage is too extensive to repair the signal for cell death is initiated leading to programmed cell death.

Maintaining genomic integrity

DNA repair encompasses all those cellular responses and biochemical pathways responsible for restoration of normal DNA from previously damaged DNA. This includes mechanisms as simple as a single polypeptide that catalyzes a single-step reaction to restore DNA to its normal state by direct reversal or as complex as elaborately regulated multi-step pathways requiring a number of large multi-subunit complexes. Multiple processes have thus been characterized such as direct reversal, excision repair and double strand break repair meant to repair the wide range of DNA damages that can occur (Figure 1.5).

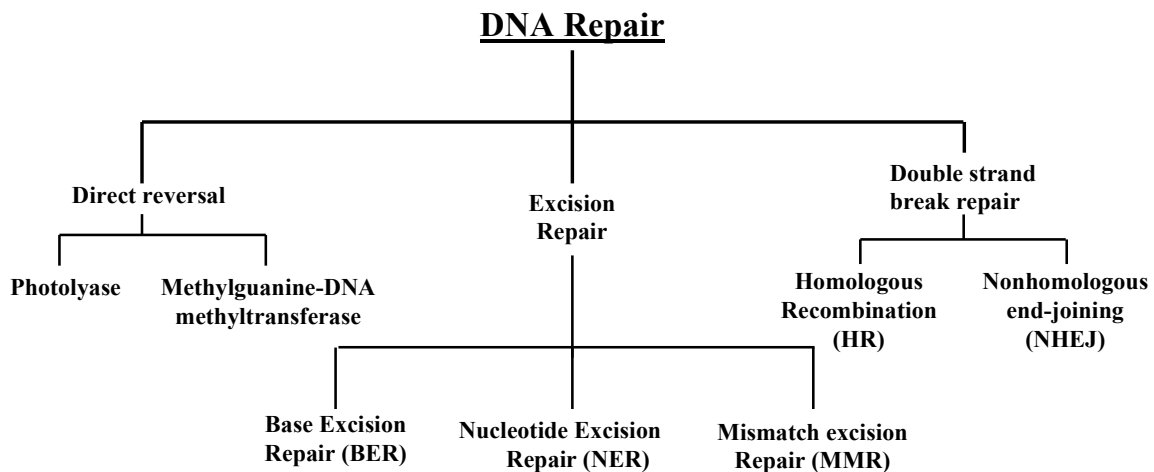


FIGURE 1.5: CLASSIFICATION OF DNA REPAIR MECHANISMS. DNA repair pathways are generally conserved among all organisms.

Direct reversal

Direct reversal is a pathway of DNA repair where cells are able to eliminate certain types of damage to their DNA by direct chemical reversal. This mechanism does not require DNA synthesis, since the damaged base is reverted back to its original form. Such repair mechanisms are specific to the type of damage incurred and do not involve breakage of the phosphodiester backbone. Two examples of proteins carrying out direct reversal include photolyases and methylbase-DNA transferases. The photolyase present in lower organisms and nonplacental mammals uses photoreactivation to reverse the formation of thymine dimers caused by UV irradiation (Weber 2005). In addition, methylation at the O⁶-position of guanine can be directly reversed by a protein named methylguanine-DNA methyltransferase (MGMT) that transfers the methyl group from O⁶-methylguanine (Figure 1.4) to itself restoring the guanine but inactivating itself in the process (Foote *et al.* 1980; Olsson and Lindahl 1980). This is an expensive process because each MGMT molecule can only be used once unlike most enzymes whose catalytic activity is replenished. Direct reversal protects cells from only a small number of base lesions but is still very critical in determining a cell's resistance to DNA damage.

Excision repair (BER/MMR/NER)

Since direct reversal is very limited in the type of damage that can be repaired, more general pathways have evolved. Excision repair excises damaged and inappropriate bases or DNA segments spanning the damage through distinct enzymatic mechanisms. Three modes of excision repair exist and differ greatly by the specific lesions repaired and the enzymatic components required. Base excision repair (BER) is responsible for repairing chemical modifications, small base adducts, AP sites and single strand breaks. The damaged base is excised and released as a free base followed by repair synthesis of one nucleotide (short patch-/single nucleotide-BER) or 2-10 nucleotides (long patch-

BER). BER will be discussed in greater detail in later sections. The second mode of excision repair is mismatch repair (MMR) and can utilize much of the components of BER but differs in the fact that mismatched base pairs are repaired. MMR is associated with replication and adds another level of fidelity to the DNA synthesis process by identifying inappropriate or mismatched bases incorporated in the nascent strand. Both BER and MMR are initiated by recognition of very specific, and sometimes small, alterations to the DNA. Unlike BER or MMR, nucleotide excision repair (NER) is quite different and is responsible for repair of large DNA adducts, dimers and intra- or interstrand crosslinks. NER uses damage specific endonucleases to excise a single-stranded oligonucleotide fragment of ~30 nucleotides (in mammals) containing the lesion followed by repair synthesis of the gap. NER can further be divided into two subpathways, global genomic and transcription coupled NER that differ only in how recognition of the DNA damage occurs. Global genomic NER repairs damage in both transcribed and untranscribed DNA strands in active and inactive genes throughout the genome unlike transcription-coupled NER that is only recruited to sites of stalled transcription in active genomic sequences repairing damage in only the transcribed strand. Excision repair comprises the majority of all DNA repair in the cell because of the large variety and frequency of DNA lesions that are repaired by this system. It is also argued that excision repair is also the most critical of all repair processes because of this and is further supported by the multiple redundancies that have been characterized within excision repair pathways.

Double strand break repair (NHEJ/HR)

Double strand breaks, with interruption in both strands are particularly toxic to the cell because they can lead to genomic rearrangements. Two distinct and complementary mechanisms exist to repair double strand breaks: non-homologous end joining (NHEJ)

and homologous recombination (HR). NHEJ occurs throughout the cell cycle while HR occurs when a sister chromatid is available during S-phase as a template through chromatid exchange for repair fidelity.

In NHEJ, DNA Ligase IV forms a complex with XRCC4 and directly joins the two ends of DNA strands (Thacker and Zdzienicka 2003). The catalytic subunit of the DNA-dependent protein kinase (DNA-PK) is the major factor in bridging the DNA ends in mammalian cells by interacting with and promoting intermolecular joining by DNA ligase IV-XRCC4 (Tomkinson *et al.* 2006). NHEJ relies on short homologous sequences called microhomologies in the single-stranded tails of the DNA ends to be joined for accurate repair. When these overhangs are compatible, repair occurs with limited processing of the DNA ends, if they are not NHEJ will still join non-matching termini generating translocations in the process. NHEJ invariably causes DNA sequence alteration during repair because the loss of nucleotides at the break site will lead to deletions. NHEJ has a repair-independent function, generating diversity of B-cell and T-cell receptors via V(D)J recombination in the immune system (Market and Papavasiliou 2003).

Homologous recombination repair requires the presence of an identical sequence to be used as a template for repair of double-strand breaks that are often associated with loss of nucleotides. This pathway allows a damaged chromosome to be repaired using the sister chromatid that is present in late S and G2 phases. Double-strand breaks caused by the replication machinery attempting to synthesize across a single-strand break or unrepaired lesions cause collapse of the replication fork and are typically repaired by homologous recombination. The enzymatic machinery responsible for this repair process catalyzes invasion of the opposite chromatid by the single-stranded DNA from one end of the break. Next, the 3' end of the invading DNA primes DNA synthesis, causing

displacement of the complementary strand, which subsequently anneals to the single-stranded DNA generated from the other end of the initial double-stranded break. The structure that results is an intermolecular-strand exchange, known as a Holliday junction. Branch migrations followed by resolution of the junction structure to separate the two DNA duplex molecules and subsequent ligation of the strand breaks repairs duplex DNA. Fortunately, DNA double strand breaks are a relatively rare occurrence in the cell but absolutely must be repaired to prevent gross chromosomal damage such as translocations.

Translesion synthesis (TLS)

As a last resort, specialized DNA polymerases have evolved that are capable of bypassing non-coding lesions. This allows tolerance of DNA lesions such as thymine dimers or AP sites. Translesion synthesis (TLS) involves switching from the replicative DNA polymerases to specialized translesion synthesis polymerases (Nikolaishvili-Feinberg and Cordeiro-Stone 2000). Polymerase switching is thought to be mediated by replication machinery upon polymerase stalling by modification of the processivity factor, PCNA, a DNA sliding clamp (Chang *et al.* 2006). The TLS polymerases often have large active site pockets facilitating nucleotide insertion opposite the blocking lesion, and are characterized as inserters or extenders based on their preference for inserting bases opposite the damage or extending from bases incorporated opposite the damaged site (Nelson *et al.* 1996; Yuan *et al.* 2000). This constitutes the two-polymerase two-step model. This process is not foolproof and is rather error-prone because TLS polymerases have a propensity to insert improper bases at lesion sites introducing point mutations (Broomfield *et al.* 2001). However, from a cellular standpoint it can occasionally be preferable to avoid more drastic mechanisms of DNA repair that could cause gross chromosomal aberrations or to prevent signaling for cell death.

BASE EXCISION REPAIR

As previously described base excision repair is the major cellular process for repairing damaged DNA bases which, involves flipping the damaged base out of the DNA helix, excision of the base and subsequent synthesis to replace the lesion (Fortini *et al.* 1998; Bjoras *et al.* 2002; Jiang and Stivers 2002; Krosky *et al.* 2004; Bellamy *et al.* 2007). BER is responsible for recognizing both sequence errors and small base lesions (adducts or chemical modifications) to prevent mutations during replication or to remove lesions that may lead to improper transcription or spontaneous strand breaks in the DNA (Ishibashi *et al.* 2005). Oxidative base lesions will be considered as the major lesions to be repaired via the BER process for the remainder of this chapter.

***E. coli* BER is a simple process**

Cells repair a wide variety of DNA lesions via one of the three broad excision repair pathways with overlapping substrate specificities. Of the three, BER is the simplest, requiring as few as 4 enzymes for complete repair (Figure 1.6). This pathway was first characterized in *E. coli*, and has since been intensively investigated in the mammal. *E. coli* BER is initiated with recognition and removal of the DNA base adduct by a DNA glycosylase followed by cleavage of the resulting abasic (AP) site by one of two AP-endonucleases (Nfo or Xth) producing a 3' -OH and 5' deoxyribosephosphate moiety. In contrast, oxidized base specific DNA glycosylases additionally cleave the ribose-phosphate backbone generating a Schiff base intermediate, the product, a 3' deoxyribosephosphate or phosphate is also processed by the AP-endonucleases. The single nucleotide gap is then filled by a DNA polymerase from the 3' -OH as well as removal of the 5' deoxyribosephosphate. The process is finally completed by a DNA ligase sealing the remaining single strand break. However, the current model for mammalian BER of oxidized bases proposed by Wiederhold *et al.* (2004) and others is

much more complex containing at least three subpathways with crosstalk and intricate coordination an integral component of successful and efficient repair.

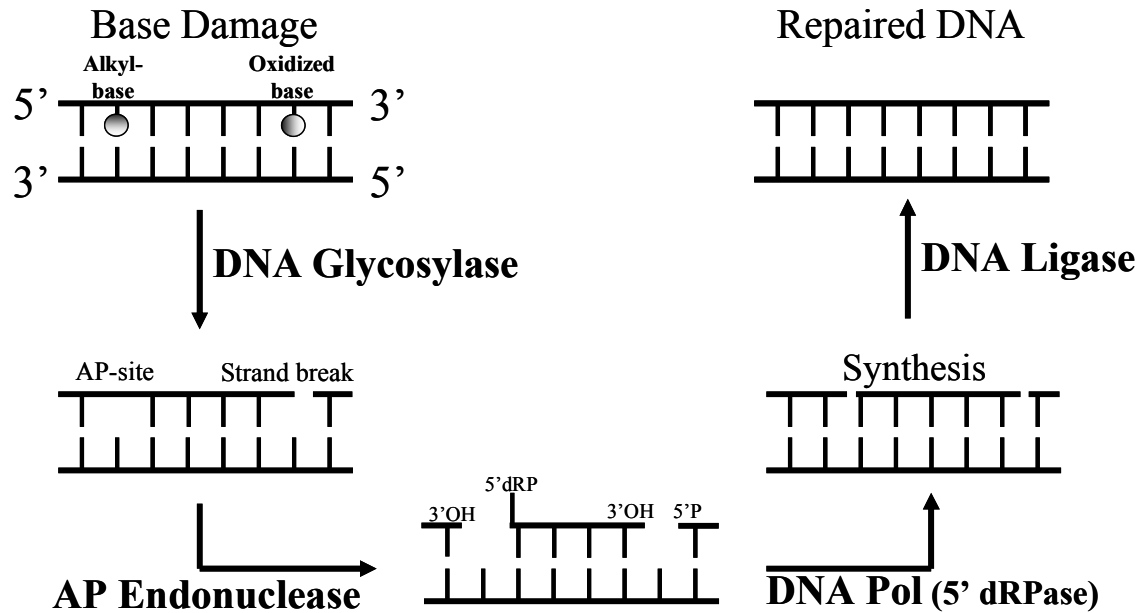


FIGURE 1.6: MINIMAL STEPS IN DNA BASE EXCISION REPAIR. BER may be carried out by as few as four enzymes.

Recognition and cleavage of modified bases

DNA glycosylases recognize modified or inappropriate bases in the genome and initiate repair without requiring a cofactor (Riazuddin and Lindahl 1978; Helland *et al.* 1987). Recent studies show that they may continue to play a role in coordinating downstream steps of the repair pathway through direct interaction (Wiederhold *et al.* 2004; Das *et al.* 2006; Hegde *et al.* 2008). A wide range of cytotoxic and mutagenic DNA bases are removed by any one of a number of different DNA glycosylases. Monofunctional glycosylases, such as uracil DNA glycosylase (UDG), hydrolyze the N-glycosylic bond between the target base and deoxyribose to generate an abasic site leaving the deoxyribose backbone of the damaged DNA strand intact. In addition, DNA

glycosylases may be bifunctional, displaying an additional lyase activity that cleaves the phosphodiester backbone 3' to the AP site generated by the glycosylase activity. Nucleotide flipping has been suggested to be actively facilitated by the enzyme and is the method for identifying modified bases (Jiang and Stivers 2002; Krosky *et al.* 2004; Bellamy *et al.* 2007). A conserved helix-hairpin-helix motif and an Asp residue are found in the active sites of most DNA glycosylases. In bifunctional DNA glycosylases, the conserved Asp works to deprotonate a N-terminal Pro or internal Lys to act as a nucleophile. This nucleophile forms a transient, covalent intermediate Schiff base with the C-1 of deoxyribose after base excision and then initiates strand cleavage via β -elimination (and β,δ - in some cases) and subsequent regeneration of the free enzyme.

Oxidized base specific DNA glycosylases

Oxidized base specific DNA glycosylases are interesting in the fact that they are all bi-functional; meaning that they have N-glycosylase activity as well as intrinsic AP lyase activity. These DNA glycosylases/AP lyases are categorized into two classes based on their reaction mechanism as was first defined in *E. coli* systems and has only recently been fully modeled in mammalian systems. Three oxidatively damaged base-specific DNA glycosylases, (Nth, Fpg and Nei) have been characterized in *E. coli* and based on their tertiary structures, active site characteristics, and AP lyase activity are divided into two groups. Nth (endonuclease III) is the prototype of one, and Fpg (foramidopyrimidine-DNA glycosylase)/Nei (endonuclease VIII) of the other (Hazra *et al.* 2007).

Thus far, five enzymes have been identified as mammalian orthologs based on the *E. coli* system. The first class of mammalian DNA glycosylases/AP lyases is composed of NTH1 (mammalian endonuclease III homolog 1) and OGG1 (8-oxoG DNA glycosylase), homologues of the *E. coli* Nth class (Table 1.1) (Ikeda *et al.* 1998; Krokan

et al. 2000; Zharkov *et al.* 2003; Fromme and Verdine 2004; Hitomi *et al.* 2007). These glycosylases catalyze β -elimination at the AP site using an internal lysine as the active site nucleophile generating a 3' phospho α,β -unsaturated aldehyde (3' puA). The second class of mammalian DNA glycosylases/AP lyases belong to the *E. coli* Fpg and Nei family named Nei-like (NEIL1, NEIL2 and NEIL3). At this time, NEIL3 has yet to be shown to have glycosylase activity and its *in vivo* function remains unclear. This family of glycosylases catalyze β,δ -elimination at the AP site generating a 3' phosphate at the strand break (Table 1.1) (Hazra *et al.* 2002; Hazra *et al.* 2002; Wiederhold *et al.* 2004). Both glycosylase families generate a 3' blocking group and a 5' terminus containing a monophosphate thus allowing a DNA ligase to seal the remaining break without further processing of the 5' terminus once the nucleotide gap is filled.

	OGG1	NTH1	NEIL1	NEIL2
Size (kD)	38	36	43	36
Preferred substrates	8-oxoG, Fapy G	Tg, 5OHU, DHU	Fapy A, Fapy G, Tg, 5OHU	Hydantoins (Sp, Gu), 5 OHU
Structural type	Nth	Nth	MutM/Nei	MutM/Nei
Conserved motif	HhH	HhH	H2TH	H2TH
Zn Finger motif	Absent	Absent	Absent	Present
[4Fe-4S] cluster loop	Absent	Present	Absent	Absent
Catalytic residue	Lys 249	Lys 212	Pro 1	Pro 1
AP lyase product	3' dRP	3' dRP	3' P	3' P
Dispensable sequences	C-terminal 20 and N-terminal 10 aa	N-terminal 80 aa	C-terminal 101 aa	C-terminal 11 aa

* Sp, Spiroiminodihydantoin; Gu, Guanidinohydantoin

Table 1.1: Comparative properties of human DNA glycosylases responsible for removal of oxidative base damage.

APE- vs. PNK-dependant BER

In *E. coli*, the 3' blocked products produced by both β - and β,δ -elimination by bi-functional DNA glycosylases are processed by the two AP endonucleases present, Xth and Nfo. Both AP endonucleases generate the 3' terminal –OH that acts as the primer terminus for repair synthesis. The AP site generated by monofunctional glycosylases are also cleaved also by these AP endonucleases on the 5' side of the AP site leaving a 5' deoxyribosephosphate and a 3' OH, both of which are substrates subsequently acted upon by DNA Polymerase β (Pol β). Surprisingly, in mammalian cells, there is only one major AP endonuclease, APE1. APE1 efficiently removes the 3' puA generated by the OGG1 and NTH1. On the other hand, APE1 has weak activity on the 3' phosphate generated through β,δ -elimination by the NEILs and presented a dilemma. However, the activity of mammalian PNK on 3' phosphates is efficient and was shown to be required for NEIL-initiated repair (Wiederhold *et al.* 2004). The 3' phosphate end is “polished” by PNK rather than by APE1 to generate a 3' OH that is used by Pol β to fill in the gap in NEIL-initiated BER (Wiederhold *et al.* 2004). In fact, NEIL1 can act like APE1 and enhance OGG1 turnover while competing for the AP site to possibly take over repair initiated by other glycosylases (Mokkapati *et al.* 2004). This sub-pathway is APE-independent and PNK-dependent.

BER in mammalian systems

The current model for mammalian BER of oxidative damage is substantially more complex than that in *E. coli*. The model proposed by Wiederhold *et al.* (Wiederhold *et al.* 2004) contains three sub-pathways that are followed based upon which particular type of DNA glycosylase initiates the pathway (Figure 1.7). Monofunctional DNA glycosylases generate AP sites after base excision that APE1 recognizes to cleave the

DNA strand 5' of the AP site. Pol β then synthesizes across the gap and removes the 5' deoxyribose phosphate moiety (Pathway II). APE1 also functions when oxidized bases are removed by OGG1 or NTH1 that carry out subsequent β -elimination generating a 3' phospho- α,β -unsaturated aldehyde. The resulting product is a 3' OH used for gap filling by Pol β (Pathway II). Exclusive to the NEIL-initiated sub-pathway is the inability of APE1 to efficiently remove the 3' phosphate generated thus requiring PNK to clear the 3' end and allow synthesis by Pol β (Pathway III). An alternate path exists with the capacity to shuttle the glycosylase reaction product from Pathway I (3' phospho- α,β -unsaturated aldehyde) or Pathway II (AP site) to Pathway III. In this case NEIL1 would override the OGG1 AP lyase reaction through displacement of OGG1 by competing for the AP site. This is possible because NEIL1 has a greater affinity for the AP site and stronger AP lyase activity than OGG1 (Mokkapati *et al.* 2004). The end product of this shuttle is the β,δ -elimination product utilized in the APE-independent BER sub-pathway. Thus, mammalian BER is defined by the enzymatic characteristics of the initiating DNA glycosylase, and is characterized by the utilization of either apurinic/apyrimidinic endonuclease (APE1) or polynucleotide kinase (PNK).

Recent reports indicate that BER is more complex, and involves many additional proteins, particularly for repair of oxidative lesions and AP sites in mammalian cells (Krokan *et al.* 2000; Slupphaug *et al.* 2003; Harrigan *et al.* 2006; Sung and Demple 2006). This is also evidenced by the interactions within the pathway along with the many interactions of repair proteins outside of repair such as those involved in replication, transcription, cell cycle progression and gene regulation. Much crosstalk occurs between these cellular processes but at the center of all these are components of BER.

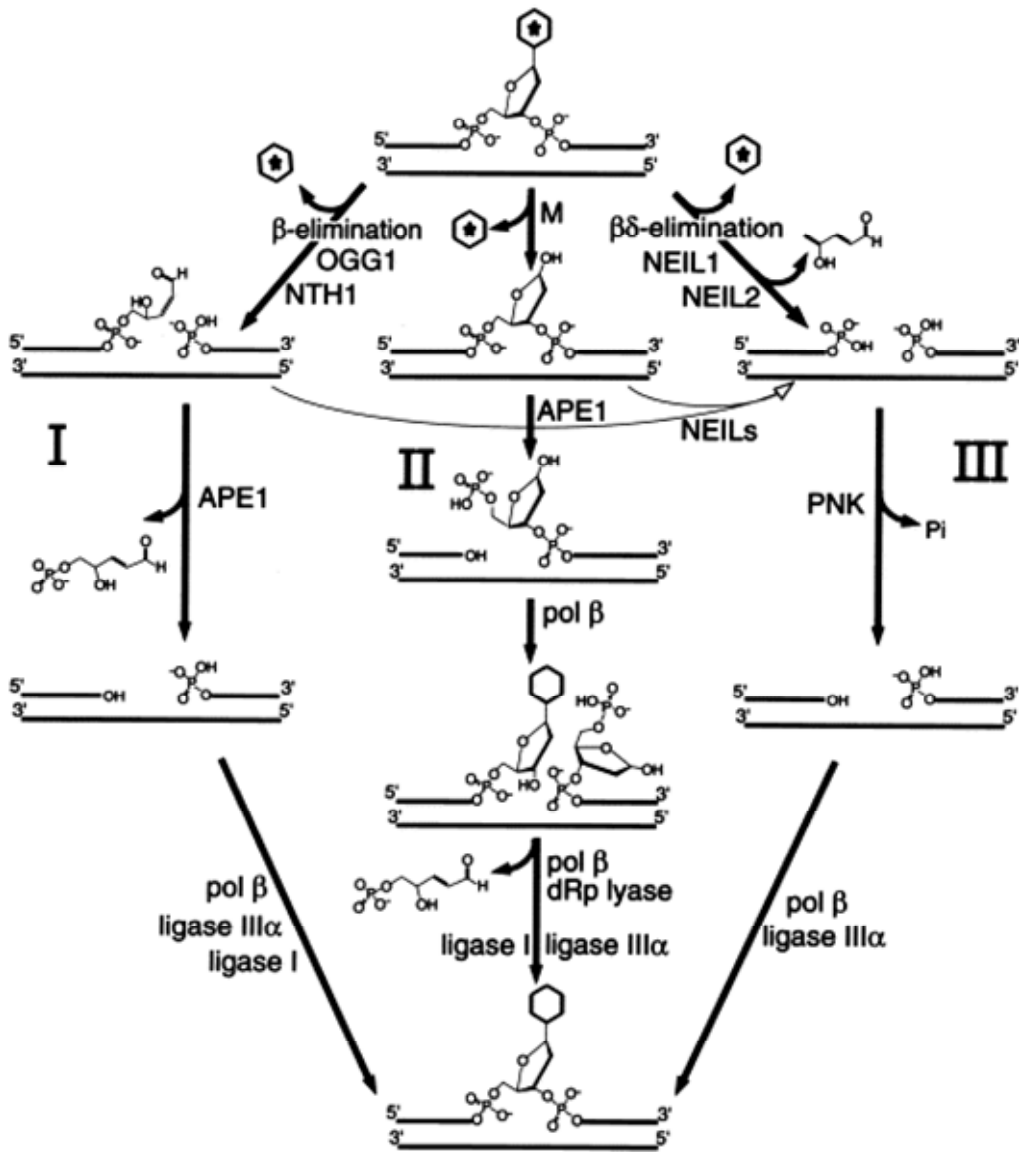


FIGURE 1.7: MAMMALIAN BER SUBPATHWAYS. Schematic of the three subpathways of BER mapped out in mammalian systems. The reaction product of the initiating DNA glycosylase determines the particular subpathway followed. The subpathways differ in the necessary enzymes required for subsequent steps of repair. Pathways I and III represent repair pathways of oxidized bases. (Wiederhold *et al.* 2004)

NEIL1

The oxidized base-specific DNA glycosylases have broad substrate specificity commensurate with the large number of such lesions that can occur, and are generally conserved in organisms ranging from bacteria to mammals (Mitra *et al.* 1997; Izumi *et al.* 2003). The newest family of mammalian DNA glycosylases, identified in 2003 by several different groups independently, has three members (Bandaru *et al.* 2002; Hazra *et al.* 2002a; Hazra *et al.* 2002b; Morland *et al.* 2002; Takao *et al.* 2002; Wiederhold *et al.* 2004). NEIL1 was the first of the mammalian Nei/Fpg type DNA glycosylases to be characterized, followed closely by NEIL2 (Hazra *et al.* 2002b). Observations were made during the initial characterization of these two enzymes that have set them apart from the other oxidative damage specific glycosylases. Further in-depth investigation since that time, primarily in our lab, have identified divergent properties within the NEIL family such as the observation that NEIL1 expression is S phase-dependent. NEIL1 expression is regulated by not only oxidative stress but also the S phase-specific *cis* element E2F based on identification of binding sites within intron 1 of the NEIL1 gene (Das *et al.* 2005). Similarly, NTH1 is regulated during the cell cycle with increased transcription during early and mid S-phase (Luna *et al.* 2000). In contrast, NEIL2 and OGG1 gene expression is not cell cycle regulated (Dhenaut *et al.* 2000; Hazra *et al.* 2002b).

Reaction mechanism and structural features

NEIL1 was first identified through a search for proteins that contain the conserved N-terminal motif “PEGP” present in all prokaryotic members of the Nei glycosylase family. The importance of this sequence is the N-terminal Pro in which the α -imino group is an active site nucleophile. It should be stated that NEIL1 is only active in its mature form since the unprocessed NEIL1 polypeptide contains Met at the N-terminus with the active site Pro as the second amino acid. NEIL1 also contains a conserved Lys

at position 56 that also acts as an active site nucleophile for *E. coli* Fpg catalysis (Bandaru *et al.* 2002). Both the Pro and Lys are required for NEIL1 activity (Bandaru *et al.* 2002). Unique to NEIL1 is the lack of the signature Zn finger motif used in DNA binding present in *E. coli* Nei and many other glycosylases, including family member NEIL2. However, it was shown by crystal structure of a C-terminally truncated NEIL1 that a “zinc-less” finger domain is present within residues 269-281 that contains a conserved Arg that is required for glycosylase activity (Doublet *et al.* 2004). The helix-two-turns-helix (H2TH) motive is another conserved DNA binding domain found within the NEIL1 structure (Doublet *et al.* 2004). The C-terminal domain of NEIL1 (residues 289-389) is not conserved and has been shown to be dispensable for glycosylase/AP lyase activity. This region has been predicted to be disordered and/or flexible rather than maintaining a uniform conformation and ordered structure which necessitated NEIL1’s C-terminal truncation for crystallization (Figure 1.8). Interestingly, our studies have shown that this domain contains the components unique for proper eukaryotic protein function including a putative nuclear localization signal (Das, unpublished observation), sites of post-translational modification (Theriot and Bhakat, unpublished observation) and protein-protein interaction motifs (Wiederhold *et al.* 2004; Dou *et al.* 2008).

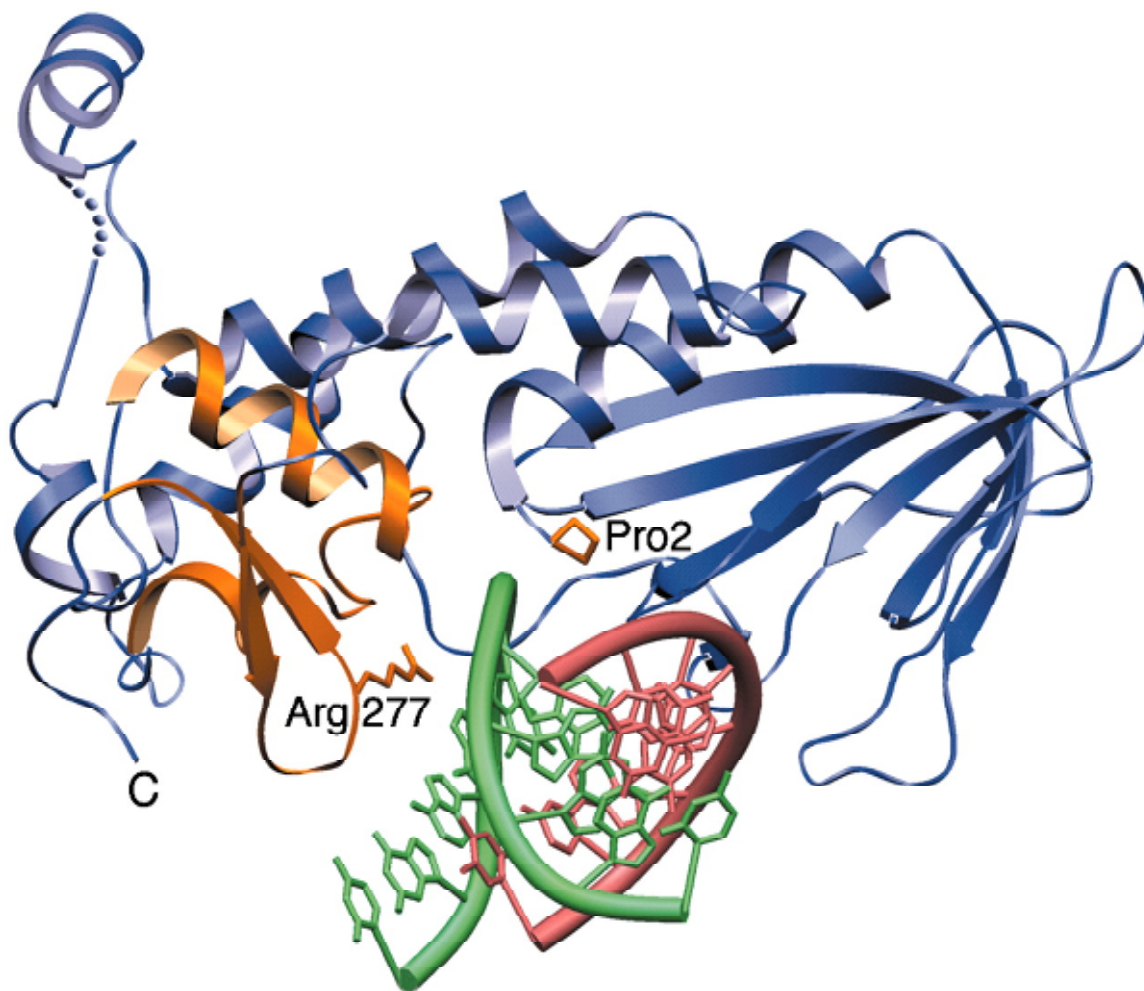


FIGURE 1.8: NEIL1–DNA MODEL. DNA from *E. coli* Nei complex (lesion-containing strand in green and complementary strand in pink) was superimposed onto human NEIL1 (blue). The zincless finger motif, H2TH domain, catalytic proline, and conserved arginine are highlighted in gold (Doublié *et al.* 2004).

Substrate specificity

NEIL1 shares a broad range of substrate lesions with the other three major oxidized base-specific DNA glycosylases OGG1, NTH1 and NEIL2. Characterization of NEIL1's activity showed that it prefers ring-opened purines Fapy A and Fapy G, 5-hydroxyuracil (5-OHU), dihydrouracil (DHU), thymine glycol (Tg) and 8-oxoG opposite C as well as hydantoins (guanidinohydantoin (Gh) and spiroiminodihydantoin (Sp)) the secondary oxidation products of 8-oxoG (Bandaru *et al.* 2002; Hazra *et al.* 2002; Rosenquist *et al.* 2003; Jaruga *et al.* 2004; Katafuchi *et al.* 2004; Miller *et al.* 2004; Hailer *et al.* 2005; Hu *et al.* 2005; Krishnamurthy *et al.* 2008). Thus far NEIL1 is the only mammalian enzyme shown to excise Fapy A highlighting its importance. Despite a preference for particular lesions DNA glycosylases are promiscuous in excising damaged bases and NEIL1 could possibly recognize even more lesions *in vivo* depending upon sequence context and DNA structure.

Unique activity on non-duplex DNA

All oxidized base specific glycosylases share a broad and overlapping range of substrates and thus provide protection from a plethora of oxidized lesions. However, they do differ greatly in the DNA structures that are substrates for activity. OGG1 and NTH1 excise lesions from only duplex DNA, which is expected because the undamaged strand provides a template for repair synthesis. In contrast, the Nei family members NEIL1 and NEIL2 share a preference for the substrate lesion in single-stranded DNA sequences, like those present in a transcription bubble or a replication fork including bubble, forked, and single-stranded structures (Dou *et al.* 2003). OGG1 and NTH1 like most other glycosylases (except the NEILs, UNG2 and SMUG1) are inactive with single-stranded DNA substrates (Dou *et al.* 2003). NEIL1 has also been shown to have affinity

for both duplex and single-stranded undamaged DNA. In addition, oxidative base lesions near the 3' proximal end of a DNA single strand break were shown to be resistant to cleavage by NTH1 and OGG1 (Parsons *et al.* 2005; Parsons *et al.* 2007). In similar studies, NEIL1 was characterized as the major DNA glycosylase that excises oxidative base damage located in close proximity to DNA single-strand breaks (Parsons *et al.* 2007). We thus hypothesized that NEIL1 and NEIL2, unlike OGG1 or NTH1, are involved in repair associated with replication and/or transcription by excising oxidized bases from transient bubble and fork intermediates generated during DNA metabolic processes (Dou *et al.* 2003). It is possible that NEIL1 and NEIL2 are involved in linking BER to transcription and/or replication because the bubble and single strand DNA substrates used in these studies represent intermediates generated during transcription and/or replication.

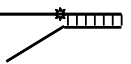
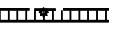
	dsDNA 	Fork 	Bubble 	Nicked 	ssDNA 
NEIL1	+	++	++	++	++
NEIL2	+	++	+++	?	++
OGG1	+	-	-	±	-
NTH1	+	-	-	±	-

Table 1.2: Comparative activities on various DNA substrates of human DNA glycosylases NEIL1, NEIL2, OGG1 and NTH1.

Phenotype of NEIL1-deficiency

Previous studies of OGG1- and NTH1-null mice and of cells derived from these mice showed lack of a major phenotype suggesting that other DNA glycosylases could provide back-up activity in the absence of OGG1 or NTH1. In fact, the OGG1- and NTH1-null cells exhibited no increase in sensitivity to ROS and radiation (Klungland *et al.* 1999; Takao *et al.* 2002). In contrast, NEIL1-depleted cells show enhanced radiation sensitivity (Rosenquist *et al.* 2003) and downregulation of NEIL1 induces a mutator phenotype as indicated by an increase in spontaneous HPRT mutations in Chinese hamster V79 and human A549 lung cells (Maiti *et al.* 2008). Enhanced mutation frequency was observed in oxidatively stressed NEIL1-downregulated cells implying NEIL1 is critical for repairing induced oxidative damage as well. In addition, inactivating mutations in the NEIL1 gene have been epidemiologically linked with gastric cancer (Shinmura *et al.* 2004). The NEIL1 knockout mice developed by Stephen Lloyd's group demonstrate a phenotype similar to the human metabolic syndrome with symptoms such as severe obesity, dyslipidemia, and fatty liver disease (Vartanian *et al.* 2006). NEIL2 knockout mice are currently being developed in T. K. Hazra's lab and it is expected that the NEIL2-null mice will show a phenotype because of its preferential repair activity. This cumulative evidence suggests that while OGG1 and NTH1 repair damage globally, NEIL1 carries out preferential repair while still retaining the ability to act as a back-up enzyme (together with NEIL2) in the complete absence of OGG1 or NTH1.

We have developed a working hypothesis based on this collection of evidence that in contrast to OGG1 and NTH1, NEIL1 is involved in a preferential repair pathway for oxidized base damage, most likely in replicating cells where repair of both transcribed and nontranscribed sequences would be equally important because a base lesion in either

strand could induce mutations. This proposed linkage of NEIL1-mediated repair to DNA replication was supported by three key observations: (1) S-phase specific activation of NEIL1, (2) NEIL1's ability to use single-stranded DNA substrates, and (3) the unique phenotype associated with NEIL1 deficiency. Thus, as a prerequisite, specific involvement of NEIL1 with the DNA replication machinery would be required to carry out repair efficiently.

DNA REPLICATION IN EUKARYOTIC CELLS

DNA replication is the semi-conservative process of copying a double-stranded DNA molecule to form two double-stranded "daughter" molecules each containing one new and one old strand. DNA replication is a fundamental process used by all living organisms to faithfully pass on the genetic information necessary for life to its descendants and is responsible for biological inheritance. Since each DNA strand holds the same genetic information, both strands can serve as templates for synthesis of the opposite strand. The ability of cells to fully and faithfully replicate their DNA is essential for ensuring genomic integrity. This task becomes even more arduous when cells experience stress that causes DNA damage while replicating the genome. Cells have evolved methods of dealing with a damaged template and other replication stressors by coordinating the replication process with cell cycle checkpoints and DNA repair. Obviously, lack of coordination between these processes could result in the accumulation of mutations leading to genome instability, cancer or cell death.

The replication fork

DNA synthesis begins at specific locations in the genome, called "origins" (ori), where the two strands of DNA are initially separated in a controlled fashion generating a

replication bubble. In eukaryotes, replication starts from many ori sequences per chromosome and continues in both directions. The unwinding of template DNA strands by a DNA helicase and synthesis of the daughter strands occurs at a complex structure called the replication fork. The replication fork is the structure created through the action of DNA helicase, which melts the hydrogen bonds holding the two DNA strands together resulting in two branching prongs, each one made up of single-stranded template DNA. However, bare single-stranded DNA has a tendency to form intramolecular hydrogen bonds to generate hairpin and loop-containing structures that can interfere with the movement of the DNA polymerase. To prevent this, single-strand binding proteins bind to the DNA preventing secondary structure formation allowing DNA synthesis to proceed. DNA polymerases use this single-stranded template and free dNTPs to synthesize the new strands of DNA in only a 5'→3' direction. This polarity necessitates the discontinuous synthesis of one of the strand, the lagging strand, generating Okazaki fragments and continuous synthesis of the other, leading strand. In addition, a number of other proteins associated with the replication fork assist in DNA synthesis (Figure 1.9). Oligomeric protein complexes form a sliding clamp around duplex DNA, helping the DNA polymerase maintain contact with its template and thereby enhancing its processivity. The hollow center of the torrid structure enables DNA to be threaded through the center of the clamp. Once the polymerase reaches the end of the template or detects double stranded DNA, the sliding clamp-polymerase complex undergoes a conformational change and releases the DNA polymerase. Clamp-loading proteins are used to initially load the clamp, recognizing the primer-template junction.

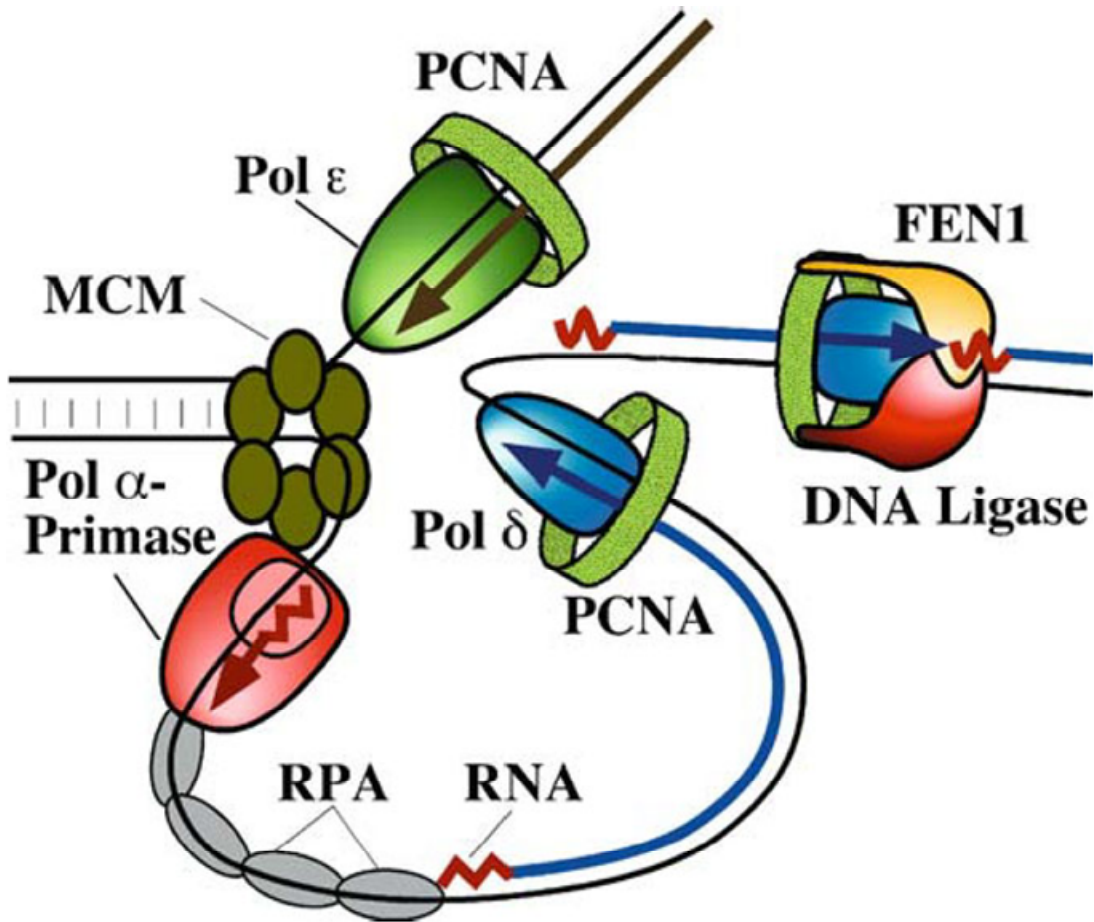


FIGURE 1.9: CORE COMPONENTS OF THE EUKARYOTIC DNA REPLICATION COMPLEX. The minimal set of proteins for fork propagation and DNA synthesis are indicated (Garg and Burgers 2005).

Proliferating cell nuclear antigen (PCNA) is a DNA sliding clamp

PCNA is a homotrimeric ring with 6-fold symmetry because of two equivalent domains in each subunit (Krishna *et al.* 1994). PCNA's central role in DNA transactions is to act as a platform for recruiting the proteins involved in DNA metabolism. PCNA is an essential factor for eukaryotic DNA replication (Tsurimoto and Stillman 1991).

PCNA has also been shown to be required in nucleotide excision repair (Nichols and Sancar 1992; Shivji *et al.* 1992), mismatch repair (Johnson *et al.* 1996; Umar *et al.* 1996) and post-replication repair (Torres-Ramos *et al.* 1996). During replication, PCNA is loaded on to DNA templates by replication factor C (RFC) at the primer-template junction of the growing chain and functions to increase the processivity of the replicative polymerases, Pol δ/ϵ , while also activating FEN1 and DNA Ligase 1 all via direct interactions (Montecucco *et al.* 1998; Warbrick 2000). In view of the trimeric nature of PCNA, it was suggested that each subunit may interact with a distinct replication or repair protein independently of the other two subunits. PCNA also activates translesion synthesis (TLS) DNA polymerases, including Pol η , when the replication complex stops at a noninstructional bulky adduct in the template (Friedberg *et al.* 2005). The polymerase switching allows the TLS polymerase to insert a base opposite the noninstructional adduct to get past the block, followed by the second switching to allow the replication complex to resume copying of the undamaged template. In recent years, a large number of additional proteins have been identified that physically interact with PCNA indicating that PCNA appears to function not just as an accessory to DNA polymerases but also as a communication point between a variety of important cellular processes including cell cycle control and several DNA repair pathways.

Relication protein A (RPA) protects single-stranded DNA

An essential player in all the DNA metabolic pathways including DNA replication, DNA repair, cell cycle checkpoints and DNA damage checkpoints is the Replication Protein A (RPA) complex (Sancar *et al.* 2004; Li and Zou 2005). Mammalian RPA is a heterotrimeric complex consisting of three subunits of varying size. The largest subunit, referred to as RPA70 or RPA1 contains three DNA binding domains (DBDs) in tandem and contains the majority of protein-protein interaction sites

(Kolpashchikov *et al.* 2001; Bochkareva *et al.* 2002; Bochkarev and Bochkareva 2004). The fourth DBD resides in the second subunit called RPA32 or RPA2 (Bastin-Shanower and Brill 2001; Bochkareva *et al.* 2002). These four DBDs bind in a sequential fashion beginning with DBD-A and -B at the 5' end occluding 8-10 nucleotides (de Laat *et al.* 1998; Kolpashchikov *et al.* 2001; Bochkareva *et al.* 2002; Cai *et al.* 2007). Then, through a conformational change DBD-C becomes involved in binding a stretch of 12-23 nucleotides (Cai *et al.* 2007). Finally, co-operative binding of all four DBDs results in a fully extended conformation of RPA occluding a stretch of approximately 30 nucleotides (Iftode *et al.* 1999; Bastin-Shanower and Brill 2001). These three distinct states of binding are thought to coexist and even be modulated through protein-mediated conformational remodeling from extended into compact conformations and vice-versa depending upon binding requirements (Jiang *et al.* 2006). The third subunit is RPA14 (RPA3) and is 14 kDa in size containing a single structural DBD that is responsible for the trimeric complex formation (Deng *et al.* 2007). Each subunit contains at least one DBD and is capable of DNA binding independently *in vitro* but is found only in its functional trimeric complex form *in vivo*. RPA's primary role is in replication where it binds, coats, and protects the single-stranded regions of template DNA strand after helicase unwinding (Iftode *et al.* 1999).

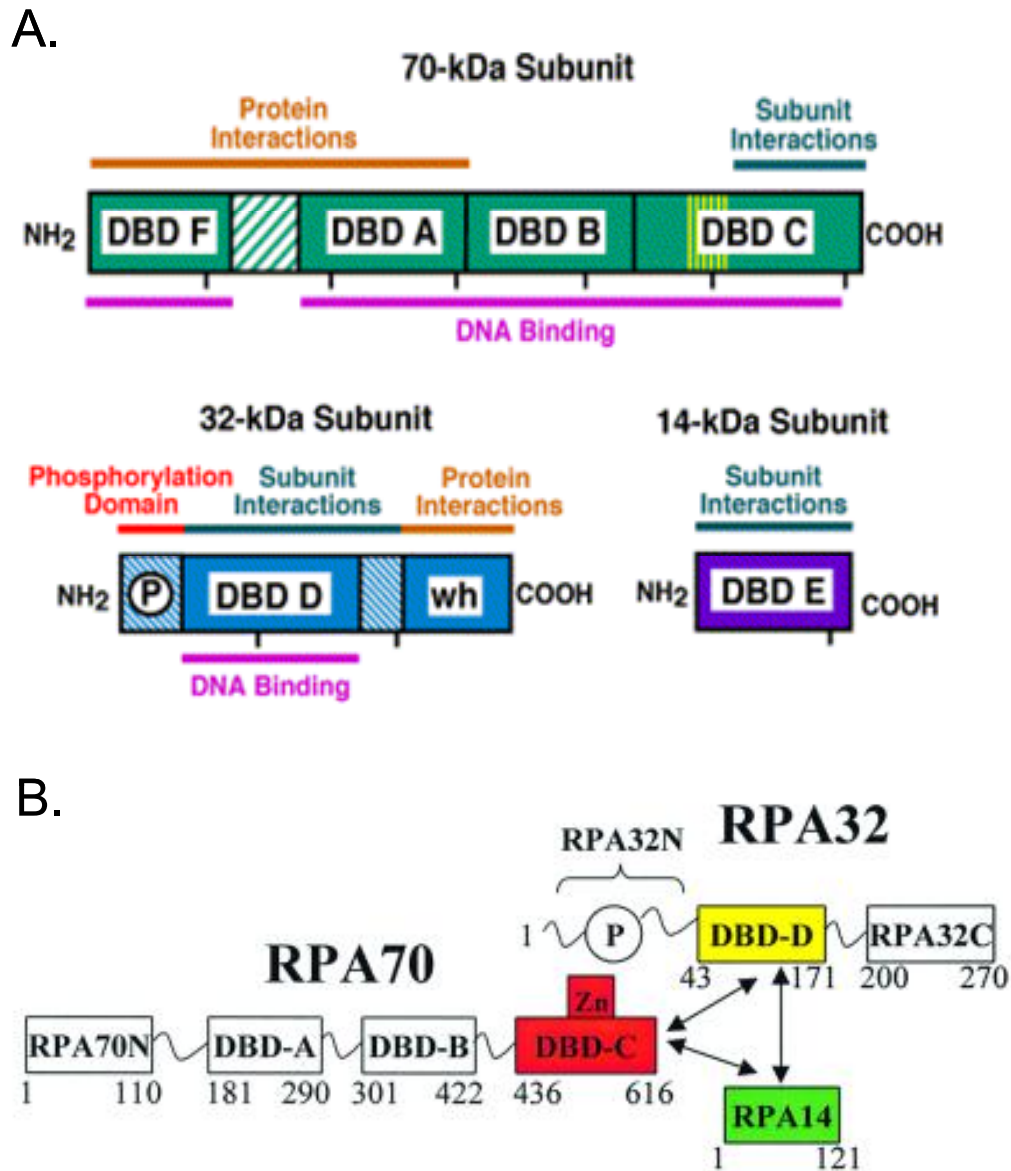


FIGURE 1.10: STRUCTURAL ORGANIZATION OF HUMAN RPA. A. Schematic representation of the three subunits of the RPA complex. Labeled are important functions associated with different domains of the protein (Binz *et al.* 2004). B. DNA binding domains C of RPA70, D of RPA32 and E of RPA14 are involved physical interaction for trimeric complex formation (Bochkareva *et al.* 2002).

Unique to RPA32 is its 40-residue unstructured N-terminus which contains nine potential phosphorylation sites thus far identified including S4, S8, S11/S12/S13, T21, S23, S29, and S33 (Binz *et al.* 2004). This region of RPA32 undergoes various levels of phosphorylation in response to cellular conditions. Four different phospho-isoforms of RPA32 have been identified each with an increasing number of phosphoresidues (Oakley *et al.* 2001). Under normal growing conditions, specifically the S-phase, RPA is hypo-phosphorylated at a low level (isoforms 2 and 3). However, exposure of cells to DNA damaging agents activates the stress response kinases leading to hyper-phosphorylation of RPA32 (isoforms 4 and 5). The primary kinases responsible for hyper-phosphorylation of RPA32 are of the phosphoinositide 3-kinase-like kinase (PI3K) family such as DNA protein kinase (DNA-PK), ATM and ATR (Oakley *et al.* 2001). RPA's requirement in such a broad range of basic cellular processes together with its role in genomic repair from DNA damage implicates its potential role in coordination and regulation of these processes.

Replication-associated repair of oxidized bases

It is evident that the sequence fidelity of only the transcribed strand and promoter regions of functional genes are critical for maintaining information fidelity in nonreplicating cells, while it is essential to maintain the integrity of both strands in replicating cells because both transmit the genetic information equally to the progeny. Unlike bulky adducts that physically block replication and induce TLS, most oxidized bases do not completely block DNA synthesis. This poses a challenge to the cell, as replication prior to repair of the ROS-generated bases such as 5-OHU from C could be mutagenic. It was also previously explained how mutation due to incorporation of A opposite 8-oxoG in the template occurs (Grollman and Moriya 1993). Additionally, unlike bulky base adducts, the oxidized nucleotides generated in the dNTP pool could be

incorporated into nascent DNA as well and thus induce mutations. For example, 8-oxoGTP, with the ability to pair with A or C, would induce a transversion mutation when incorporated opposite A in the template DNA. In spite of a report indicating 8-oxoGTP is a poor DNA polymerase substrate, inactivation of MutT, an 8-oxoGTPase that prevents incorporation of 8-oxoG into nascent DNA, induces a strong mutator phenotype in *E. coli*. This indicates a potential mutagenic role of incorporated 8-oxoG in DNA originating from 8-oxoGTP in the nucleotide pool.

Thus for oxidatively damaged bases such as 8-oxoG, we propose distinct post-replicative vs. pre-replicative repair modes in replicating genomes. For pre-replicative repair, oxidized bases in the template strand are preferentially repaired in replicating DNA, possibly triggered by a signal. This also raises the question of whether the leading and lagging strand template are similarly repaired. Enhancement of repair in the lagging strand template in replicating cells relative to the leading strand was recently reported. Post-replicative repair, on the other, as in classical mismatch repair or MYH-dependent BER, involves nascent strand-specific removal of the incorporated base. We envision that NEIL1 could repair incorporated damage either by excising it at the 3' terminus like an editing enzyme or by excising it after incorporation of additional nucleotides.

CHAPTER II

NEIL1 Associates With Proteins Of The Replisome

INTRODUCTION

NEIL1 has previously been shown to be functionally associated with proteins involved in SN- BER namely, Pol β , Ligase III α and XRCC1 (Wiederhold *et al.* 2004). Stable interaction of NEIL1 with the downstream repair proteins led us to propose the concept that the DNA glycosylase, as the initiating enzyme in the BER process, determines the specific sub-pathway for repair and plays a role in coordinating the subsequent steps of repair (Wiederhold *et al.* 2004; Das *et al.* 2006). Tainer's group and others have proposed a "hand-off" mechanism that would facilitate this coordination by recognition of a product-enzyme complex by the next enzyme in the pathway (Mol *et al.* 2000; Hitomi *et al.* 2007). In addition, Wilson and Kunkel proposed a similar "passing the baton" model in which the product of one reaction is passed on to the next enzyme in a mechanism centered around the preformed distortions in the DNA (Wilson and Kunkel 2000). No single model of coordinated repair has been clearly enunciated which may involve a combination of protein-protein interaction, recognition of enzyme-substrate complexes and careful passing of the distorted DNA molecule that allows efficient repair to occur.

The observation of participation by replication proteins in the long patch BER subpathway suggests that this repair process is performed during replication of chromosomal DNA (Fortini and Dogliotti 2007). It was previously shown that a BER pathway indeed operates in replication foci (Otterlei *et al.* 1999). Recently, studies carried out by Parlanti *et al.* showed that components of the human BER complex are

associated with the DNA replication machinery (Parlanti *et al.* 2007). The hypothesis that cells maintain classical BER during conditions of rest and another subpathway of BER for preferential repair of replicating DNA during cell division would ensure genetic integrity of the replication products (Fortini and Dogliotti 2007). We and others have termed this subpathway of BER replication-associated repair (RAR). Since NEIL1 has a unique preference for excising lesions from bubble, forked and single-stranded DNA (Dou *et al.* 2003) and is activated in S-phase (Hazra *et al.* 2002a), our hypothesis is that NEIL1 is involved in the repair of oxidized base lesions in single-stranded template DNA generated during replication prior to DNA synthesis. A likely prerequisite of RAR is the crosstalk between DNA replication proteins and BER enzymes, specifically NEIL1 (Hazra *et al.* 2002).

We previously provided evidence that NEIL1 is involved in coordinating the steps in SN- BER and it is logical that NEIL1 would also assume a similar role in RAR of oxidative base damage. Thus, we hypothesized that the prerequisite would be physical and functional association of NEIL1 with proteins involved in DNA replication. In order to test our hypothesis we set out to identify NEIL1-interacting partners that are well established for their function in the DNA replication process (Figure 1.9).

MATERIALS AND METHODS

Construction of a NEIL1-FLAG expression plasmid: To generate the FLAG-tagged NEIL1 expression construct, hNEIL1 cDNA encoding residues 1-390 was PCR amplified with primers NEIL1-5'-EcoRI and NEIL1-3'-XbaI (Table 2.1) using template pRESETB-NEIL1 (Hazra *et al.* 2002). The PCR products were digested with EcoR I and Xba I, then ligated into pFLAG-CMV 5.1 (Sigma) expression vector generating a C-terminally FLAG-tagged NEIL1. The cloned NEIL1 gene sequence was confirmed by DNA

sequencing using CMV30 and CMV24 (Sigma) sequencing primers. For stable expression of NEIL1, the NEIL1-FLAG sequence was amplified by PCR then ligated into the pcDNA 3.1/Zeo (+) (Invitrogen) vector at EcoR I and Xho I sites.

Name	Sequence	Purpose
hNEIL1-5'-EcoRI	5'-CGGAATTCGCTATGCCTBAGGGCCCGAGC-3'	5' primer of hNEIL1 in pFLAG-CMV 5.1
hNEIL1-3'-XbaI	5'-GCTCTAGAGGCTGAGGTCCCTCTG-3'	3' primer of hNEIL1 in pFLAG-CMV 5.1

Table 2.1: Sequence of primers used for generation of NEIL1-FLAG expression plasmid.

Cell culture: The human colorectal tumor line HCT116 (expressing wild type p53) was grown in McCoy's 5A medium containing 10% FBS, 100 U/ml penicillin, 100 µg/ml streptomycin at 37°C, 5% CO₂. For selection of stably transfected colonies, cells were grown in the presence of 200 ng/mL Zeocin 24 hours after transfection. Individual colonies were isolated, checked for level of expression and maintained in McCoy's 5A complete media supplemented with 200 ng/mL Zeocin. All media and other reagents were purchased from Invitrogen/Gibco-BRL (Gaithersburg, MD).

Enzymes and Proteins: Recombinant wild type (WT) NEIL1, PNK, Pol δ, RFC, DNA Ligase I, Pol β, DNA Ligase IIIα and FEN1 were purified as described previously (Fien and Stillman 1992; Prasad *et al.* 1993; Singhal *et al.* 1995; Prasad *et al.* 1996; Hill *et al.* 2001; Hazra and Mitra 2006). The NEIL1 protease (endoproteinase Asp-N) resistant domains were cloned, expressed and purified in the laboratory as follows: The DNA sequence encoding NEIL1 (1-311), (1-349), (312-389), (312-349) were amplified by PCR using appropriate primers to select positive clones. After DNA sequence confirmation, the truncated NEIL1 cDNAs were subcloned into different plasmid vectors.

The NEIL1 cDNA encoding (1-311) and (1-349) were subcloned as C-terminal His-tag in pET 22(b) vector with Nde I and Xho I restriction sites. The NEIL1 cDNAs (312-349) and (312-389) were subcloned as N-terminal GST-tag into pGEX 2T plasmid vectors with EcoR1 and Xho1. His-tagged NEIL1 domains (1-311), (1-349) were purified from the extract of plasmid-bearing *E. coli* by affinity chromatography on nickel-sepharose. After elution with imidazole, the proteins were dialysed against 25 mM Tris-HCl (pH 7.5), and finally purified by cation -exchange on SP-sepharose.

The GST-fusion NEIL1 domains (312-349) and (312-389) were expressed in *E. coli* and purified from the cell extract by glutathione-sepharose affinity chromatography, the protein being eluted with 200 mM reduced glutathione. The GST-fusion peptides were then dialyzed and its aliquots stored for GST-pull down assay after subsequent purification using cation-exchange chromatography. To remove GST from the truncated NEIL1 peptides, the proteins were digested with thrombin followed by chromatography on SP-sepharose.

In vivo NEIL1-FLAG Co-Immunoprecipitation: Stably transfected cells were grown to ~75% confluency and then were lysed in lysis buffer (50 mM Tris-HCl, pH 7.5, 150 mM NaCl, 1 mM EDTA, 1% Triton X-100, 1mM NaF, 1 mM Na-orthovanadate, 10 mM Na-butyrate and protease inhibitor mixture), The extract was immunoprecipitated by rocking for 3h at 4°C with FLAG M2 antibody crosslinked to agarose beads (Sigma). The beads were collected by centrifugation, washed three times with cold TBS (50 mM Tris-HCl, pH 7.5, 150 mM NaCl), and NEIL1-FLAG was eluted from the immunocomplex by adding SDS loading buffer. The immunocomplex was separated in 12% SDS-PAGE and immunoblotting was carried out using antibodies for RFC1, Pol δ , FEN1, Ligase I, PCNA and RPA1 and the corresponding secondary antibodies.

Far-Western analysis: For Far Western Analysis, proteins were separated by 10% SDS-PAGE, transferred to a nitrocellulose membrane, denatured with 6M guanidine-HCl, and then slowly renatured by soaking in successive dilutions of guanidine-HCl in PBS with 1 mM DTT (Jayaraman et al, 1998). After blocking with 5% non-fat dry milk in PBS, 0.5% Tween 20, the membrane was incubated with the interacting protein in the blocking buffer for 3h at 4°C before immunoblot analysis with the appropriate antibodies.

Surface plasmon resonance (SPR) analysis: Interaction between NEIL1 and FEN1 or Pol β was analyzed by SPR using Biacore 3000 (GE Healthcare). Full-length NEIL1 (197 RU) or NEIL1 N-311 (193.5 RU) was directly immobilized onto a CM5 sensor chip via the amine coupling method. FEN1 or Pol β (62.5 nM to 2 μ M) was injected over the sensor chip at 50 μ L/min for 2 min in buffer (10 mM Tris (pH 7.5), 0.1 M NaCl, 1 mM MgCl₂ and 1 mM DTT). The response units were corrected for the blank from a reference flow cell and analyzed by curve fitting using a 1:1 (Langmuir) binding model (BIAevaluation software, GE Healthcare).

Circular dichroism spectroscopy: The CD spectra (195–260 nm) were recorded for NEIL1 (312-389) in 10 mM PBS, pH 7.5, 5% glycerol buffer at 25°C on a AVIV 60 DS Spectropolarimeter. The cell length was of 1 mm width and 1 mm length. Each spectrum was the average of four repetitions. 1 μ M protein was used for each measurement.

RESULTS

In vivo association of NEIL1 with proteins of DNA replication

In order to characterize NEIL1's association with the proteins of DNA replication machinery, we first set out to identify potential NEIL1 interacting protein partners by *in vivo* co-immunoprecipitation analysis. HCT116 cells were stably transfected with NEIL1-FLAG, or empty-FLAG expression plasmids and transgenic clones expressing 3 to 4 fold level of overexpression compared with endogenous NEIL1 were selected. Whole cell extracts were isolated from NEIL1-FLAG and empty FLAG expressing cells were then immunoprecipitated with α -FLAG. We identified by immunoblot analysis the presence of RFC, Pol δ , FEN1, Ligase I, PCNA and RPA in the NEIL1-FLAG IP (Figure 2.1, lane 2). The 140 kDa subunit of RFC identified in the NEIL1-FLAG complex (Figure 2.1) is unique to the RFC complex that serves as the loader for the PCNA sliding clamp. We used antibodies against the p125 subunit of Pol δ and the large 70 kDa subunit of RPA for identification of those particular proteins. FEN1, Ligase I and PCNA are all either single subunit proteins or, in the case of PCNA, homotrimeric with identical subunits. None of these proteins could be detected when the cells were transfected with the empty FLAG vector (Figure 2.1, lane 4). These results along with another recent study from our lab showing the presence of the WRN protein, a member of the RecQ helicase family (Das *et al.* 2007), in the NEIL1-IP suggests that NEIL1 associates with proteins involved in DNA replication.

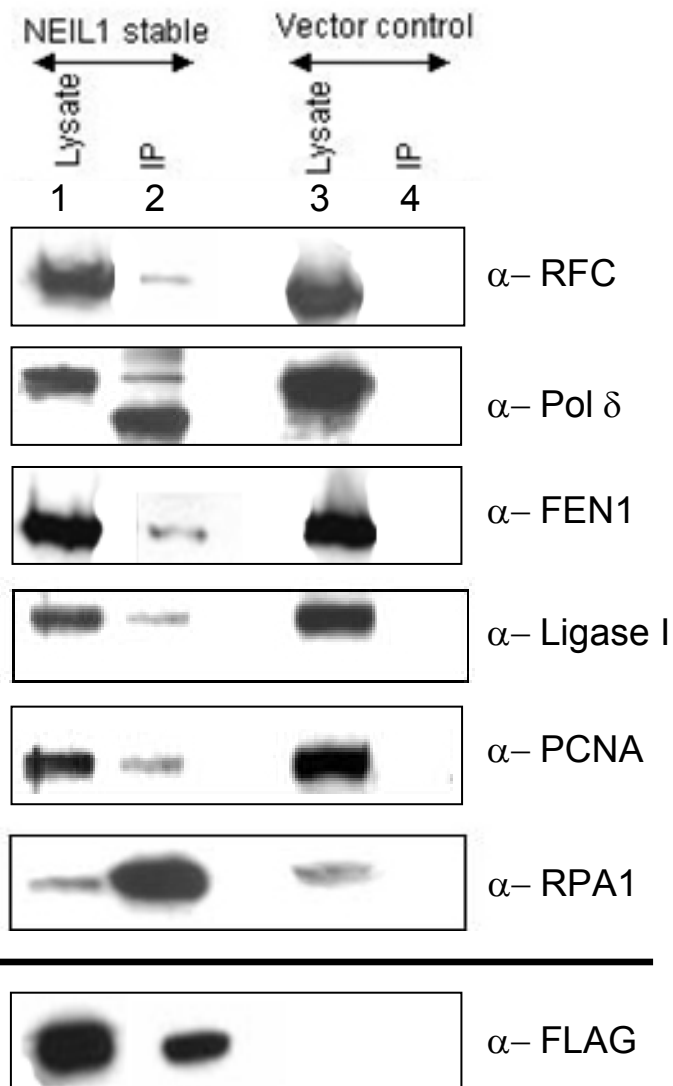


FIGURE 2.1: NEIL1 ASSOCIATES WITH REPLICATION PROTEINS. Western analysis of endogenous proteins found in the NEIL1-FLAG immunoprecipitate (IP) isolated from stably expressing cells. Lanes 1 and 3 are lysate (10% input) from NEIL1 expressing and empty vector cells, respectively, showing comparable levels of protein in each lysate. Lane 2 contains the FLAG immunoprecipitate isolated from NEIL1 expressing cells and lane 4 contains the immunoprecipitate from the empty vector cells. The primary antibodies used for immunodetection of each protein are listed to the right of the corresponding panel.

Direct physical association of NEIL1 with DNA polymerase δ , RFC and DNA ligase I

To test the direct physical interaction between NEIL1 and replication associated proteins shown to be part of the NEIL1 IP, we performed Far Western analysis and surface plasmon resonance experiments. The fine-structure mapping of the interaction interface was carried out using various recombinant NEIL1 fragments purified as explained in the Materials and Methods section. We used limited endoprotease Asp-N (cleaves at N-terminus of aspartate and glutamate) proteolysis of NEIL1 (1-389) to yield two stable, distinct fragments 1-311 and 312-389, the identity of which were confirmed by sequencing their amino-terminal residues and mass-spectrometry analysis. These two NEIL1 fragments and others, namely, 1-288 (C Δ 101), 1-349 (C Δ 40), and 312-349 were then expressed and purified as individual peptides as explained previously (Hazra *et al.* 2002; Das *et al.* 2007). Far Western analysis of NEIL1's interaction with the replication proteins showed that NEIL1 physically interacts with Pol δ , RFC and Ligase I (Figure 2.2B-C). It was evident that residues 312-349 of NEIL1 constitute the common interface for all these interactions. The fine-structure domain mapping of this interacting region indicated that the binding sequences are slightly different but overlapping for different proteins. For example, Pol δ binds to sequence 288-349 (Figure 2.2B), RFC prefers the more extreme C-terminus from residues 312-389 (Figure 2.2C) while Ligase I primarily binds to residues 312-349 (Figure 2.2D).

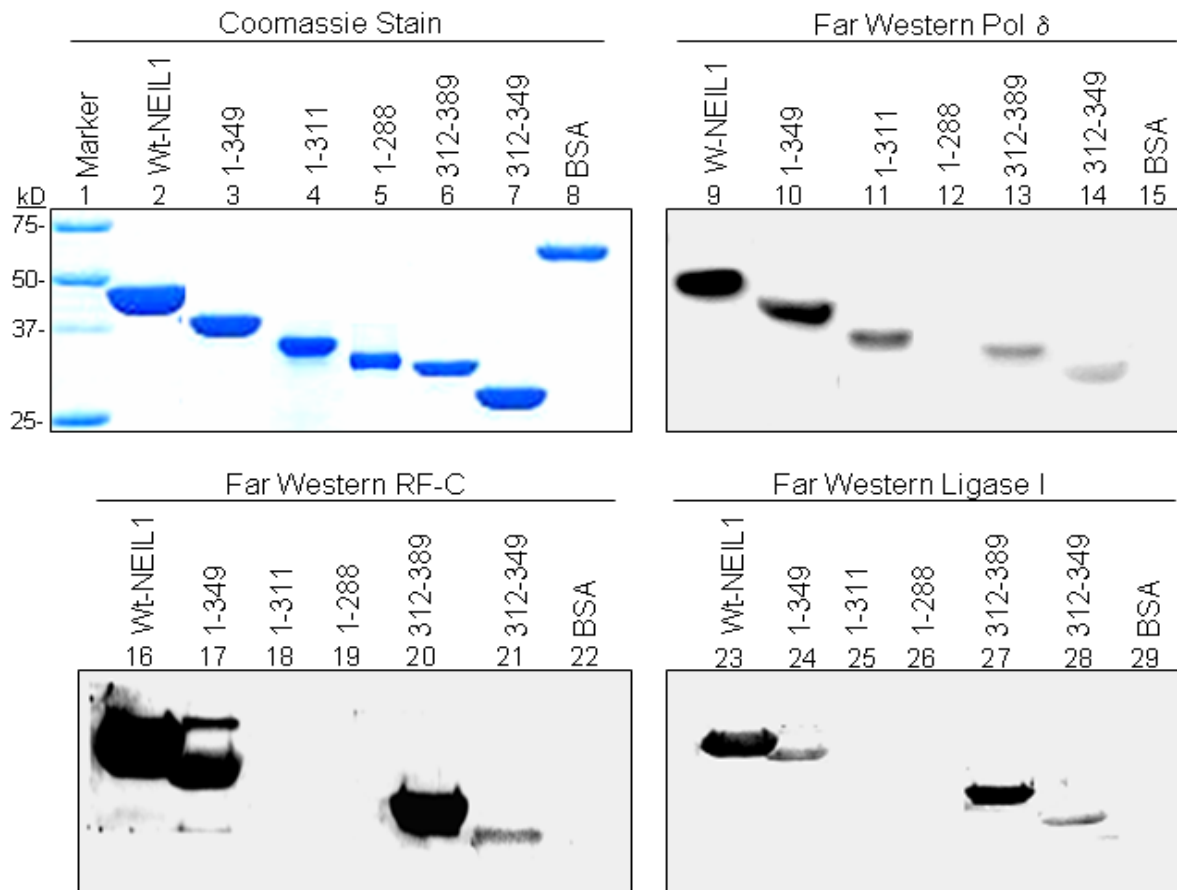


FIGURE 2.2: MAPPING NEIL1'S INTERACTION WITH POL δ , RFC AND LIGASE I. A. Coomassie staining after SDS-PAGE of WT NEIL1 (lane 2), truncated fragments of NEIL1 (lanes 3-5), GST-tagged C-terminal domains (lanes 6 and 7) and BSA (lane 8). B-D. The membrane after protein transfer and renaturation was probed with Pol δ (panel B, lanes 9-15), RFC (panel C, lanes 16-22) or Ligase I (panel D, lanes 23-29) followed by Western blot analysis with the proper antibodies.

In reciprocal experiments, we immobilized FEN1 and Ligase I in addition to SN-BER components Pol β and Ligase III α , and probed for interaction with WT NEIL1 (Figure 2.3B) or NEIL1 fragment 1-311 (Figure 2.3C). We used Pol β and Ligase III α as controls because each was previously shown to interact with NEIL1. BSA, as a negative control, was shown to have no association with NEIL1 in such experiments (Wiederhold *et al.* 2004). Figure 2.3 shows that WT NEIL1 interacts with all four proteins. However, NEIL1 1-311 only showed wild type interaction with Pol β , very weak signal with Ligase III α and no apparent interaction with FEN1 or Ligase I. Weak binding was observed with Ligase I probably because of the lack of native structure due to improper refolding on the membrane (Figure 2.3, lane 10) similar to our previous experience working with other proteins. However, when NEIL1 was on the membrane and probed with Ligase I, a strong association between NEIL1 and Ligase I was observed (Figure 2.2D). We provide additional evidence for the binding of NEIL1 to FEN1 in a separate study identifying that FEN1 also binds to residues 312-349 (Hegde *et al.* 2008). Among the proteins studied, binding in all cases involved residues 289-389 at the C-terminus of NEIL1. No interaction was seen with residues 1-288 (CA101) for any of the NEIL1 associated proteins further supporting our conclusion that the C-terminus is the sole interaction domain in the NEIL1 polypeptide. In further support of these conclusions, more extensive studies were carried out for PCNA and RPA as is covered in later chapters or were recently published in the case of the NEIL1-FEN1 functional interaction (Hegde *et al.* 2008).

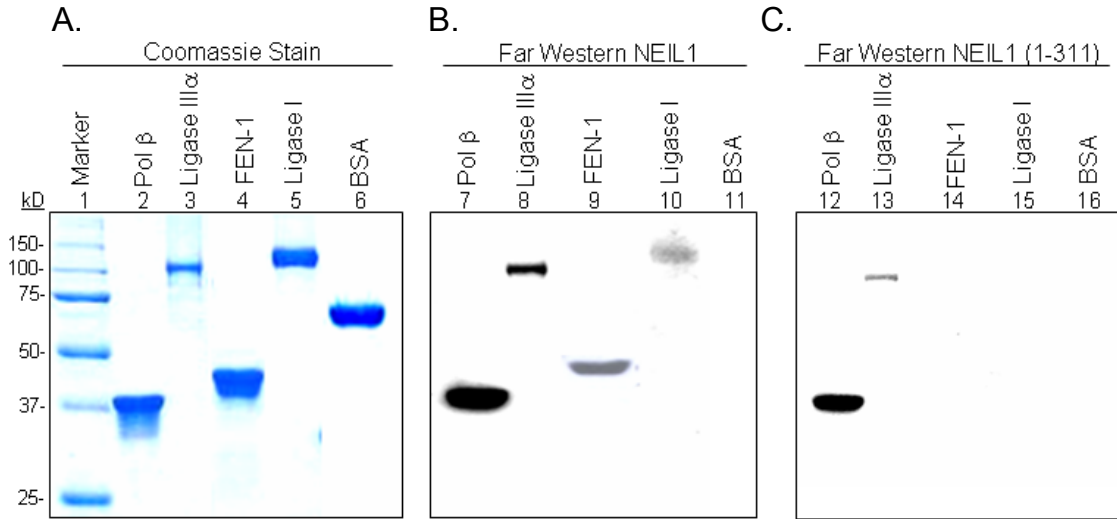


FIGURE 2.3: FAR WESTERN ANALYSIS USING WT NEIL1 AND NEIL1 (1-311).
 A. Coomassie staining after SDS-PAGE of Pol β (lane 1), Ligase IIIα (lane 3), FEN1 (lane 4), Ligase I (lane 5) and BSA (lane 6). B. Far Western analysis of proteins membrane immobilized and renatured then probed for interaction with WT NEIL1. C. The membrane was prepared as in B. but then probed for interaction with C-terminally truncated NEIL1 1-311.

Surface Plasmon Resonance (SPR) analysis of WT NEIL1 and NEIL1 1-311 binding affinities.

To further test the difference in the binding affinity of WT NEIL1 and NEIL1 (1-311) for replication proteins we utilized SPR technology. We used Pol β, a central component of the core SN-BER complex, and FEN1, a component of both long patch BER and replication complexes, for these studies. They were chosen because they interacted differently with NEIL1 1-311 in the previous Far Western analysis (Figure 2.3C). We immobilized equal levels of WT NEIL1 and NEIL1 (1-311) onto a CM5 sensor chip then flowed either Pol β or FEN1 over the sensor surface while recording the binding. The sensorgrams in Figure 2.5 indicate that NEIL1 and NEIL1 1-311 bind to both Pol β and FEN1. SPR technology is a powerful tool for characterizing interactions

because it records binding in real-time allowing for simultaneous calculation of the on- and off-rates. The dissociation constant of Pol β for WT NEIL1 (2.89^{e-6} M) and NEIL1 (1-311) (3.97^{e-6} M) were similar with less than a fold change in K_D (Table 2.2) suggesting that residues beyond 311 have little effect on binding to Pol β . However, the binding of FEN1 for NEIL1 (1.37^{e-7} M) versus NEIL1 (1-311) (4.05^{e-7} M) was significantly different with a 3 fold change in K_D (Table 2.2). It is interesting that k_d of FEN1-complex with both NEIL1 and NEIL1 (1-311) are nearly identical, and that the decrease in the rate of NEIL1-FEN1 complex formation (k_a) is what is responsible for the significant increase in K_D . This suggests that particular residues missing in NEIL1 (1-311) may regulate the initial binding and that modification of those specific residues regulate the NEIL1-FEN1 association. Our Biacore results were unlike the Far Western analysis where NEIL1 1-311 did not show any interaction with FEN1. This may be due to limited mobility of FEN1 on the membrane versus in solution or due to the increased sensitivity of the SPR assay. Regardless, the calculated affinities explain the differences seen in Far Western analysis.

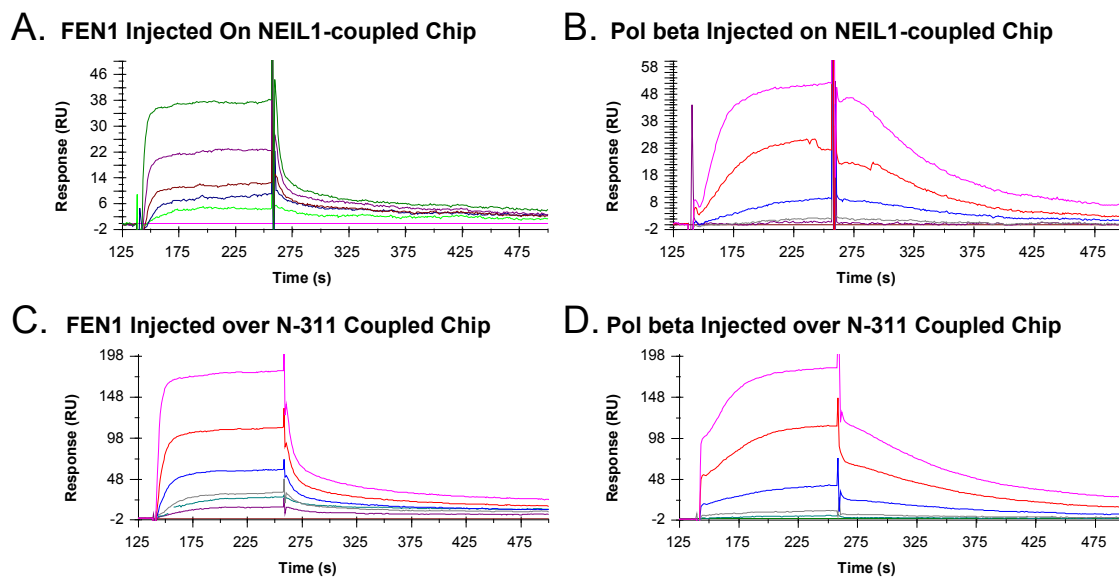


FIGURE 2.4: SPR ANALYSIS OF NEIL1 AND NEIL1 1-311 INTERACTIONS. Sensorgrams showing the interaction between NEIL1 and FEN1 (panel A) or Pol β (panel B) as well as between NEIL1 (1-311) and FEN1 (panel C) or Pol β (panel D). Various concentrations (62.5 nM to 2 μ M) of FEN1 or Pol β in the analyte were passed over the sensor chip at 50 μ L/min. Sensorgrams were calculated using BIAevaluation software and a 1:1 (Langmuir) binding model.

		<u>ka (1/Ms)</u>	<u>kd (1/s)</u>	<u>KA (1/M)</u>	<u>KD (M)</u>
NEIL1	FEN1	7.19E+04	9.86E-03	7.29E+06	1.37E-07
	Pol beta	3.54E+03	1.01E-02	3.51E+05	2.85E-06
N-311	FEN1	2.44E+04	9.88E-03	2.47E+06	4.05E-07
	Pol beta	1.53E+03	6.09E-03	2.52E+05	3.97E-06

Table 2.2: Binding constants of Pol β and FEN1 interaction with WT NEIL1 and NEIL1 1-311. Affinity and dissociation constants were calculated from the sensorgrams in Figure 2.5 using a 1:1 (Langmuir) binding model.

Analysis of the NEIL1 C-terminal domain

The fine-mapping of interactions between replication associated proteins and NEIL1 fragments has been summarized in Figure 2.5. The binding sequences for these proteins on NEIL1 are closely located at its C-terminus from residues 289-389, with an overlapping common interaction interface spanning 38 residues (312-349). Though the exact binding residues appear to be unique for each protein partners, they still appear to be close enough to prevent formation of a ternary complex on a single molecule of NEIL1. Although it is possible that the overlap in the binding sequence allow for displacement of one interacting partner by another

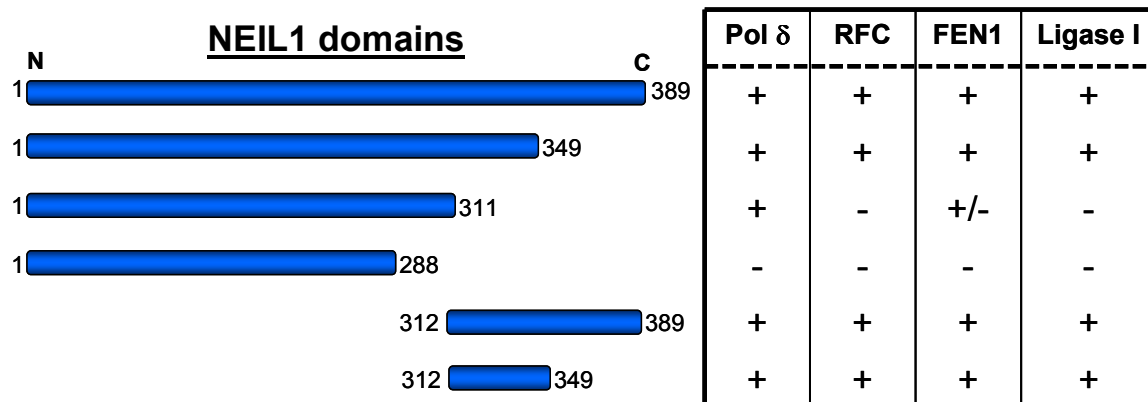


FIGURE 2.5: SCHEMATIC OF THE INTERACTION DOMAIN OF NEIL1. NEIL1 domains used in previous experiments are diagrammed to the left with the minimal interaction domain (312-349) shown on the bottom. Results of our *in vitro* studies of the interaction of NEIL1 with Pol δ , RFC, FEN1, and Ligase I are summarized in the table to the right.

It is intriguing that a relatively small region near the C-terminus of NEIL1 could bind with such a large number of proteins. It is important to note, however, that this segment was absent in the crystal structure of NEIL1 (Doublié *et al.* 2004) and that its disordered nature and flexibility was suggested as the primary reason for difficulties in crystallization. The C-terminus has also been shown to be dispensable for enzymatic activity as well. To understand the basic mechanism of these interactions we analyzed the conformation of the NEIL1 C-terminus (residues 312-389) using both a molecular modeling approach and experimentally by fluorescence spectroscopy. The PONDR (Predictor of Naturally Disordered Regions) analysis software uses the primary amino acid sequence to predict disorder in a given region. A PONDR score near 1.0 means that the region is predicted to assume a disordered conformation. Through this analysis the C-terminal 100 residues of NEIL1 were predicted to be completely unfolded or disordered (Figure 2.6A). Circular dichroism (CD) spectra of a NEIL1 fragment containing residues 312-389 further confirmed this prediction (Figure 2.6B). We used this fragment because it was determined to be stable by our previous endoproteinase cleavage experiment. The analysis of the CD spectra for calculation of relative protein conformations using CD Pro and K2D software suggested that the C-terminus of NEIL1 contains a major portion (85-92%) random coil conformation and a negligible amount of α -helix (3%), β -sheet (3-9%) and β -turn (0-5%) structures (Figure 2.6B). The property of NEIL1's C-terminus being intrinsically disordered potentially explains how NEIL1 manages to interact with such a diverse set of protein partners with a common interacting interface by containing overlapping sites of interaction that assume particular conformations during specific interactions.

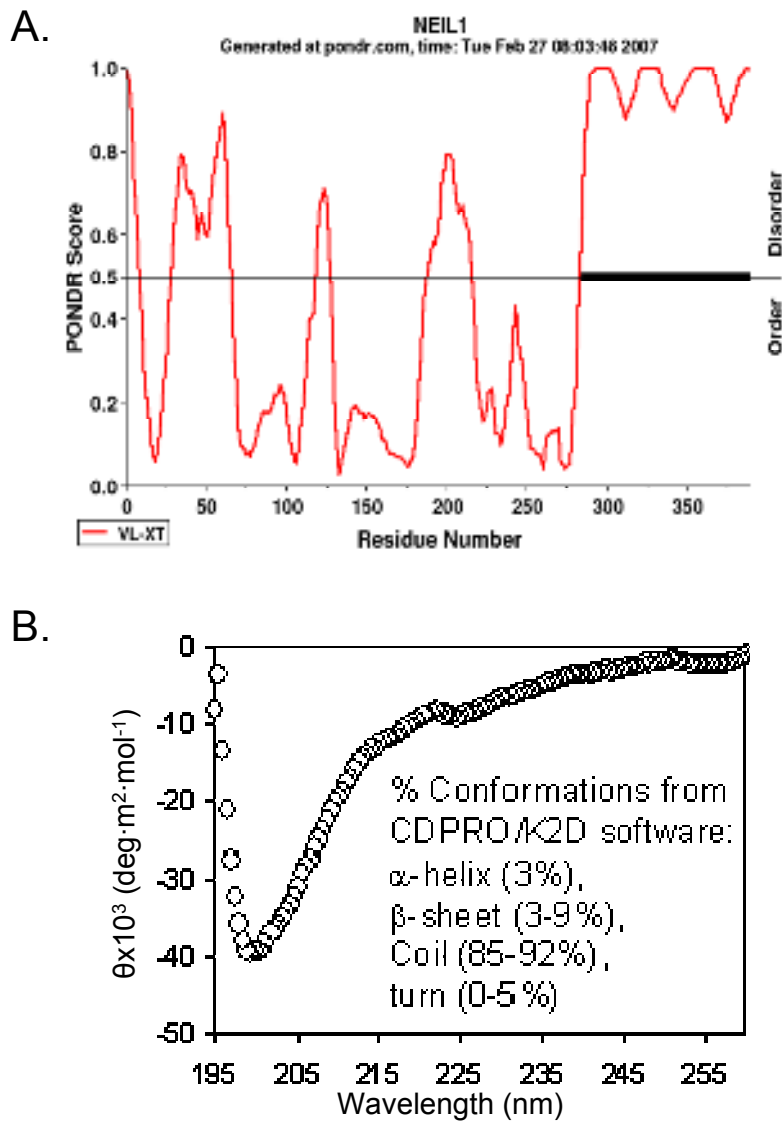


FIGURE 2.6: NEIL1 C-TERMINAL DOMAIN IS PREDICTED TO BE DISORDERED.
 A. PONDR analysis output showing overall disorder predicted from the primary sequence of WT NEIL1 residues 1-389 as depicted on the X-axis. Y-axis represents the PONDR score with 0.0 predicting an ordered conformation and 1.0 predicting disorder within that region. B. Circular dichroism (CD) spectra of the C-terminus of NEIL1 residues 312-389 across increasing wavelengths of light (nm). Composition of relative protein conformation are given as percentages and listed in the graph. Calculations were performed using CD Pro and K2D software.

DISCUSSION

Based on our previous observations suggesting NEIL1's likely involvement in preferential repair of oxidized bases in the replicating genome, we analyzed the proteins present in the NEIL1 immunoprecipitate from human cell extracts. We have identified a large number of proteins in NEIL1's interactome that can be grouped based on their potential functions. Previously published results demonstrated PNK, Pol β , XRCC1 and Ligase III α as components of a BER core complex (Wiederhold *et al.* 2004). We also observed here the presence of several proteins of the DNA replication machinery in the NEIL1-immunocomplex namely, RFC, Pol δ , FEN1, Ligase I, PCNA and RPA. This was the first evidence implicating physical association of NEIL1 with replication proteins suggesting that NEIL1 may in fact be a component of the replication complex.

We then established binary interaction of NEIL1 with Pol δ , RFC and Ligase I. In a separately published study, we reported that NEIL1 and FEN1 are mutually stimulatory and stably interact through the C-terminal domains of NEIL1 in similar fashion as Pol δ , RFC and Ligase I (Hegde *et al.* 2008). All proteins have been shown to interact with residues 312-349 of NEIL1 signifying that this is a common interface and the minimal interaction domain. The interfaces for proteins such as RFC and FEN1 extend further toward the C-terminus, while the interaction interface of others like Pol δ interface with residues N-terminal of the minimal interaction domain. It is interesting to note that residues 289–349 of NEIL1 are also important for its interactions with Pol β (Wiederhold *et al.* 2004), DNA ligase III (Wiederhold *et al.* 2004), XRCC1 (Wiederhold *et al.* 2004), WRN (Das *et al.* 2007b) and others. How so many protein partners interact with NEIL1 within this common region is still unclear.

We further characterized the C-terminal domain of NEIL1 in order to understand how a small domain is responsible for interfacing with many other interacting partners.

First, residues 290-389 of NEIL1 were predicted to be disordered by PONDR analysis. In contrast, the rest of the protein was predicted to prefer an ordered state. It is also important to mention that residues 290-389 are not conserved in the prokaryotic homologs. The predicted disorder of NEIL1's C-terminus was later confirmed by CD analysis with random coil structures formed 85% - 90% of the residue 312-389 fragment. This fragment was determined to be stable independent of the rest of the protein and shown to contain the minimal interaction domain for all protein interactions. The physical and structural properties described here help explain how this domain of NEIL1 is capable of interacting with the large number of proteins using such a small domain.

These results strongly support our hypothesis that NEIL1 associates with DNA replication as an initiator of a preferential pathway for repair of oxidative base damage. These results also suggest that NEIL1 may initiate long patch BER because of the presence of the necessary components of that pathway. Based on the comprehensive details emerging from recent studies it is probable that NEIL1-initiated repair associated with replication would follow the long patch pathway. These results prompted us to continue our investigation into NEIL1's interaction with several of the proteins identified in our screen, specifically FEN1 (Hegde *et al.* 2008), PCNA (Chapter III) and RPA (Chapter V).

CHAPTER III

Functional Interaction Of NEIL1 With PCNA

INTRODUCTION

Our observation, that unlike the other three mammalian DNA glycosylases (OGG1, NTH1, and NEIL2) specific for repair of oxidized bases, NEIL1 shows strong S-phase-specific activation, provided the rationale for investigating NEIL1's interaction with proteins of replication. We and others have postulated preferential repair of oxidized bases in replicating cell genomes based on the reasoning that bulky base adducts induce persistent strand breaks by blocking chain elongation which may activate signals for repair. In contrast, most oxidized base adducts allow replication (and transcription) to proceed past the damage site and could thus induce mutations (Guschlbauer *et al.* 1991; Tornaletti *et al.* 2004; Maga *et al.* 2007). Therefore, while the signaling for repair of such damage could be subtle, the repair should still be extremely urgent.

We identified the DNA sliding clamp, PCNA, in our coimmunoprecipitation screen for replication proteins. It is loaded onto double stranded DNA at 3' primer-template junctions by the clamp loader complex, RFC, which was also found in the NEIL1 IP and shown to directly interact (Chapter II). Once loaded, PCNA is free to slide along the DNA where it functions as a scaffold not only in replication but also other DNA metabolic processes. We hypothesized that the association of NEIL1 with PCNA serves to place NEIL1 at the core of the replication complex where it would have access to the DNA acting as a "cowcatcher" scanning the template DNA for base lesions.

Many proteins have been shown to interact with PCNA with functional relevance including two other DNA glycosylases. Uracil-DNA glycosylase (UNG2) and 8-oxoG•A specific adenine-DNA glycosylase (MYH) have been shown to have functional interaction with PCNA. In the case with MYH, the association works in a post-replicative repair pathway to prevent mutation from uracil incorporation or when A is misincorporated opposite a persistent 8-oxoG in the template. These observations set a precedent that PCNA plays a multi-faceted role during the S-phase beyond that of a polymerase processivity factor. Specifically, PCNA now appears to be a component of a BER pathway in concert with DNA replication suggesting the presence of independent pools of PCNA for DNA replication and repair. These previous studies gave us reason to believe that PCNA could serve as a recruitment site and scaffold for NEIL1 within the replication complex. In support of this, we investigated the stable interaction of NEIL1 with the PCNA sliding clamp and tested the functional consequence of this interaction on NEIL1's glycosylase and DNA binding properties.

MATERIALS AND METHODS

Oligonucleotide substrates: A 51-mer oligo containing 5-OHU at position 26 from the 5'-end, was purchased from Midland Co., TX. The undamaged 51-mer control oligo contained C at position 26; the sequences of complementary oligos had G opposite the lesion for generating duplex, or contained noncomplementary sequences for producing bubble and fork structures as shown in Table 3.1. For optimal annealing, the equimolar mixture of lesion-containing and the complementary strand were heated to 94°C for 2 min in phosphate-buffered saline (PBS), and then slowly cooled to room temperature. The 5-OHU-containing oligo was ³²P-labeled at the 5' terminus with [γ -³²P] ATP using T₄-PNK prior to annealing when necessary.

Plasmids: Mammalian expression plasmids for FLAG-tagged NEIL1 and NEIL2 were previously described (Das *et al.* 2006; Guan *et al.* 2007). Generation of bacterial expression plasmids for the production of N-terminal GST-fused NEIL1 C-terminal domains was described previously (Hegde *et al.* 2008). To generate plasmids for the mammalian two-hybrid system (Stratagene), NEIL1 and PCNA were PCR amplified and subcloned using BamH I and Xba I sites into pCMV-BD and pCMV-AD, respectively. Site-directed mutants of PCNA and NEIL1 were generated using Quick-change® site directed mutagenesis kit (Stratagene). All recombinant plasmid sequences were confirmed by DNA sequencing.

Expression and purification of recombinant proteins: Recombinant WT NEIL1, WT NEIL2 and truncated NEIL1 polypeptides were purified to homogeneity from *E. coli* as described previously (Hazra *et al.* 2002a; Hazra *et al.* 2002b; Wiederhold *et al.* 2004; Das *et al.* 2006). His-tagged PCNA was purified by affinity chromatography on a Ni²⁺ column followed by chromatography for final purification in a HiTrap-SP column (GE Healthcare). Recombinant wild type PCNA was expressed in *E. coli* and purified as before (Matsumoto *et al.* 1999). The GST-fused NEIL1 domains (289-349) and (289-389) were expressed in *E. coli*, purified from the cell extract by glutathione-sepharose affinity chromatography (GE Healthcare) and then eluted using 200 mM reduced glutathione. The GST-fusion peptides were dialyzed and subjected to another step of purification by cation-exchange chromatography.

Assay of DNA glycosylase activity: The DNA glycosylase activity of NEILs was quantitated on the basis of strand incision at the 5-OHU site after its excision from 5'-³²P-labeled DNA oligo substrates. After incubation of the DNA (25 nM) with NEIL1 or NEIL2 in a 10 µl reaction mixture containing 40 mM HEPES-KOH, pH 7.5, 50 mM KCl, 1 mM MgCl₂, and appropriate amount of bovine serum albumin (BSA) to maintain a

constant protein level in the presence or absence of PCNA at 37°C for indicated times, the reaction was stopped with 70% formamide/30 mM NaOH. The alkali in the stop buffer cleaves any uncleaved AP sites escaping NEILs' AP lyase activity. The intact and cleaved oligos were then separated by denaturing gel electrophoresis in 20% polyacrylamide containing 7M urea, 90 mM Tris-borate (pH 8.3) and 2 mM EDTA, and the radioactivity in the DNA bands was quantitated in a PhosphorImager using ImageQuant software (Molecular Dynamics).

For single-turnover enzyme kinetics, we incubated 5-OHU bubble oligo substrate (2 nM) with excess NEIL1 (20 nM) alone or in the presence of PCNA (0.5 μ M) at 37°C in a buffer containing 40 mM Hepes-KOH, pH 7.5, 50 mM KCl, 1mM MgCl₂. The reaction was stopped at the designated times and cleaved products were quantitated as before.

Immunoblotting: Proteins were separated by 10% SDS-PAGE and transferred to nitrocellulose membranes which then were blocked in TBS (50 mM Tris-HCl, pH 7.5, 150 mM NaCl) with 0.05% Tween 20, 5% NFDM and incubated with specified primary and appropriate secondary antibodies. The immunocomplexes were detected by enhanced chemiluminescence (Pharmacia). Antibodies used include mouse α -PCNA (PC-10 clone), rabbit polyclonal α -NEIL1(Hazra *et al.* 2002a), HRP-conjugated α -FLAG M2 (Sigma), HRP-conjugated α -His-tag (Santa Cruz) or goat α -GST (GE Healthcare) antibodies.

Co-immunoprecipitation assay: The human embryonic kidney cell line HEK293 was maintained and grown in DMEM at 37°C, 5% CO₂. HEK293 cells were transfected with empty FLAG, NEIL1-FLAG or NEIL2-FLAG plasmids. The cells were collected 48 hours after transfection and lysed by sonication (15% output, 10sec) in buffer (20 mM Tris-HCl, pH 7.5, 150 mM NaCl, 1 mM EDTA, 1% Triton X-100, and 0.5 mM, 1 mM

NaF, 1 mM Na-orthovanadate, β -mercaptoethanol, plus protease inhibitors). In several experiments, the cell lysates were digested with 500 units/ml DNase I (Ambion) at 37°C for 30 min, and cleared by centrifugation. The lysates were then immunoprecipitated, separated and immunoblotted as previously described (Chapter II).

In vitro pulldown assay: Wild type NEIL1 or its truncated mutants (20 pmol) were incubated with His-tagged PCNA (10 pmol) in 0.5 ml TBS for 1 h at 4°C and then mixed with HIS-Select HC nickel beads (Sigma) with constant rotation for 1 h at 4°C. The beads were subsequently washed extensively with wash buffer (50 mM Tris-HCl, pH 7.5, 500 mM NaCl). After elution of the proteins with SDS sample buffer and SDS-PAGE, the presence of NEIL1 was tested by immunoblotting.

GST pull down assays were performed as described previously (Das *et al.* 2007a). Briefly, proteins were mixed with Glutathione-sepharose beads (20 μ l) alone or bound to GST-tagged truncated NEIL1 domains (312-349 and 312-389) (10 pmol), incubated with PCNA (2.5 pmol) in 0.5 ml. After washing the bound proteins were separated by SDS-PAGE and the presence of PCNA was tested by immunoblotting.

Mammalian two hybrid analysis: WT NEIL1 was cloned into the pCMV-BD vector containing five tandem repeats of the GAL4-binding sites (PFR-Luc; Stratagene) and named pCMV-NEIL1_{BD} which encodes a GAL4-NEIL1 fusion protein. WT PCNA was cloned into pCMV-AD vector and named pCMV-PCNA_{AD} containing the transcriptional activation domain of the mouse NF- κ B (Stratagene) to encode a PCNA fusion protein. HCT116 cells were co-transfected with pCMV-NEIL1_{BD} and pCMV-PCNA_{AD} or equivalent amount of the empty vector; pCMV- β -gal was used as an internal standard. Luciferase activity was measured in a luminometer using a luciferase assay kit (Promega) at 48h after transfection and normalized with co-expressed β -galactosidase activity.

Electrophoretic gel mobility shift analysis (EMSA): The 5' ³²P-labeled 5-OHU-containing 51-mer oligo and a control oligo of identical sequence except for substitution of 5-OHU with C at position 26 (Table 3.1) were used. The DNA (15 fmol) was incubated with NEIL1 (5 nM) and various amounts of PCNA for 10 min at 22°C in a buffer containing 40 mM HEPES (pH 7.3), 50 mM KCl, 12% glycerol and appropriate amount of BSA to maintain an equal amount of total protein in each reaction. After electrophoresis in nondenaturing 10% polyacrylamide gels in Tris-glycine buffer (pH 8.4), the protein DNA complex was quantitated by band intensity.

Surface plasmon resonance (SPR) analysis of NEIL1 DNA binding: The effect of PCNA on the interaction between NEIL1 and bubble DNA was analyzed by SPR using Biacore X (GE Healthcare). 5' biotinylated bubble oligo (Table 3.1) was bound to sensor chip SA according to the manufacturer's instructions. Interaction analysis was carried out using HEPES buffered saline (HBS) buffer containing (50 mM EDTA, 0.005% Tween-20) with NEIL1 alone or together with PCNA. The analyte solution was passed over the sensor chip at 20 µl/min and the response units were corrected for the blank reading. Regeneration buffer (HBS with 350 mM EDTA, 0.005% Tween-20) was injected at 20 µl/min to regenerate the surface in between analysis cycles. This procedure did not reduce binding of the sensor chip surface.

Kinetic constants were calculated from the sensorgrams using the BIAevaluation software (version 3.1, Biacore), and a global fitting model. Response curves were prepared for fitting by subtraction of the signal generated simultaneously on the BSA control flow cell and then globally fitted to a bivalent analyte model (first step: $A+B \rightleftharpoons AB$; second step: $AB+B \rightleftharpoons AB_2$; where A = ligand and B = analyte).

RESULTS

NEIL1 association with PCNA in vivo

Our previous observation of NEIL1's unique activity on single-stranded and bubble DNA substrates and its S-phase-specific activation suggested linkage of NEIL1's *in vivo* function to DNA replication (Dou *et al.* 2003). Because of PCNA's established role as a scaffold during DNA replication we tested for *in vivo* association between NEIL1 and PCNA by performing co-immunoprecipitation of extracts from HEK293 cells expressing either the NEIL1-FLAG or NEIL2-FLAG polypeptide. We tested NEIL2 because it shares NEIL1's preference for single-stranded region containing substrates but unlike NEIL1 is not cell cycle-regulated. PCNA was found to be present in both NEIL1 and NEIL2 immunocomplexes but to a greater extent in the NEIL1 immunoprecipitate (Figure 3.1A, lanes 2 and 4). PCNA was not found in the FLAG immunocomplex obtained from empty FLAG vector control transfected cells (Figure 3.1A, lane 1)

Furthermore, to address the possibility that the presence of contaminating DNA contributed to PCNA's detection in the NEILs immunoprecipitates, we treated the lysate with DNase I. DNase treatment removed most contaminating genomic DNA (data not shown). The removal of DNA did not diminish the amount of PCNA present in either the NEIL1 or NEIL2 immunocomplex (Figure 3.1A, lanes 3 and 5) suggesting that DNA is not required for the stable association of NEILs with PCNA. Immunoblot analysis using an α -FLAG antibody demonstrated that equal amounts of NEIL1-FLAG or NEIL2-FLAG was present in both untreated and DNase-treated samples. Although these results do not establish binary interaction between PCNA and NEIL1, they strongly suggest that endogenous NEIL1 and PCNA are present in the same *in vivo* complex even in the absence of DNA. This prompted us to test for direct interaction of NEIL1 with PCNA.

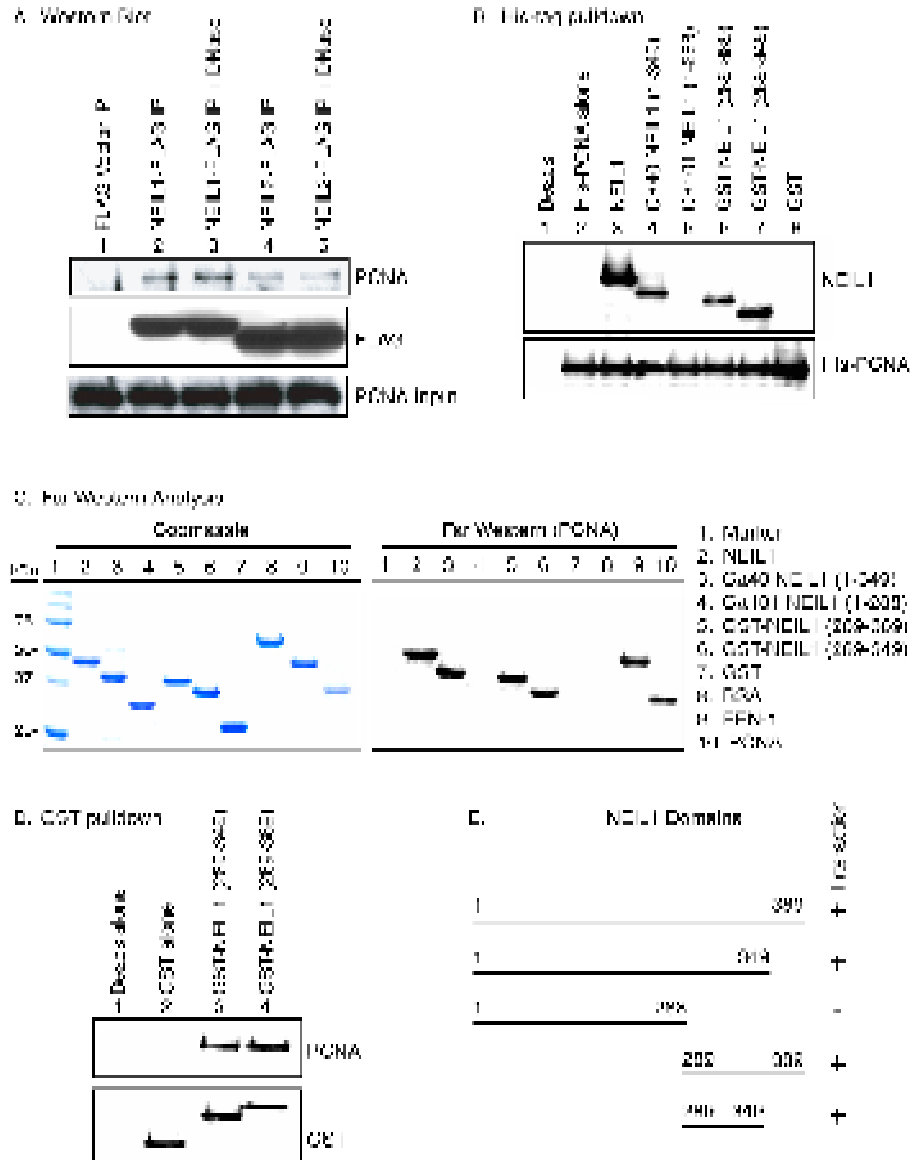


FIGURE 3.1: NEIL1 INTERACTS WITH PCNA THROUGH ITS UNCONSERVED C-TERMINAL DOMAIN. A. Western analysis of endogenous PCNA in the NEIL1-FLAG and NEIL2-FLAG IP isolated from HEK 293 cells. Top panel: Detection of PCNA in IP of empty FLAG vector control (lane 1), NEIL1-FLAG (lanes 2 and 3) and NEIL2-FLAG (lanes 4 and 5). Lanes 3 and 5 were pretreated with DNase I. Middle panel: Western analysis comparable levels of NEIL1-FLAG and NEIL2-FLAG. Bottom panel: Levels of total PCNA in the cell lysate by immunoblotting with PCNA antibody. B. Mapping of NEIL1's interaction with PCNA. His-PCNA (10 pmol) was used as bait to identify the interaction domain of NEIL1 (20 pmol). Top panel: Immunoblot analysis of His-PCNA bound to WT NEIL1 (lane 3) and truncated fragments of NEIL1 (lanes 4-7). Lane 8, GST alone control. Bottom panel: Western analysis of His-tag epitope to confirm equal

level of His-PCNA. C. Far Western analysis of PCNA interaction with NEIL1. Left panel: Coomassie staining after SDS-PAGE of WT NEIL1 (lane 2) and truncated fragments (lanes 3-6), GST (lane 7), BSA control (lane 8), FEN-1 (lane 9) and PCNA (lane 10). Lanes 2-9 contain 40 pmol of each protein and lane 10 contains 5 pmol of PCNA. Right panel: The membrane was probed with PCNA (10 pmol/ml) for interaction (lanes 2-9) followed by Western blot analysis with PCNA antibody (lane 10, positive control). D. GST pulldown assay of PCNA interaction with C-terminal segments of NEIL1. Glutathione-sepharose beads alone (lane 1) or bound to 10 pmol GST (lane 2) or GST-tagged C-terminal domains of NEIL1 (lanes 3 and 4) were incubated with PCNA (2.5 pmol). Top panel: Immunoblot analysis of eluate for PCNA. Bottom panel: Immunoblot analysis for GST to confirm comparable levels of GST-tagged proteins. E. Schematic representation of NEIL1's interacting domain for PCNA.

Mapping the interaction domain of NEIL1

We previously showed that NEIL1 interacts with several proteins involved in short patch BER, including DNA ligase III α , Pol β , and XRCC1 (Wiederhold *et al.* 2004). The interacting domain of NEIL1 for all of these proteins is localized within the C-terminus (Wiederhold *et al.* 2004). In addition, we identified another subset of interacting protein partners that are part of the replication machinery that also utilize this interaction domain of NEIL1, including RFC, FEN1, Pol δ and Ligase I (Chapter II). To test the possibility that the same region also includes the binding site for PCNA, we used His-tag (Figure 3.1B) or GST-tag (Figure 3.1D) pulldown assays and Far Western (Figure 3.1C) analysis.

We confirmed that NEIL1 and PCNA directly interact and that the interaction domain of NEIL1 is localized within the C-terminal domain. Figure 3.1B shows that His-tagged PCNA interacts with full-length and C Δ 40 NEIL1 but not the C Δ 101 truncated mutant (top panel, lanes 3-5). We also fused NEIL1 C-terminal regions to GST and showed that PCNA interacts with this fusion protein (Figure. 3.1B, lanes 6 and 7) demonstrating that NEIL1's interaction domain alone is sufficient for stable binding to PCNA. Used as a control, GST alone did not interact with PCNA (Figure 3.1B, lane 8).

In a reciprocal pulldown assay, we used the GST-tagged NEIL1 domains to confirm that the C-terminal interaction domain of NEIL1 alone was sufficient for interaction. Indeed, C-terminal fragments of NEIL1 in absence of the rest of the protein were sufficient for stable interaction with PCNA (Figure 3.1D, lanes 3 and 4). Again, GST itself was unable to interact with PCNA (Figure 3.1D, lane 2).

These results were confirmed by Far Western analysis where PCNA in solution was incubated with various membrane-immobilized proteins (Figure 3.1C, right panel). Once again deletion of 101 C-terminal residues of NEIL1 abolished interaction and the C-terminal domain fused to GST was sufficient for interaction. As controls we immobilized GST and BSA (Figure 3.1C, lanes 7 and 8) which did not show interaction. FEN1, whose interaction with PCNA was well established, was used as a positive control (Figure 3.1C, lane 9). In a reciprocal Far Western analysis, we could not detect interaction when PCNA was present on the membrane after SDS-PAGE (data not shown). This was perhaps expected because denatured PCNA in the gel was unlikely to refold to the native trimeric structure after the renaturation procedure needed for binding to NEIL1.

ss DNA Oligo

5' - GCT TAG CTT GGA ATC GTA TCA TGT AXA CTC GTG TGC CGT GTA GAC CGT GCC - 3'

Duplex Oligo

5' - GCT TAG CTT GGA ATC GTA TCA TGT AXA CTC GTG TGC CGT GTA GAC CGT GCC - 3'
3' - CGA ATC GAA CCT TAG CAT AGT AGA TGT GAG CAC ACG GCA CAT CTG GCA CCG - 5'

Bubble (11-nt) Oligo

5' - GCT TAG CTT GGA ATC GTA TC ATGTAXACTCG TG TGC CGT GTA GAC CGT GCC - 3'
3' - CGA ATC GAA CCT TAG CAT AG GQACCCGACAA AC ACG GCA CAT CTG GCA CCG - 5'

5' Fork Oligo

5' - GCT TAG CTT GGA ATC GTA TCA TGT AXA CTC GTG TGC CGT GTA GAC CGT GCC - 3'
3' - CGA ATC GAA CCT TAG CAT AGT AGA TCA CTC GTG TGC - 5'

3' Fork Oligo

5' - GCT TAG CTT GGA ATC GTA TCA TGT AXA CTC GTG TGC CGT GTA GAC CGT GCC - 3'
3' - GAT TCA TGT ACT GAG CAC ACG GCA CAT CTG GCA CCG - 5'

Table 3.1: Sequences of 5-OHU containing oligodeoxynucleotides. "X" represents 5-OHU.

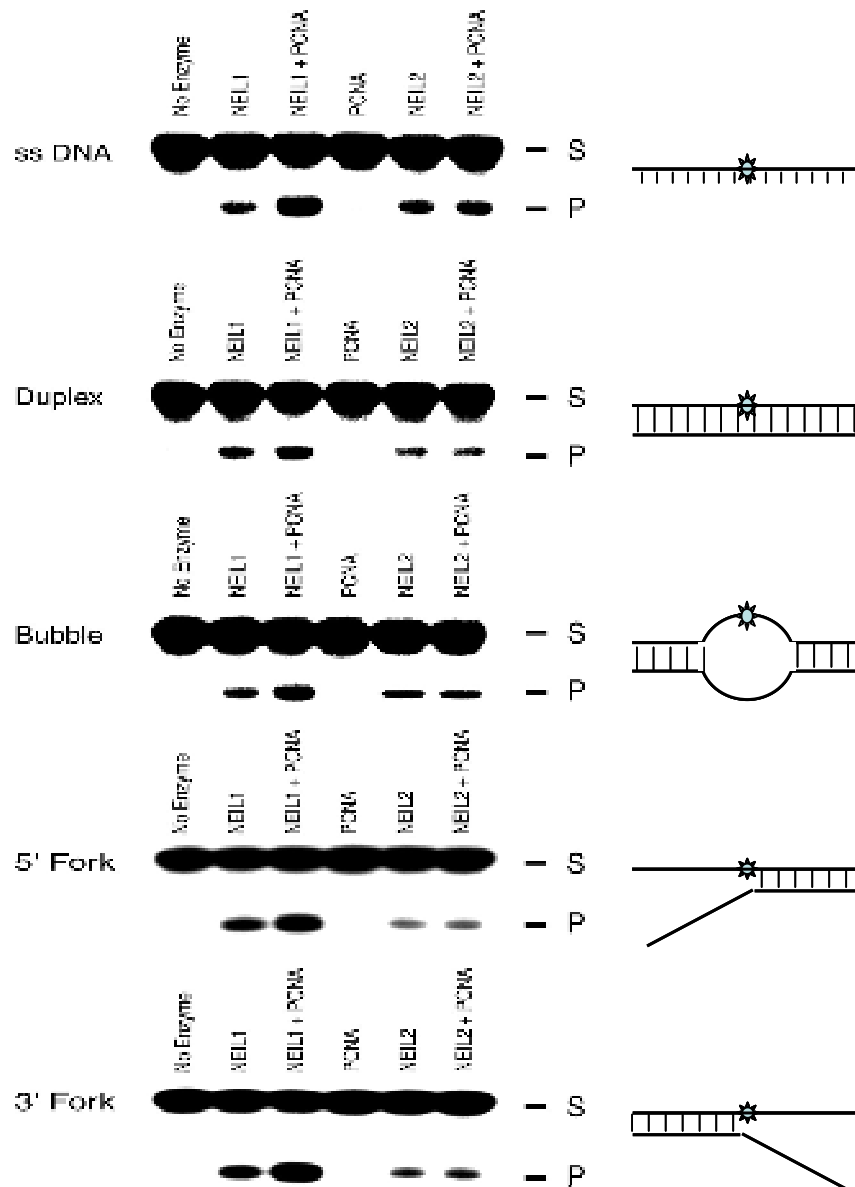


FIGURE 3.2: EFFECT OF PCNA ON NEIL1 AND NEIL2 FOR 5-OHU EXCISION FROM VARIOUS DNA STRUCTURES. A 51-mer 5-OHU-containing oligo (25 nM) was used alone (ss) or annealed with various complementary strands to generate duplex, 11-nt bubble or 3' and 5' fork structures (see Table 1). S and P indicate 3' 32 P-labeled uncleaved oligo substrate and β,δ -elimination product, respectively. NEIL1 (3 nM) or NEIL2 (6 nM) was added to the reaction alone or together with PCNA (0.2 μ M, lanes 3 and 6). PCNA was also added to the reaction alone as a control.

PCNA stimulates NEIL1 in a DNA structure-specific manner

We examined the activities of NEIL1 and NEIL2 which are able to excise the same base lesion (5-OHU) from similar substrate structures (Dou *et al.* 2003), in the presence of PCNA, using oligo substrates of several structures containing duplex and single-stranded regions, specifically fork structures with the lesion placed 3' or 5' of the branch point (Table 3. 1). Only slight stimulation of NEIL1 activity was observed with duplex DNA substrate in the presence of PCNA, however, significant enhancement in NEIL1 activity was observed when the lesion was located in a bubble, single-stranded oligo or in the single-stranded region near the junction of a fork oligo (Figure 3.2). PCNA enhancement of NEIL1 activity was comparable for oligo substrates with 3' vs. 5' fork (Figure 3.2). Similar increase in activity was also observed with fork substrates when the lesion in the single-stranded region was placed as far away as 10 nt away from the fork junction (data not shown). In contrast to the results with NEIL1, NEIL2's activity with all substrates was barely affected by the presence of PCNA (Figure 3.2). An earlier report described a similar finding with NTH1 which also excises 5-OHU, but only from duplex DNA. NTH1 was shown to bind to PCNA but was not stimulated as a result of such binding (Oyama *et al.* 2004). We also showed concentration dependence of NEIL1 stimulation by PCNA for all substrates. The extent of stimulation was highest with the 3' fork substrate, intermediate for single-stranded or bubble substrate and negligible for the duplex DNA (Figure 3.3A). PCNA's stimulation of NEIL1 activity could be due to its ability to load NEIL1 on the lesion site when PCNA is concentrated at the fork junction of a partially duplex DNA (e.g., a primed template). PCNA could also alter NEIL1's conformation thus facilitating its substrate binding on single-stranded lesions. Again no significant stimulation in NEIL2 activity was observed in the presence of increasing concentration of PCNA, which confirmed the results in Figure 3.2.

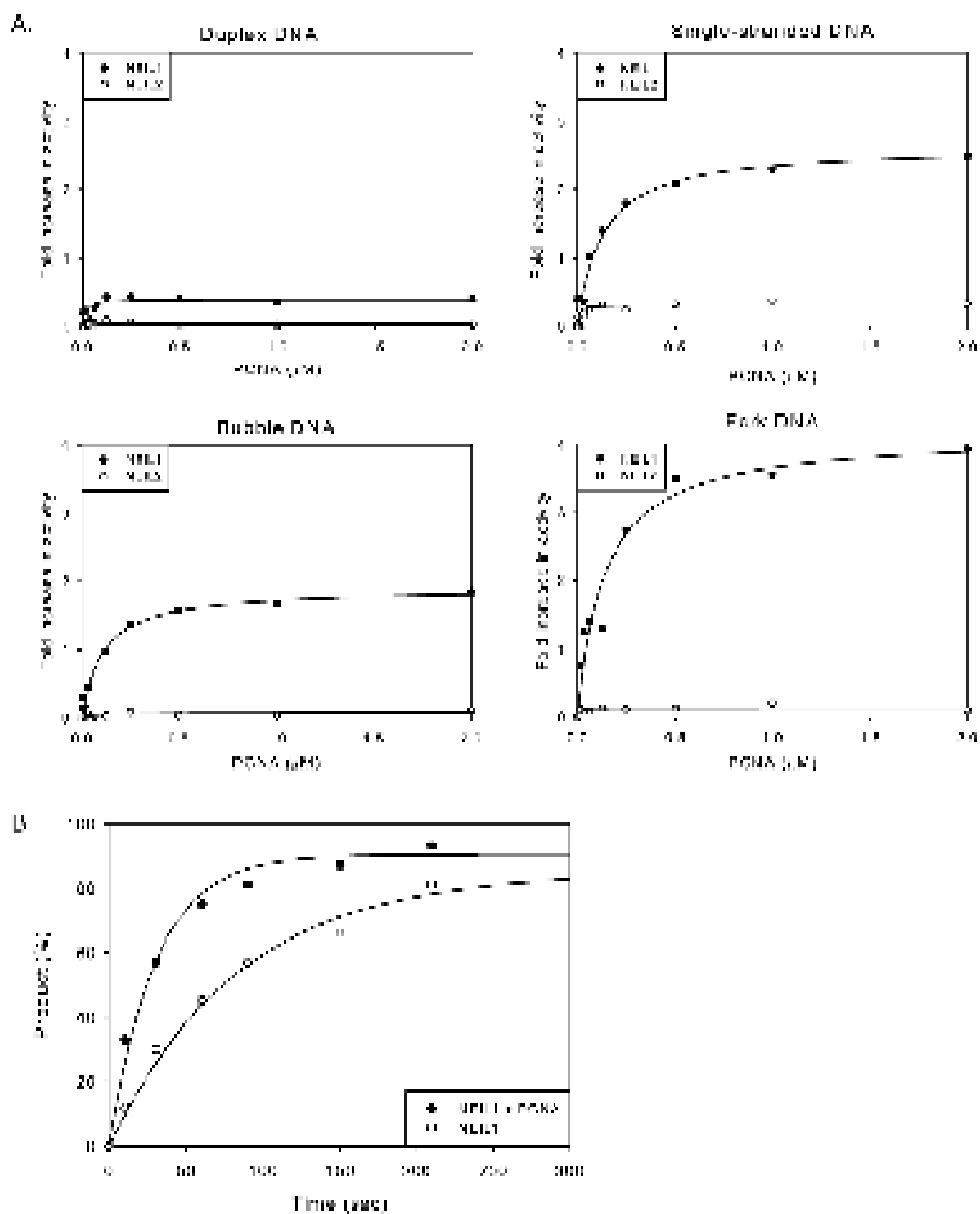


FIGURE 3.3: PCNA DOSE-DEPENDENT STIMULATION OF NEIL1 ACTIVITY AND SINGLE-TURNOVER KINETICS. A. The fold increase in activity ($\text{Activity}_{\text{NEIL-PCNA}} - \text{Activity}_{\text{NEIL}} / \text{Activity}_{\text{NEIL}}$) is plotted for NEIL1 (3 nM) and NEIL2 (6 nM) with duplex (top left), bubble (top right), single-stranded (bottom left) and 3' fork (bottom right) DNA structures (all at 25 nM) was plotted as a function of PCNA concentration. B. Effect of PCNA (0.5 μM) on single-turnover kinetics of NEIL1 (20 nM) using 5-OHU-containing bubble oligo (2 nM) substrate.

We then determined the kinetic parameters of NEIL1's activity on a bubble DNA substrate in the presence or absence of PCNA, using conditions for single turnover in which the enzyme is present in excess, and product formation follows the first-order kinetics (Porello *et al.* 1998). The data were analyzed using the first-order rate equation $[P] = A_0 (1 - \exp(-\kappa_{\text{obs}} t))$, where A_0 represents the amplitude of the exponential phase and κ_{obs} is the rate constant correlated with the reaction (Figure 3.3B). For NEIL1 alone, the κ_{obs} was 0.012 ± 0.002 (sec^{-1}), and with PCNA, it was 0.033 ± 0.002 , sec^{-1} . Because $v_0 = \kappa_{\text{obs}}[S_0]$, it is evident that PCNA stimulates the turnover of NEIL1 by increasing the release of the damaged base product.

Effect of PCNA on NEIL1's affinity for bubble DNA

Enhancement of NEIL1's activity by PCNA with the bubble substrate suggested that NEIL1 has intrinsic affinity for the single-stranded DNA. We tested this by using EMSA and surface plasmon resonance. We used a control oligo whose sequence is identical to that of the 5-OHU-containing oligo except for the substitution of 5-OHU with C. We could not carry out the binding studies with the lesion-containing DNA because the activity of wild type NEIL1 could not be inhibited during execution of the experiment. Figure 3.4A shows representative data on the WT NEIL1-DNA complex in the presence or absence of PCNA. PCNA showed no direct binding to the DNA oligo. We observed a second slower migrating complex with bubble DNA that appears to be due to the binding of two NEIL1 molecules to a single oligo, which became more pronounced with increasing protein concentration. NEIL1 had no excision activity on these oligos lacking an oxidatively damaged base, as expected (data not shown).

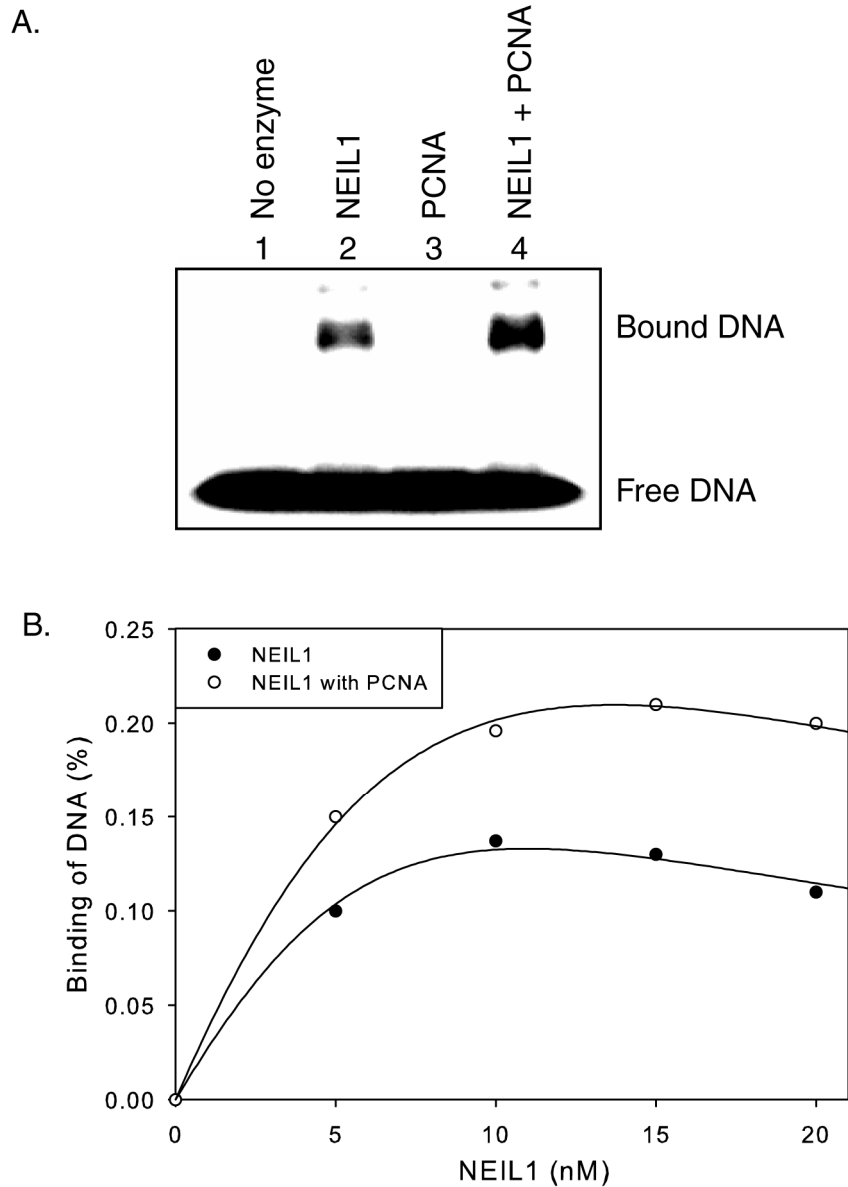


FIGURE 3.4: EFFECT OF PCNA ON NEIL1'S DNA BINDING. A. EMSA of no enzyme (lane 1), NEIL1 (5 nM) alone (lane 2), PCNA (0.2 μ M) alone (lane 3), or NEIL1 plus PCNA (lane 4) binding to undamaged DNA oligo (150 fmol). B. Binding isotherm of NEIL1 alone (filled circles) or in the presence of PCNA (0.5 μ M, empty circles). Other details are given under Experimental Procedures.

We observed increased affinity of NEIL1 for DNA in the presence of PCNA (Figure 3.4B and Table 3.2). A similar trend was also observed when we used the catalytically inactive NEIL1 K53L mutant with the 5-OHU containing substrate (data not shown). We utilized surface plasmon resonance (SPR) to examine real-time kinetics of NEIL1 binding to bubble DNA as before (Figure 3.5). The NEIL1-PCNA complex demonstrated about 2-fold higher affinity than NEIL1 alone for the bubble oligo. The binding constants calculated from EMSA and SPR studies are not identical, presumably because of the different ionic strengths of the reaction mixtures used in these studies. Low salt concentration used in EMSA, cannot be used in the SPR studies because of nonspecific binding to the sensor chip. Taken together, these data show that PCNA increases NEIL1's affinity for the substrate, and thus its enzymatic activity, and that NEIL1 has intrinsic affinity for single-stranded regions in DNA bubble and fork structures.

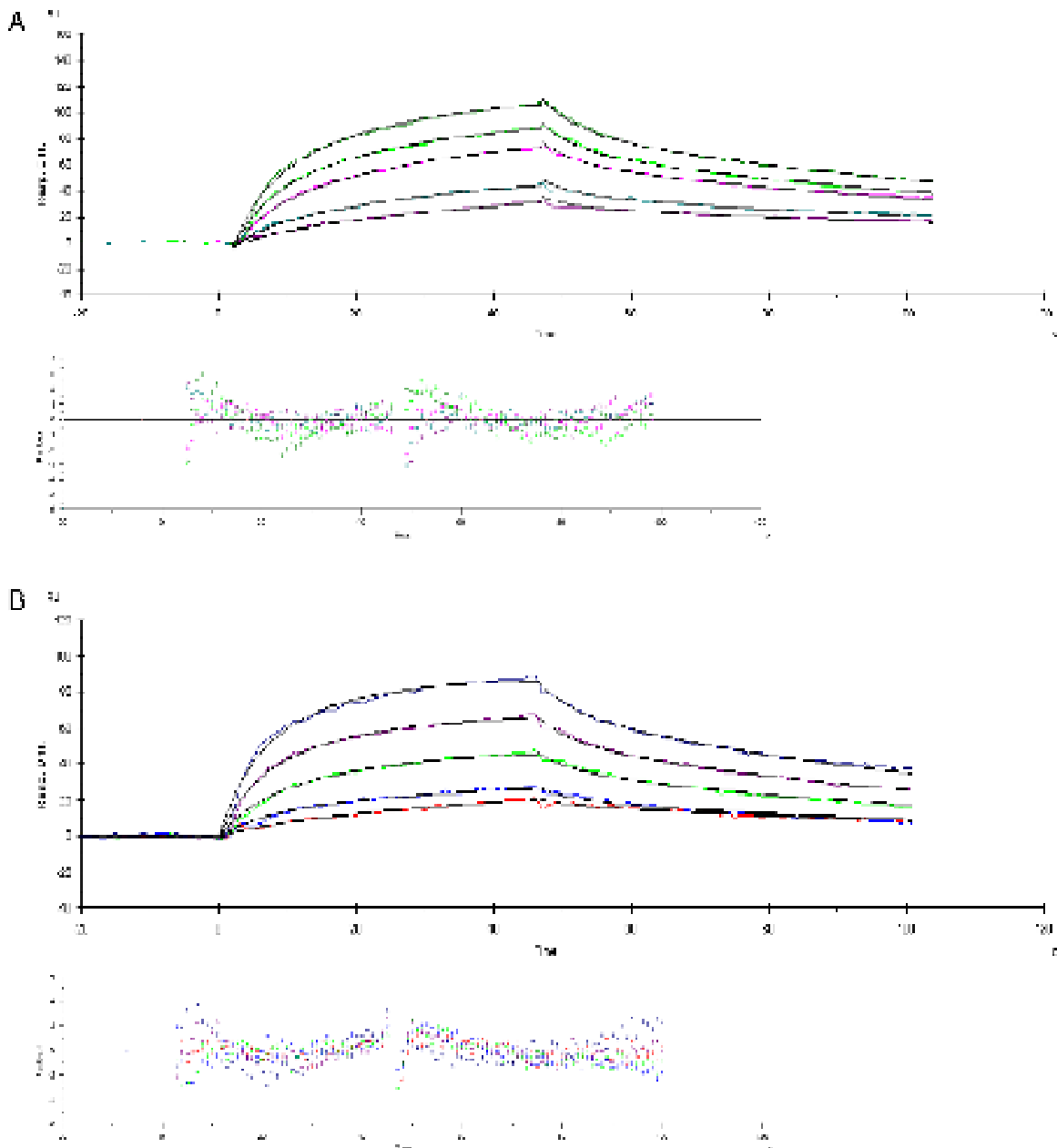


FIGURE 3.5: SURFACE PLASMON RESONANCE ANALYSIS OF NEIL1 DNA BINDING. NEIL1 binding to undamaged 11-nt bubble DNA ligand attached to the sensor chip was determined using a Biacore X. Various concentration of NEIL1 (0.125 – 2 nM) alone or together with PCNA (0.5 μ M) in the analyte was passed over the sensor chip at 20 μ l/min. A, NEIL1 alone. B, NEIL1 with PCNA. The distribution of residuals is given below the isotherms.

Mammalian two-hybrid analysis for in vivo NEIL1-PCNA interaction

Using a mammalian two-hybrid assay system, we analyzed the *in vivo* interaction between NEIL1 and PCNA (Figure 3.6). A major advantage of this system is that, unlike with *E. coli* or yeast two-hybrid systems, interaction among proteins occurs in the native environment where these interacting partners could be covalently modified. In this system, the GAL4 DNA binding domain fused to NEIL1 (pCMV-NEIL1_{BD}) binds to its cognate site in the GAL4 containing promoter, thus directly recruiting NEIL1 to the promoter. A functional transcriptional activator is created by bringing the NF- κ B activation domain that is fused to PCNA (pCMV-PCNA_{AD}) in close proximity to the GAL4 binding domain which is accomplished when NEIL1 interacts with PCNA. HCT116 cells were co-transfected with these plasmids. Simultaneous expression of pCMV-NEIL1_{BD} and pCMV-PCNA_{AD} enhanced luciferase reporter activity by over 7-fold compared to expression of GAL4 (pCMV-GAL4) alone (Figure 3.6, lane 1 vs. 4). Although, the modest stimulation could be explained by the competition of ectopic PCNA with the endogenous protein. No increase in luciferase activity was observed when either pCMV-NEIL1_{BD} or pCMV-PCNA_{AD} was transfected alone (Figure 3.6, lanes 2 and 3). These results further confirm that NEIL1 and PCNA interact *in vivo*.

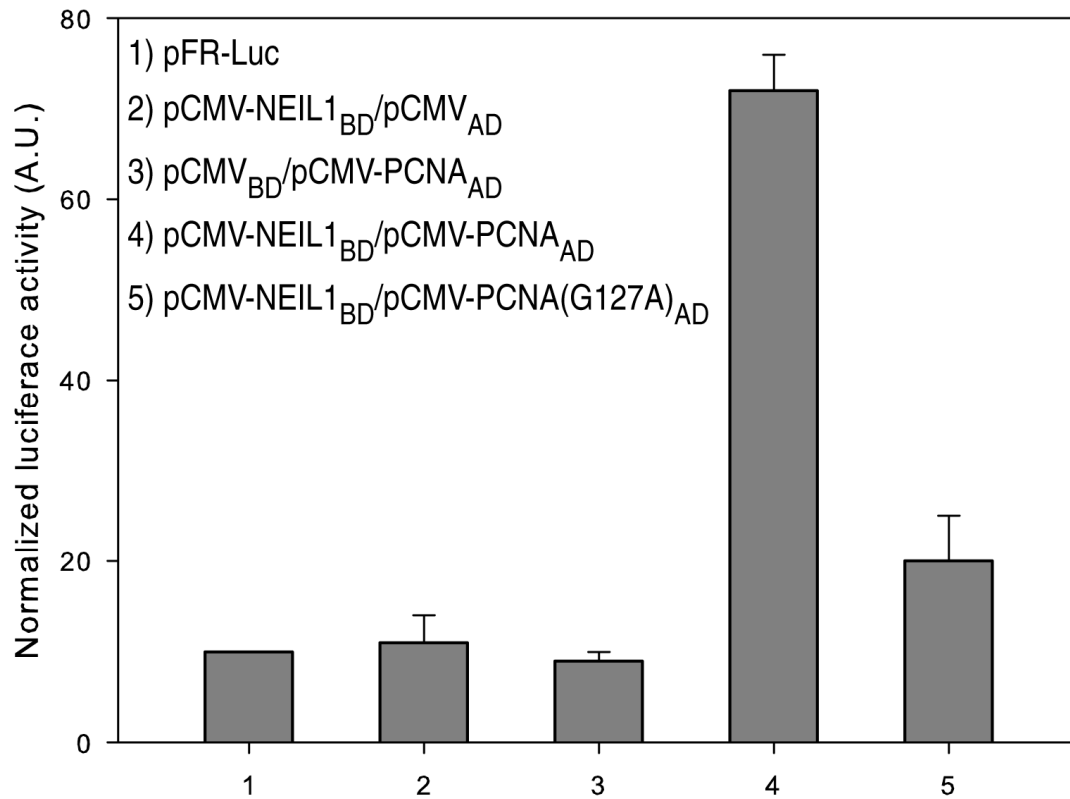


FIGURE 3.6: MAMMALIAN TWO-HYBRID ASSAY OF NEIL1-PCNA INTERACTION. HCT116 cells were transfected with a promoter-reporter plasmid (pFR-Luc; 0.75 μ g) alone (lane 1) or cotransfected with separate expression plasmids (0.2 μ g each) containing the binding domain fused to NEIL1 and the activation domain alone (lane 2) or the binding domain alone and the activation domain fused to PCNA (lane 3) as described in Experimental Procedures. Cotransfection with fusion plasmids for NEIL1 and PCNA as in lanes 2 and 3 (lane 4); with fusion plasmids for NEIL1 (KA mutant) and PCNA (lane 5); or with fusion plasmids for NEIL1 and PCNA (G127A mutant) (lane 6). Luciferase activity was measured at 48h after transfection and normalized with coexpressed galactosidase activity.

NEIL1 interacts with the interdomain connector loop of human PCNA

Because of our characterization that the PCNA interacting sequence is located in the unconserved C-terminal region of NEIL1, we analyzed the NEIL1 sequence for the canonical PCNA-interacting sequence (PIP-box) present in many PCNA partners. However, such a motif is absent in NEIL1, on the other hand, we have identified a sequence which is nearly identical to the N4 region present in the 125 kD subunit of mammalian Pol δ (Zhang *et al.* 1995). The alignment of NEIL1 residues (296-311) with the N4 region of the 125 kD subunit of Pol δ as shown in Table 3.3, demonstrating sequence conservation between the two, specifically the KATQ sequence. Mutation of the KA in this sequence lead to significant decrease in the interaction between NEIL1 and PCNA as indicated by mammalian two-hybrid analysis (Figure 3.6, lane 5).

RAT Polδ	R A E K K A T L C Q L E V D V L
HAMSTER Polδ	R T E K K A T Q C Q L E V D V L
Human Polδ	R L K E K A T Q C Q L E A D V L
Human NEIL1	296 K K K S K A T Q L S P E D R V E₃₁₁
	: * * * * . * *

Table 3.2: Conserved KA-containing sequences in mammalian Pol δ and human NEIL1.

A loop structure in PCNA corresponding to residues 121 to 132 connects the N-terminal and C-terminal domains in a PCNA monomer. This sequence called the interdomain connector loop, is involved in PCNA's direct interaction with many proteins including human Pol δ (Zhang *et al.* 1998). Site-directed mutagenesis of a single amino acid residue G127 to A in this loop of PCNA significantly reduced this interaction

(Zhang *et al.* 1998). We observed that the G127A mutant significantly reduced the affinity of NEIL1 for PCNA using the mammalian two-hybrid assay (Figure 3.6, lane 6). This suggests that the interdomain connector loop of PCNA is important for interaction with residues 296-311 in the C-terminus of NEIL1.

G127A mutation in the interdomain connector loop of human PCNA diminishes stimulation of NEIL1

We then examined whether reduced interaction between NEIL1 and the PCNA G127A mutant affected PCNA's stimulating function. Using EMSA, we observed that the G127A mutant did not significantly enhance NEIL1's affinity for the fork DNA substrate unlike WT PCNA (Figure 3.7 A & B). Furthermore, the PCNA G127A mutant did not stimulate NEIL1's base excision activity with the 3' fork DNA substrate to the same level as an equimolar level of WT PCNA (Figure 3.7C, lanes 3 and 4). However, 10-fold excess of the mutant could restore NEIL1 stimulation near to the same level as WT PCNA (Figure 3.7C, lane 5). These results are consistent with our conclusion that the interaction of the interdomain connector loop of PCNA with the C-terminus of NEIL1 stimulates loading of NEIL1 onto the substrate thus stimulating its activity.

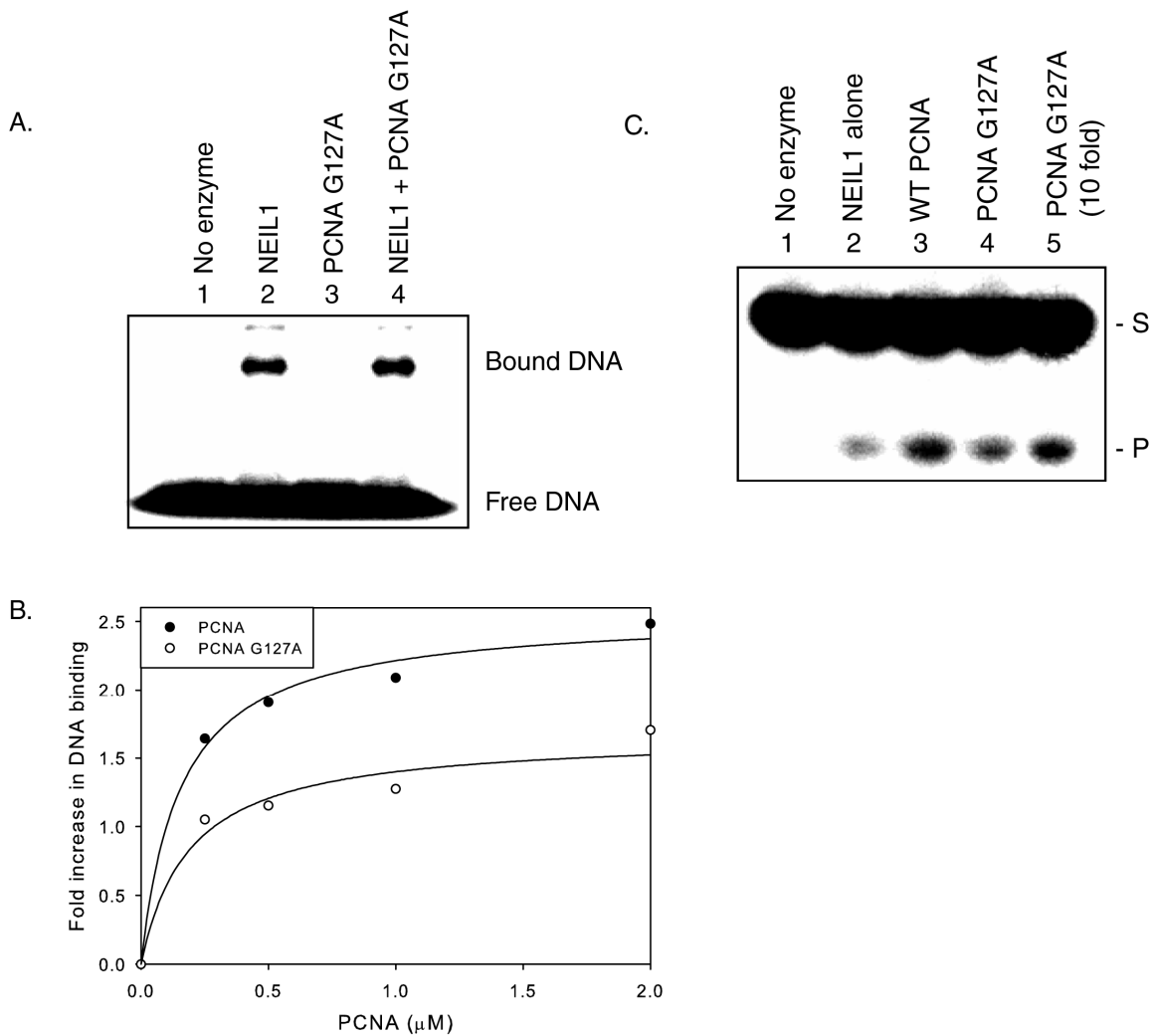


FIGURE 3.7: REDUCED STIMULATION OF NEIL1 WITH PCNA G127A MUTANT. A. EMSA with no enzyme (lane 1), NEIL1 (5 nM) alone (lane 2), PCNA G127A (0.2 μM) alone (lane 3), or NEIL1 in the presence of PCNA G127A (lane 4) binding to undamaged 3' fork DNA oligo (150 fmol). B. Binding of NEIL1 (1 nM) to undamaged 3' fork DNA in the presence increasing concentration of PCNA or PCNA. C. NEIL1 activity on the 5-OHU-containing 3' fork substrate (25 nM); NEIL1 (3 nM) alone (lane 2) or in the presence of 0.5 μM WT PCNA (lane 3) and PCNA G127A (lane 4) or 10-fold higher (5 μM) of G127A PCNA mutant (lane 5). S and P indicate 3' ³²P-labeled uncleaved oligo substrate and β,δ-elimination product, respectively.

DISCUSSION

Our previous observation that NEIL1 is cell cycle regulated, strongly suggested that NEIL1 has a unique role in repair of replicating DNA and that it may have functional interactions with proteins of the replication machinery. This was further supported by our results in Chapter II. We show here that: (1) PCNA preferentially stimulates NEIL1 with single-stranded or fork DNA substrates, and (2) NEIL2 is also active on ssDNA substrates and its immunocomplex contains PCNA, but is not stimulated by PCNA. NTH1, another oxidized base-specific DNA glycosylase was also shown to interact with PCNA but without activation (Oyama *et al.* 2004). Two other DNA glycosylases, namely, uracil-DNA glycosylase (UNG2) and 8-oxoG•A specific adenine-DNA glycosylase (MYH) were also shown to be stimulated by PCNA (Lu *et al.* 2006). UNG2 was suggested to have a preferential activity on repairing misincorporated U in nascent DNA (Otterlei *et al.* 1999). A recent study documented the presence of many replicative proteins in the UNG2 immunocomplex (Parlanti *et al.* 2007). MYH is similarly responsible for removing misincorporated A, opposite 8-oxoG in the template strand (Boldogh *et al.* 2001). This provides an opportunity to prevent mutation due to unrepaired 8-oxoG in the template DNA. Thus repair by UNG2 and MYH should be nascent strand-specific and further supports replication-associated BER (Hazra *et al.* 1998).

Many PCNA partners including MYH and UNG2 interact via the consensus PIP motif (Matsumoto 2001; Helt *et al.* 2005). In the case of the NEIL1 polypeptide lacking this motif, we have identified the interacting domain to be in the C-terminus which contains a sequence not entirely conserved in mammalian NEIL1 but conserved in mammalian Pol δ (Zhang *et al.* 1995). The interaction involving this region appears to be weaker than that for the PIP motif. Although the PIP motif was the first to be discovered

for the PCNA binding interface, it now appears, consistent with the plethora of PCNA's interacting partners, that other peptide sequences are also involved in binding to this sliding clamp (Warbrick 2000). For example, the human translesion synthesis DNA polymerase lambda lacks the PIP motif but binds to PCNA (Shimazaki *et al.* 2002). On the other hand, a sequence in the interdomain linker region of PCNA appears to be the common interacting interface for its partners (Warbrick 2000). We confirmed that this region containing Gly127 is also involved in interaction with NEIL1 because the G127A mutant showed reduction in binding to and activating NEIL1 with a fork substrate.

The PCNA sliding clamp lacking affinity for DNA is loaded in topologically constrained duplex DNA by the clamp loader RFC. In studies using linear duplex DNA with unblocked termini, RFC was not shown to be required for loading PCNA which could presumably slide on and off DNA using the ends. PCNA could thus maintain a steady state equilibrium between the free and sliding fractions, when present in excess. However, it is interesting that we observed the presence of RFC along with PCNA in the NEIL1 immunocomplex and showed that NEIL1 has direct interaction with the clamp loader as well (Chapter II).

Most studies of base damages imply that their repair occurs in regions of the genome consisting of only the duplex form. Such repair involves either single nucleotide incorporation in the short patch BER pathway or long patch repair synthesis by using PCNA and FEN1 together with Pol δ and Lig 1. Earlier studies confirmed the possibility of LP-BER *in vitro* for repair of synthetic or reduced AP sites which could not be repaired via Pol β -dependent short patch BER (Klungland and Lindahl 1997; Kim *et al.* 1998). APE1 cleaves AP sites, as well as its reduced form or tetrahydrofuran which mimics the AP site (Wilson *et al.* 1995). Interaction of APE1 with PCNA is consistent with the involvement of PCNA in long patch BER (Dianova *et al.* 2001). More recent

studies showed that long patch BER could also be mediated by Pol β where FEN1 could remove the 5' terminal region instead of the β lyase activity of Pol β (Podlutzky *et al.* 2001). Stable interaction of Pol β with FEN1 and PCNA strongly suggests that LP-BER could be mediated by either Pol β or Pol δ while short patch BER uniquely requires Pol β . We have earlier shown that NEIL1 stably interacts with Pol β as well as XRCC1 and Ligase III α to carry out short patch BER (Wiederhold *et al.* 2004). Our observation in this study of the interaction between NEIL1 with PCNA suggests that NEIL1 may also be involved in APE1-independent LP-BER, presumably concurrent with DNA replication.

CHAPTER IV

NEIL1 Interacts With The Checkpoint Activated 9-1-1 Clamp Complex

INTRODUCTION

Repair of ionizing radiation and UV-induced DNA damage is coordinated with cell-cycle progression and DNA-damage checkpoints (Bartek *et al.* 2004; Sancar *et al.* 2004). Checkpoints are activated upon DNA damage in order to arrest cell cycle progression and to enhance DNA repair or to induce apoptosis caused by excessive DNA damage. The loss of proper response to DNA damage can lead to genomic instability, and has been implicated in carcinogenesis. This activation requires the action of DNA-damage sensors and transducers, and effectors (Zhou and Elledge 2000). Among these, Rad9, Rad1, and Hus1 form a heterotrimeric complex (the 9-1-1 complex) that exhibits structural similarity with the homotrimeric PCNA sliding clamp (Venclovas and Thelen 2000; Burtelow *et al.* 2001; Shiomi *et al.* 2002). The 9-1-1 complex is loaded onto DNA by an alternative clamp loader Rad17/RFC2-5 (Bermudez *et al.* 2003; Ellison and Stillman 2003; Majka and Burgers 2003). Moreover, the 9-1-1 complex, Rad17/RFC2-5 and PCNA co-localize in foci formed upon DNA double-strand breaks and upon replication block in late S-phase (Dahm and Hubscher 2002; Meister *et al.* 2003). These data suggest a mechanism in which Rad17/RFC2-5 localizes to DNA lesions, allowing the recruitment of the 9-1-1 complex to these sites. Subsequently, the 9-1-1 complex serves as a recruitment platform for the checkpoint effectors kinase such as Chk1 or Chk2, which are subsequently phosphorylated by ATM or ATR. Additionally, a model has recently been proposed by two different groups, where the 9-1-1 complex and the

Rad17/RFC2-5 clamp loader could stabilize stalled replication forks (Ellison and Stillman 2003; Zou *et al.* 2003).

The link between checkpoint activation and recruitment of repair machineries to DNA lesions has been demonstrated through interaction and co-localization of checkpoint sensors with proteins involved in multiple DNA-repair processes upon DNA damage (Kai and Wang 2003; Meister *et al.* 2003; Giannattasio *et al.* 2004). However, the mechanism by which the sensor checkpoint proteins detect different types of DNA lesions remains elusive. It has been suggested that the checkpoint proteins may detect a common intermediate, such as single-stranded DNA coated by RPA (Zou and Elledge 2003). RPA has been shown to directly interact with the 9-1-1 complex (Wu *et al.* 2005). Recently, several reports support a hypothesis that checkpoint proteins may require a series of “adaptors” to recognize DNA damage (Wang, and Qin 2003; Giannattasio *et al.* 2004; Lavin 2004; Yoshioka *et al.* 2006). Such adaptor proteins may be the DNA damage recognition proteins involved in MMR, NER, BER and double-strand break repair.

Previous studies on 9-1-1 complex activation and activity was carried out in response to double-strand breaks and large bulky adducts that activate DSB repair and NER pathways. Only recently have investigations established a link between the human 9-1-1 complex and the BER pathway. It was shown that the 9-1-1 complex physically and functionally interacts with the MutY homologs (MYHs) of *S. pombe* and the human (Chang and Lu 2005; Shi *et al.* 2006). The 9-1-1 complex has also been shown to interact with and stimulate other BER enzymes, which include Pol β (Touelle *et al.* 2004), FEN1 (Wang, *et al.* 2004; Friedrich-Heineken *et al.* 2005), and DNA ligase 1 (Smirnova *et al.* 2005; Wang, *et al.* 2006). The potential involvement of NEIL1 in replication-associated repair like MYH lead us to hypothesize that the 9-1-1 complex also

interacts with NEIL1 and that this interaction has functional relevance in much the same manner as PCNA with NEIL1 (Hazra *et al.* 1998; Lu and Fawcett 1998). 9-1-1 would essentially replace PCNA as the sliding clamp in NEIL1-initiated repair when PCNA is inhibited by p21 upon cell cycle arrest.

MATERIALS AND METHODS

Human cell culture: The human HeLa S3 cell line was purchased from American Type Cell Culture (ATCC). HeLa cells were cultured in Dulbecco's modified Eagle medium (DMEM) supplemented with 10% FBS. At 90% confluence, cells were transfected with NEIL1-FLAG using Fugene 6 (Roche). The cells were replanted at 24 h after the transfection. Cell extracts were prepared as described (Parker *et al.* 2001; Gu *et al.* 2002).

Construction and expression of hRad9, hRad1 and hHus1 in E. coli: The cDNA of Hus1, Rad1 and Rad9 were amplified by PCR from GST-Rad9, GST-Rad1 and GST-Hus1 plasmids. The sequences of forward and reverse primers for these PCR reactions are given in Table 4.1. The Hus1 gene was cloned between the BamH1 and Not1 sites of pET-21a (EMD Biosciences) to obtain the clone pET21a-Hus1 as described (Shi *et al.* 2006). The Rad9 gene was cloned between the BglIII and XhoI sites of pACYCDuet-1 (EMD Biosciences) to obtain the clone pACYCD-Rad9. The Rad1 gene was cloned between the BamH1 and Sall sites of pACYCD-Rad9 to obtain pACYCD-Rad1-Rad9. The Hus1, Rad1, and Rad9 proteins were tagged with a C-terminal His, N-terminal His, and C-terminal S-tag, respectively.

The BL21 Star cells (Stratagene, La Jolla, CA, USA) harboring the expression plasmids, pET21a-Hus1 and pACYCD-Rad1-Rad9, were cultured in LB broth containing 100 µg/ml of ampicillin and 50 µg/ml of chloramphenicol at 37°C. Protein expression

was induced at an A590 of 0.6 by the addition of IPTG to a final concentration of 0.2 mM and the cells were grown at 20°C and then harvested 16 h later.

Name	Sequence	Purpose
hHus1-5-Bam	5'-GATCGCGGATCCATGAAGTTTCGGGCCAAGATC-3'	5' primer of hHus1 in pET-21a
hHus1-3-Not	5'-TCGAGTGCGGCGCGGACAGCGCAGGGATGAAATA-3'	3' primer of hHus1 in pET-21a
hRad1-F	5'-GAGGATCCGATGCCCGTTGTGACC-3'	5' primer of hRad1 in pACYCDuet-1
hRad1-R	5'-GACCBTCGACTCATACTCAABACTCAG-3'	3' primer of hRad1 in pACYCDuet-1
hRad9-F	5'-GGTAGATCTCATGAAGTGCCTGGTC-3'	5' primer of hRad9 in pACYCDuet-1
hRad9-R	5'-GACTCGAGGCCCTCAGCCGTCACTG-3'	3' primer of hRad9 in pACYCDuet-1

Table 4.1: Sequences of primers used for 9-1-1 PCR reactions.

Expression and purification of Rad9, Rad1, Hus1 and the 9-1-1 complex in baculovirus system: The Sf9 insect cells (Invitrogen, Princeton, NJ, USA) were grown in 80 ml of Sf-900 II SFM complete medium (GIBCO/BRL) in suspension to 3×10^6 cells/ml and then infected with baculovirus vectors containing cDNA encoding FLAG-Rad9 (obtained from Dr Alan Tomkinson), FLAG-Rad1 (obtained from Dr Aziz Sancar), or FLAG-Hus1 (obtained from Dr Aziz Sancar) and supplemented with 0.2% FBS. For expression of the 9-1-1 complex, 500 ml culture of the Sf9 insect cells were co-infected with a mixture of three viruses carrying cDNA encoding Rad9, Rad1 and Hus1. About 48 h after infection, the cells were harvested by centrifuge at 1500 x g for 2 min. The cell pellets were lysed in 10 times the cell volume of a lysis buffer [(50 mM Tris-HCl, pH 7.5, 0.5% Nonidet P-40, 0.3 M NaCl, and 0.1 mM phenylmethylsulfonyl fluoride (PMSF)] and incubated on ice for 15 min before centrifugation for 30 min at 32 000 x g. The supernatants were incubated with 1 ml (for the 9-1-1 complex) or 0.5 ml (for each subunit) of 50% slurry of Anti-FLAG M2 Affinity Gel (Sigma) at 4°C overnight. The

resin was then washed four times with lysis buffer and the proteins were eluted with 1 ml (for h9-1-1 complex) or 0.45 ml (for each subunit) elution buffer [50 mM Tris-HCl, pH 7.5, 0.05% Nonidet P-40, 0.3 M NaCl, 0.1 mM PMSF and 200 µg/ml FLAG peptide (Sigma)]. FLAG-Rad9, FLAG-Rad1 and FLAG-Hus1 were dialyzed against lysis buffer without Nonidet P-40 and stored at -80°C. The 9-1-1 complex was further purified by a Sepharose-12 gel filtration column (GE Health) with a buffer containing 20 mM KPO₄, pH 7.4, 0.1 mM EDTA, 0.2 M KCl, 10% glycerol, 0.5 mM dithiothreitol (DTT), 0.1 mM PMSF. By comparison to the size markers (bovine thyroglobin, apoferritin, β-amylase, and bovine serum albumin), the 9-1-1 complex eluted in a position corresponding to a mass of about 120 kDa, which is in line with the predicted molecular mass (110 kDa) of the heterotrimeric complex.

Other proteins used: Untagged NEIL1 and deletion constructs were purified as described (Hazra *et al.* 2002; Hazra and Mitra 2006). His-tagged NEIL1 was expressed and purified as described (Hazra *et al.* 2002; Hazra and Mitra 2006).

GST pull-down assay: The BL21 Star cells (Stratagene) harbouring the GST expression plasmids were cultured in LB broth containing ampicillin (100 µg/ml). Protein expression was induced as described above. The cell paste, from a 500 ml culture, was resuspended in 9 ml of buffer G (50 mM Tris-HCl, pH 7.4, 150 mM NaCl and 2 mM EDTA) containing 0.5 mM DTT and 0.1 mM PMSF and treated with lysozyme (1 mg/ml) for 30 min at 4°C. After sonication, the solution was centrifuged at 10 000 x g for 20 min and the supernatant was saved. The GST-tagged proteins were immobilized on glutathione-sepharose 4B (GE Health) as described earlier (Parker *et al.* 2001). GST fusion proteins (500 ng) were incubated with purified protein or cell extracts in 0.2 ml volume at 4°C with shaking overnight. After centrifugation at 1000 x g for 2 min, the pellets were washed five times with 1 ml of buffer G containing Nonidet P-40. Bound

proteins were eluted by boiling in SDS loading buffer and resolved by 12% SDS-PAGE. The proteins were subsequently analyzed by Western blot using the corresponding antibodies according to established methods.

Ni-affinity binding: His-Select (Sigma) magnetic beads (20 μ l suspension) were washed once with water, equilibrated with binding buffer (50 mM Tris-HCl, pH 7.5, 200 mM NaCl, 10 mM imidazole), and then incubated with His-tagged Hus1 (500 ng) in binding buffer for 1 h at 4°C with gentle rocking. After pelleting using a magnetic separator the beads were washed three times with binding buffer and then equilibrated with interaction buffer (50 mM Tris-HCl, pH 7.5, 400 mM NaCl, 10 mM imidazole). Wild-type or mutant NEIL1 (250 ng) was incubated with the beads for 2 h at 4°C with gently rocking, pelleted and washed three times with final wash buffer (50 mM Tris-HCl, pH 7.5, 500 mM NaCl, 10 mM imidazole). The NEIL1/Hus1 complex was eluted with 20 μ l of SDS loading buffer and resolved by 12% SDS-PAGE. The presence of NEIL1 was examined by immunoblot analysis using NEIL1 antibodies.

Far Western analysis: Wild-type and mutant NEIL1 were treated as described earlier (Chapter II) and incubated with 10 pmol/ml of his-tagged Hus1 in blocking solution containing 1 mM DTT and 100 mM TMAO for 3 h at 4°C. Subsequent Western blotting was performed using α -His-tag antibody followed by α -Rabbit IgG HRP-conjugated secondary antibody (Amersham Biosciences, Piscataway, NJ).

Co-immunoprecipitation: Extracts of HeLa cells expressing NEIL1-FLAG were precleared by adding 30 μ l Protein G agarose (Invitrogen) for 1–4 h at 4°C. After centrifugation at 1000 x g, the supernatant was incubated with 4 μ g of polyclonal α -FLAG or α -His overnight at 4°C. Protein G agarose (30 μ l) was added and incubated for 4–12 h at 4°C. After centrifugation at 1000 x g, the supernatant was saved and the pellet

was washed. Both the supernatant (~10% of total volume) and pellet fractions were resolved on a 12% SDS-PAGE and Western blot analysis for Rad9 was performed.

NEIL1 glycosylase activity assay: The sequence of the 54-mer duplex DNA substrate containing Tg for the NEIL1 activity assay is given in Table 4.1. The Tg-containing strand was labeled and annealed with the complementary strand as described before (Lu *et al.* 1995). The NEIL1 assay mixture (10 μ l) contained 2.5 mM HEPES (pH 7.8), 1 mM DTT, 2.5% glycerol, 50 mM KCl, 50 μ g/ml bovine serum albumin, 0.5 mM EDTA and 1.8 fmol oligo. The Hus1 or 9-1-1 complex was added immediately after NEIL1 for incubation at 37°C for 30 min. The NEIL1 reaction was stopped and the gel imaged as described earlier (Chapter III). The area at the product position in the no protein control lane was used to subtract out the background signal. The NEIL1 cleavage activity was calculated by the percentage of product over total DNA (product plus substrate).

Name	Sequence
Tg-54	5'-ATTCCAGACTGTCAATAACACGG <u>Tg</u> GGACCAGTC GATCCTGGGCTGCAGGAATTC-3'
A-54	5'-GAATTCCTGCAGCCAGGATCGACTGGTCC <u>A</u> GTGT TATTGACAGTCTGGAAT-3'

^a Mismatched base is underlined. Tg represents thymine glycol.

Table 4.2: Sequences of thymine glycol containing oligodeoxynucleotides.

RESULTS

The human 9-1-1 complex interacts with NEIL1

It was previously shown that the Rad9/Rad1/Hus1 heterotrimer interacts with MYH in *S. pombe* and human cells (Chang and Lu 2005; Shi *et al.* 2006). To determine whether the 9-1-1 complex interacts with other DNA glycosylases, we tested NEIL1 because it is also involved in the oxidative stress response. We used the GST pull-down assay to show the physical interactions of NEIL1 with Rad9, Hus1 and Rad1. GST-Hus1, GST-Rad1, or GST-Rad9 fusion protein bound to glutathione-Sepharose was incubated with purified NEIL1. As shown in Figure 4.1A, NEIL1 can be pulled down by GST-Hus1, GST-Rad1 and GST-Rad9. As a negative control, NEIL1 did not bind to GST alone (lane 5). In reciprocal experiments, GST-NEIL1 fusion protein bound to glutathione-Sepharose could pull down Rad9, Rad1 and Hus1 expressed in the baculovirus-transfected insect cells (Figure 4.1B). Both phosphorylated and unphosphorylated Rad9 interact with NEIL1 (Figure 4.1B, lane 2). Thus, NEIL1 binds to all three subunits of the 9-1-1 complex. The individual proteins used in Figure 4.1A, B were expressed separately in *E. coli* or insect cells; thus, NEIL1 can interact with Hus1, Rad1 and Rad9 binarily and individually. In addition, we incubated immobilized GST-NEIL1 fusion protein and pulled down all three subunits of the partially purified 9-1-1 complex expressed in *E. coli* (Figure 4.1C, lane 2). In addition, the physical interaction between NEIL1 and Hus1 is further demonstrated in Figure 4.2.

The interaction between NEIL1 and the 9-1-1 complex was also demonstrated by co-immunoprecipitation. We used FLAG antibody to co-immunoprecipitate Rad9 from extracts derived from HeLa S3 cells being transfected with NEIL1-FLAG expressing

plasmid. Rad9 can be immunoprecipitated from extracts derived from HeLa cells expressing FLAG-tagged NEIL1 (Figure 4.1D, lane 2).

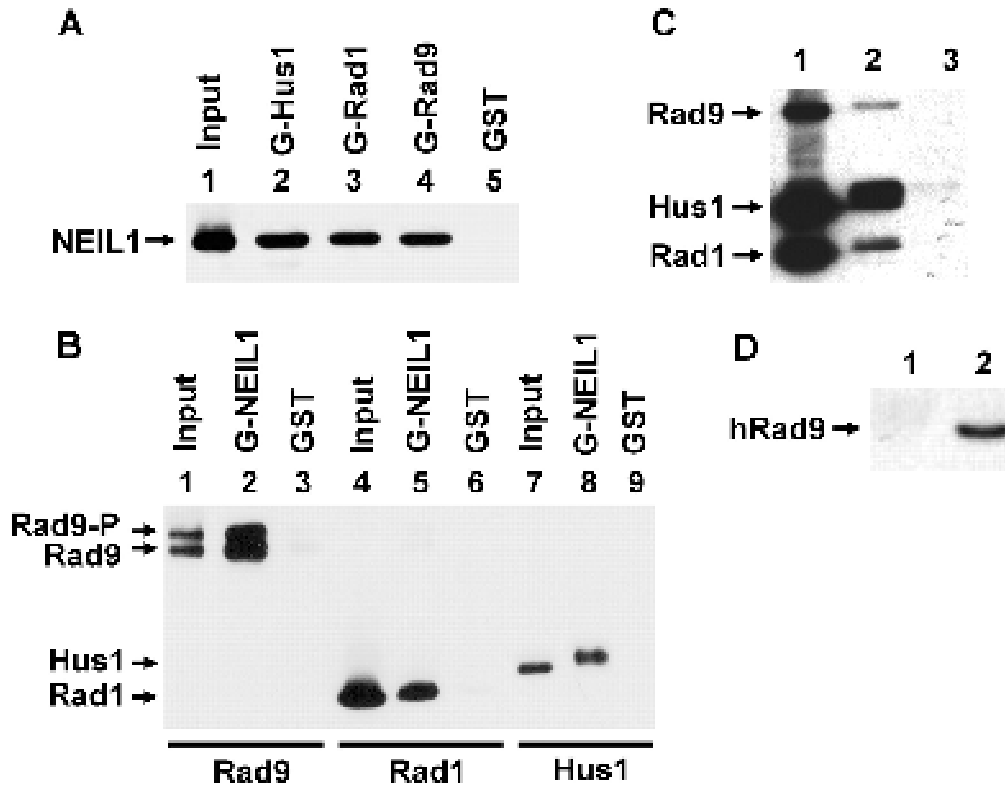


FIGURE 4.1: PHYSICAL INTERACTION BETWEEN NEIL1 AND THE 9-1-1 COMPLEX. A. NEIL1 binds to subunits of the 9-1-1 complex. GST-Hus1 (lane 2), GST-Rad1 (lane 3), GST-Rad9 (lane 4), and GST alone (lane 5) were immobilized and incubated with NEIL1 (100 ng) then separated by 10% SDS-PAGE and Western blotted for NEIL1. Lane 1 - 30 ng (30% of the total input) of NEIL1. B. Binding of Rad9, Rad1, and Hus1 to GST-NEIL1. GST-tagged NEIL1 (lanes 2, 5, and 8) or GST beads (lanes 3, 6, and 9) were incubated with Rad9, Rad1, or Hus1 (300 ng). The pellets were separated by 10% SDS-PAGE followed by Western blot analysis for FLAG. Lanes 1, 4, and 7 contain 10 ng (10% of the total input) of Rad9, Rad1, and Hus1, respectively. C. Binding of the 9-1-1 complex to GST-NEIL1. GST-tagged NEIL1 (lane 2) or GST beads (lane 3) were incubated with the partially purified 9-1-1 complex (300 ng). The Hus1, Rad1, and Rad9 proteins were tagged with a C-terminal His, N-terminal His, and C-terminal S-tag, respectively. Lane 1 contains 90 ng (30% of the total input) of the partially purified 9-1-1 complex. The Western blot was detected by a mixture of the antibodies against His-tag and S-tag. D. Coimmunoprecipitation of Rad9 with FLAG-tagged NEIL1. HeLa cell extracts expressing NEIL1-FLAG were immunoprecipitated using α -FLAG and Western blotted for the presence of Rad9 (lane 2). Lane 1 is a negative control using a His-tag antibody.

Mapping the 9-1-1 interacting domain within NEIL1

By using truncated NEIL1 proteins, we mapped NEIL1's domain for the physical interaction with the 9-1-1 complex. The results are shown in Figure 4.2A–C and summarized in Figure 4.2D. In Figure 4.2A, immobilized GST-Hus1, GST-Rad1 and GST-Rad9 proteins were incubated with 100 ng each of wild type NEIL1 or C Δ 40 (residues 1–349) and C Δ 101 (residues 1–288). The NEIL-C Δ 40 construct retained interactions with Hus1, Rad1 and Rad9; however, the C Δ 101 construct exhibited no interaction with the 9-1-1 complex. Ni affinity binding (Figure 4.2B) and Far-western analysis (Figure 4.2C) further confirmed that each subunit of the complex interacted with the C Δ 40 but not with the C Δ 101 deletion protein. Thus, residues 288–349 of NEIL1 are essential for its interaction with the 9-1-1 complex (Figure 4.2D).

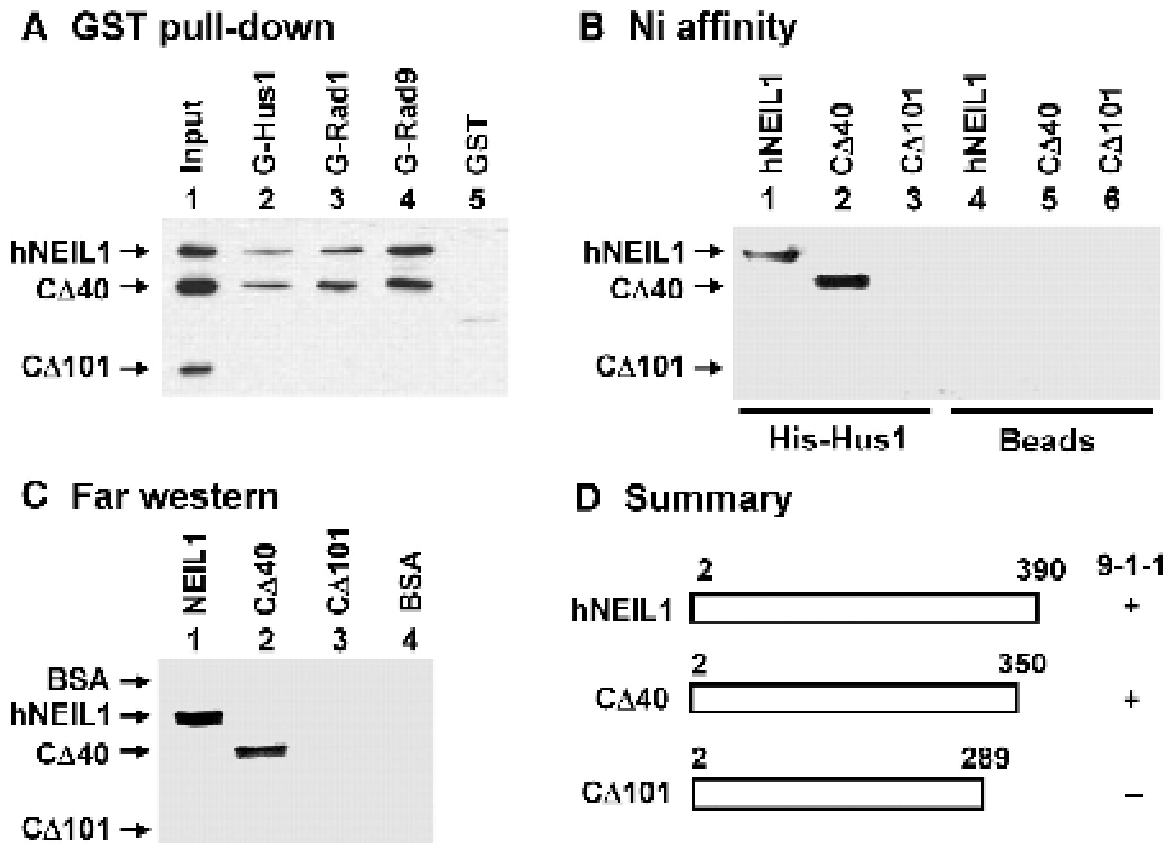


FIGURE 4.2: DETERMINATION OF REGIONS WITHIN NEIL1 INVOLVED IN BINDING TO THE 9-1-1 COMPLEX. A. Binding of NEIL1 deletion mutants to GST-Rad9, GST-Rad1, and GST-Hus1. Immobilized GST-Hus1 (lane 2), GST-Rad1 (lane 3), GST-Rad9 (lane 4), and GST alone (lane 5) were incubated with a mixture of 100 ng NEIL1, NEIL1-CΔ40 and NEIL1-CΔ101. The pellets were fractionated by 10% SDS-PAGE followed by Western blot analysis for NEIL1. Lane 1 contains 30 ng each of NEIL1, NEIL1-CΔ40, and NEIL1-CΔ101 (30% of the total input). B. Binding of NEIL1 deletion mutants to His-tagged Hus1. His-Hus1 bound to beads (lanes 1-3) or beads alone (lanes 4-6) were incubated with wild-type or truncated NEIL1. The presence of NEIL1 was examined by Western analysis against NEIL1. C. Far Western analysis. Wild-type and mutant NEIL1 were separated by 10% SDS-PAGE and transferred onto nitrocellulose membrane. Lane 4 contains BSA. The membrane was probed with His-tagged Hus1 (10 pmol/ml) and Western blotted using His-tag antibody. D. Schematic of NEIL1 constructs and summary of the binding studies with the 9-1-1 complex. The amino acid residues of NEIL1 constructs are indicated.

Colocalization between NEIL1 and 9-1-1

Next, we tested by immunofluorescent staining analyses whether NEIL1 and Rad9 translocate to the same nuclear foci following H₂O₂ treatment. FLAG-NEIL1 appeared granulated in faint spots throughout the nucleus of untreated HeLa cells expressing NEIL1-FLAG (Figure 4.3B). Rad9 molecules, as detected with its polyclonal antibody were distributed in both the nucleus and cytoplasm in untreated cells (Figure 4.3C). A few sites of its nuclear co-localization with NEIL1 were observed in control cells (Figure 4.3D). However, in H₂O₂-treated cells, NEIL1 and Rad9 formed many discrete nuclear foci (Figure 4.3F and G) and the majority of NEIL1 nuclear foci localize with the Rad9 foci (Figure 4.3H). This data support the notion that NEIL1 and the 9-1-1 complex translocate to repair foci following DNA damage.

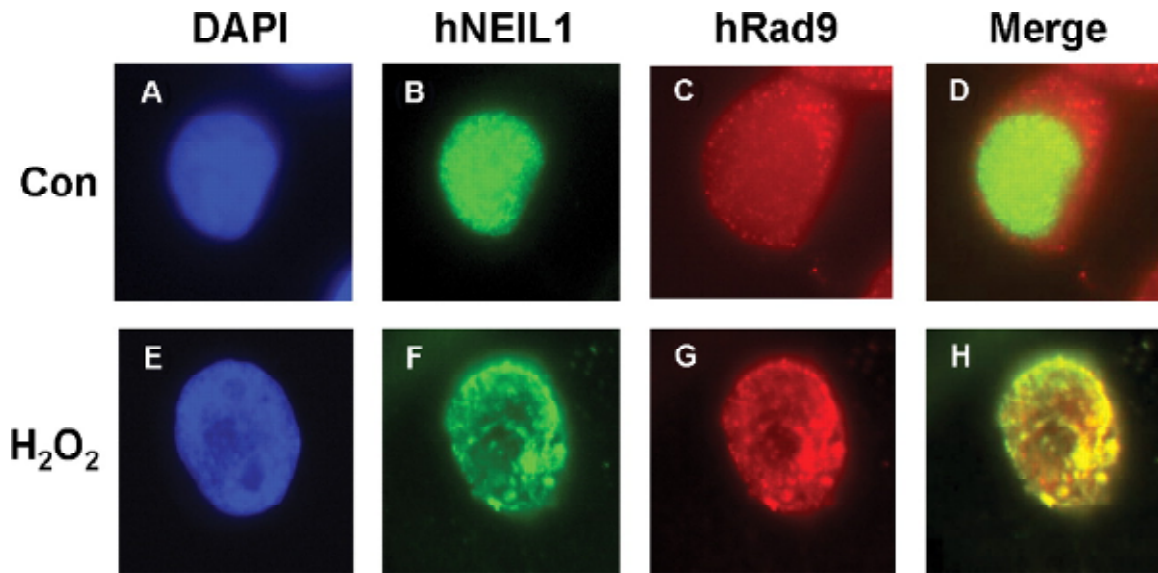


FIGURE 4.3: CO-LOCALIZATION OF NEIL1 WITH RAD9 FOLLOWING OXIDATIVE STRESS. HeLa cells were transiently transfected with NEIL1-FLAG vector. 24 h later, cells were treated with 2 mM H₂O₂ for 40 min and allowed to recover for 1 h (E–H). Control cells were not treated with H₂O₂ (A–D). The cells were stained with antibody against FLAG (Sigma) (green, B and F) and anti-Rad9 antibody (Stratagene) (red, C and G). (A) and (E) are DAPI-stained. (D & H) are the merged images, co-localization of NEIL1 (green) and Rad9 (red) is visualized as yellow.

NEIL1 activity is enhanced by Hus1, Rad1, Rad9 and the 9-1-1 complex

The above results show that NEIL1 physically interacts individually with Hus1, Rad1 and Rad9 and also the 9-1-1 complex. We then tested whether NEIL1's base excision and AP-lyase activities were affected by these proteins. We added increasing amounts of purified Hus1, Rad1, Rad9 and the 9-1-1 complex to the NEIL1 assay mix with Tg oligo as before. As shown in Figure 4.4A (lanes 3–7), NEIL1's strand cleavage activity due to combined glycosylase/AP lyase reactions was significantly enhanced by Hus1 alone. The increase in activity of NEIL1 (1 nM) was 5-fold in the presence of 20 nM of Hus1 (Figure 4.5B, diamonds). Hus1 alone (50 nM) did not have any activity as expected (data not shown). Similar stimulation of NEIL1's strand cleavage activity was observed individually with recombinant Hus1, Rad1, Rad9 alone or the 9-1-1 complex purified from the insect cells (Figure 4.4A–D, lanes 1–6). Interestingly, Hus1, Rad1, Rad9, separately or together in the 9-1-1 complex stimulated NEIL1 activity to comparable levels suggesting that the formation of the 9-1-1 complex does not further enhance stimulation of NEIL1 (Figure 4.5A–D, diamonds).

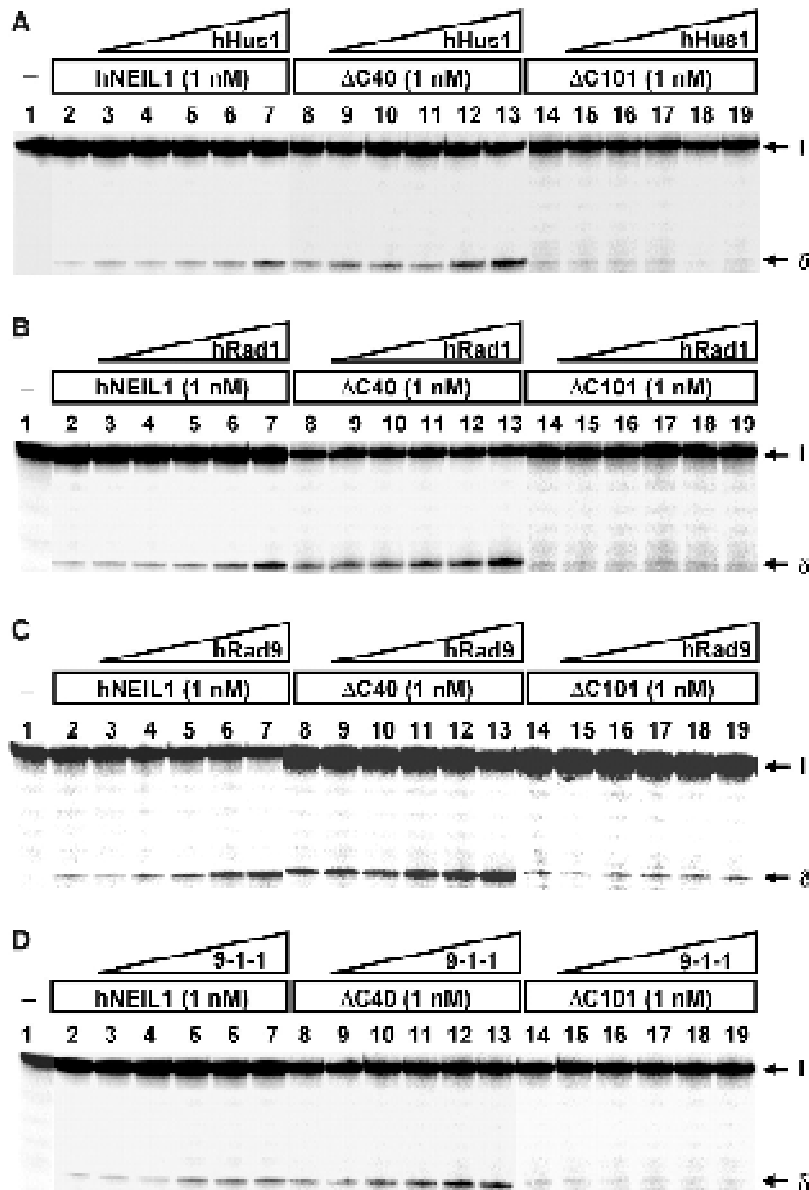


FIGURE 4: NEIL1 ACTIVITY WAS STIMULATED BY HUS1, RAD1, RAD9 AND THE 9-1-1 COMPLEX. Human Hus1 (A.), Rad1 (B.), Rad9 (C.), and the 9-1-1 complex (D.) enhance the activities of full-length NEIL1 and NEIL1-C Δ 40, but not NEIL1-C Δ 101. A. – D., Lane 1, 1.8 fmol (90 pM) of thymine glycol (Tg)/A-containing DNA substrate was incubated with NEIL1 (1 nM). A. – C., Lanes 2-6 are similar to lane 1 but with added 3.125, 6.25, 12.5, 25, and 50 nM Hus1, Rad1, or Rad9, respectively. D., Lanes 2-6 are similar to lane 1 but with added 4, 8, 16, 32, 64 nM of the 9-1-1 complex, respectively. Lanes 7-12 are similar to lane 1-6 except using 1 nM NEIL1-C Δ 40. Lanes 13-18 are similar to lane 1-6 except using 1 nM NEIL1-C Δ 101. The products were separated on a 14% DNA sequencing gel. Arrows mark the intact DNA substrate (I) and the β,δ -elimination product (δ).

Both C-terminal truncated NEIL1, C Δ 40 and C Δ 101 polypeptides, retain the strand cleavage activity on the Tg substrate (Figure 4.4A–D, lanes 2, 8, 14) confirming that NEIL1’s interaction region (residues 289–349) is not essential for its activity. The strand cleavage activity of C Δ 40 could be enhanced by Hus1, Rad1, Rad9 and the 9-1-1 complex (Figure 4.4A–D, lanes 8–13; and Figures 4.3B, 4.5A–D, squares). However, Hus1, Rad1, Rad9 and the 9-1-1 complex could not enhance the activity of the C Δ 101 polypeptide (Figure 4.4A–D, lanes 14–19; and Figures 4.3B, 4.5A–D, triangles). Thus, the 9-1-1 complex enhances the NEIL1 activity through direct physical interaction with the minimal interaction domain containing residues 289-349.

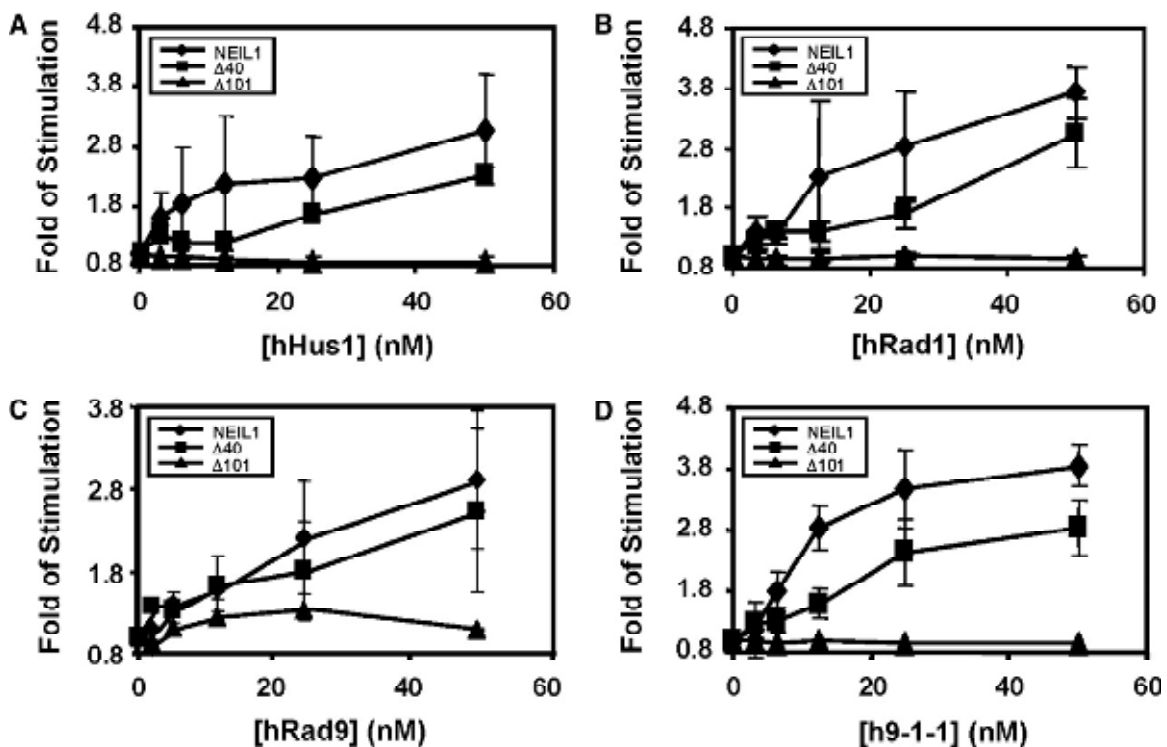


FIGURE 4.5: QUANTITATIVE ANALYSES OF NEIL1 STIMULATION. Fold stimulation of Hus1, Rad1, Rad9 and the 9-1-1 complex expressed in the baculovirus system on processed full-length NEIL1 (diamonds), NEIL1-C Δ 40 (squares), and NEIL1-C Δ 101 (triangles) activities from three experiments.

DISCUSSION

Mammalian cells express an alternative DNA clamp, 9-1-1, linked to ATR-dependent checkpoint activation in response to radiation and other damage during the S-phase (Roos-Mattjus *et al.* 2002; Lupardus and Cimprich 2006). 9-1-1, like PCNA, forms a toroidal structure consisting of Rad 9, Rad 1 and Hus1 (Burtelow *et al.* 2001; Ellison and Stillman 2003). Activation of MYH, Pol β , FEN1 and Ligase 1 by 9-1-1 suggests its role in DNA repair (Wang *et al.* 2004; Shi *et al.* 2006; Gembka *et al.* 2007). We have demonstrated that the NEIL1 DNA glycosylase physically and functionally interacts with Rad9, Rad1, and Hus1 as individual proteins and as a complex. In addition, NEIL1 and 9-1-1 colocalize to a significant extent in cells exposed to H₂O₂. The interacting site of the 9-1-1 complex is localized to the C-terminal domain of NEIL1 as is consistent with previous results demonstrating a region in the C-terminus of NEIL1 to be disordered which functions as the site of protein partner interaction.

We have also shown that the strand cleavage activity of NEIL1 is stimulated by Hus1, Rad1, Rad9, separately and the 9-1-1 complex to a similar extent. Thus, the formation of the 9-1-1 complex is not a prerequisite for NEIL1 stimulation *in vitro* but may be required *in vivo*. Because the functional interaction is parallel with the physical interaction between NEIL1 and the 9-1-1 complex, the 9-1-1 complex stimulates NEIL1 through direct physical contact with NEIL1. Thus, the 9-1-1 complex is not only a DNA damage sensor (Zhou and Elledge 2000) but is also likely involved in the NEIL1-dependent BER pathway, specifically in response to oxidative DNA damage and cell-cycle arrest.

Our mapping analyses indicate that the 9-1-1 complex interacting domain is localized to residues 288–349 of NEIL1. The crystal structure of NEIL1 containing

residues 1–341 has been determined (Doublié *et al.* 2004). However, since there is no defined electron density map beyond residues 290, the region containing residues 290–349 of NEIL1 is likely flexible as modeled in Chapter II. It is possible that this region becomes structured in the presence of the 9-1-1 complex and then this conformational change promotes the catalytic activity of NEIL1.

Our results strongly suggest that the 9-1-1 complex not only serves as a damage sensor to activate checkpoint control, but it is also a component of the NEIL1 BER pathway and may provide a platform for different factors involved in BER. This may be crucial under conditions of stress when p21 is activated, which inactivates PCNA by binding to PCNA's interdomain connector loop with high affinity preventing any other protein from binding. This mechanism effectively blocks DNA replication in response to cell cycle checkpoint activation. In this situation when PCNA is unavailable, 9-1-1 would become the crucial sliding clamp used for DNA repair.

CHAPTER V

Regulation of NEIL1 activity at the Replication Fork

INTRODUCTION

Our previous results showed direct physical interaction of NEIL1 with the sliding clamps PCNA and 9-1-1. Their stimulation of NEIL1 activity further supported our hypothesis of the role NEIL1 has in replication-associated repair. We continued our investigations into NEIL1's role in the replication complex by investigating the interaction with RPA and characterizing the role RPA has in regulating NEIL1's activity. This was a critical interaction to explore because unregulated NEIL1 cleavage of single-stranded template DNA would lead to dangerous double strand breaks and collapse of the replication fork. Not only would replication be unable to continue at that fork but double strand break responses and cell cycle checkpoints would be activated blocking global genome replication and cell division.

RPA is a heterotrimeric single-stranded DNA binding complex representing the major cellular single-stranded DNA binding protein initially identified as an essential factor in SV40 DNA replication and later shown as a critical element of cellular DNA replication (Melendy and Stillman 1993; Iftode *et al.* 1999). RPA functions to protect the exposed template DNA during replication by binding to and coating the DNA (Alani *et al.* 1992). The formation of RPA-DNA filaments also prevents secondary structure formation enhancing replication efficiency (Braun *et al.* 1997). Structural studies of RPA reveal four domains (DNA-binding domains (DBD) A-D) that each independently bind to single-stranded DNA with decreasing affinity from A to D. Three of them (DBD-A, -B and -C) are located in the 70 kDa subunit while the fourth DBD resides within the 32

kDa subunit. These four DBDs bind in a sequential fashion beginning with DBD-A and -B at the 5' end occluding 8-10 nucleotides (de Laat *et al.* 1998; Iftode and Borowiec 2000). Then, through a conformational change DBD-C becomes involved in binding a stretch of 12-23 nucleotides (Bastin-Shanower and Brill 2001). Finally, co-operative binding of all four DBDs results in a fully extended conformation of RPA occluding a stretch of approximately 30 nucleotides (Arunkumar *et al.* 2003; Wyka *et al.* 2003). These three distinct states of binding are thought to coexist and even be modulated through protein-mediated conformational remodeling from extended to compact conformations and vice-versa depending upon binding requirements.

RPA is one of the most abundant cellular proteins present at approximately 100,000 molecules per cell (Wold 1997). RPA interacts with a wide variety of protein partners and participates in various DNA metabolic pathways including DNA replication, repair, recombination and damage checkpoints (Zou *et al.* 2006). An understanding of the multiple roles that RPA plays and how it functions in processes other than DNA replication is now slowly unraveling. One hypothesis is that RPA is a central component because of its binding to DNA where processing proteins compete in a hand-off mechanism allowing them access as the pathway progresses. Additionally, RPA is well established as part of the damage sensing complex in the NER pathway for repair of bulky adducts (Wood 1999). In some cases RPA plays an active role by either activating or repressing the activity of the interacting partner. In the case of APE1, RPA specifically inhibits the nontemplated single-stranded AP site cleavage activity without direct protein-protein interaction (Fan *et al.* 2006).

Recently, RPA was shown to be involved in the cell-cycle signaling pathway by regulating the function of ATR-ATRIP complex (Zou and Elledge 2003). The formation of long single-stranded DNA-RPA filaments function as a DNA damage signal to recruit

down-stream proteins involved in DNA repair or cell apoptosis. The establishment of RPA as a protector of single-stranded DNA and sensor of damage lead us to hypothesize that NEIL1 activity would be closely regulated at the replication fork through a coordinated effort by PCNA, as already shown, and RPA. RPA's function would be to prevent the formation of double strand breaks by inhibiting the single-strand cleavage activity of NEIL1. To support our hypothesis, we investigated the physical interaction of NEIL1 with the RPA complex while also testing for the regulation of NEIL1 by RPA on substrates mimicking replication intermediates.

MATERIALS AND METHODS

Oligonucleotide substrates: The 51-mer 5-OHU containing oligo was labeled and annealed as described before (Chapter III). The sequences of complementary oligos had G opposite the lesion for generating duplex or were truncated from the 3' end to produce 3' primer-template structures as shown in Table 5.1.

Plasmids: The expression plasmid for His-tagged RPA uses a bi-cistronic IPTG inducible system encoding all three subunits in a single plasmid. This largest subunit contains an N-terminal His-tag.

Expression and purification of recombinant proteins: Recombinant WT NEIL1 and truncated NEIL1 polypeptides were purified to homogeneity from *E. coli* as described previously (Hazra *et al.* 2002a; Hazra *et al.* 2002b; Wiederhold *et al.* 2004; Das *et al.* 2006). His-tagged RPA was purified on a Ni²⁺ column followed by chromatography through a HiTrap-SP column (GE Healthcare). The GST-fused NEIL1 domains (289-349) and (289-389) as well as PCNA were expressed and purified as previously described (Chapter III).

Co-immunoprecipitation assay: The cell line HeLa S3 was maintained and transfected as described earlier (Chapter IV). The cells were collected 48 hours after transfection

and lysed in buffer (20 mM Tris-HCl, pH 7.5, 150 mM NaCl, 1 mM EDTA, 1% Triton X-100, and 0.5 mM, 1 mM NaF, 1 mM Na-orthovanadate, β -mercaptoethanol, plus protease inhibitors). In certain experiments, the cells were treated with Antimycin A (25 μ M) for 1 hr prior to harvesting. In other experiments the cell lysates were digested with 500 units/ml DNase I (Ambion) at 37°C for 1 hr, and cleared by centrifugation as previously described (Dou *et al.* 2008). The immunoprecipitation and immunoblotting was conducted as described earlier (Chapter II)

In vitro pulldown assay: Wild type NEIL1 or its truncated mutants (5 pmol) were incubated with His-tagged RPA (5 pmol) in 0.5 ml TBS for 1 h at 4°C and then treated as previously described for His-tag pulldown analysis. After elution and SDS-PAGE, the presence of NEIL1 was tested by immunoblotting.

GST pull down assays were performed as described previously (Das *et al.* 2007a). Proteins mixed with Glutathione-sepharose beads (20 μ l) alone or bound to GST-tagged truncated NEIL1 domains (312-349 and 312-389) (10 pmol) were incubated with RPA or PCNA (2.5 pmol each) in 0.5 ml. After washing the bound proteins were separated by SDS-PAGE followed by immunoblot analysis.

Fluorescence analysis: Interaction of RPA with NEIL1 C-terminal peptide (residues 312-349, which lacks aromatic residues) was monitored for change in the intrinsic tryptophan fluorescence of RPA ($\lambda_{\text{ex}} = 295$, $\lambda_{\text{em}} = 300\text{-}450$ nm) upon titration in an LS50 spectrofluorimeter (Perkin Elmer Life Sciences). For all binding experiments, the proteins in 10 mM PBS, pH 7.5, 5% glycerol were incubated at 25°C for 5 min. The binding constant K_D was calculated by plotting ΔF (change in RPA fluorescence at 345 nm) versus ligand concentration according to the equation $\Delta F = \Delta F_{\text{max}} \cdot [\text{ligand}] / K_D + [\text{ligand}]$.

Assay of DNA glycosylase activity: The DNA glycosylase activity of NEIL1 was quantitated as described before (Chapter III). When appropriate the DNA (25 nM) was preincubated with RPA for 15 min at 4°C in a 10 µl reaction mixture containing 40 mM HEPES-KOH, pH 7.5, 50 mM KCl, 1 mM MgCl₂, and appropriate amount of bovine serum albumin (BSA) to maintain a constant protein level prior to addition of NEIL1 and incubation at 37°C. The reaction was stopped after 10 min with 70% formamide/30 mM NaOH. The intact and cleaved oligos were then separated and quantitated as previously described (Chapter III).

Electrophoretic gel mobility shift analysis (EMSA): The 5' ³²P-labeled 51-mer oligo containing 5-OHU or C at position 26 annealed to various complementary sequences (Table 5.1) were used. The DNA (25 nM) was then incubated with various amounts of RPA or RPA and NEIL1 (as indicated) for 30 min at 4°C in a buffer containing 40 mM HEPES (pH 7.5), 50 mM KCl, 15% glycerol and appropriate amount of BSA to maintain an equal amount of total protein in each 20 µL reaction. Electrophoresis was performed at 4°C in 6% nondenaturing polyacrylamide gels in Tris-borate-EDTA buffer (pH 7.5 or 8.3), the protein-DNA complexes were visualized using a PhosphorImager and ImageQuant software (Molecular Dynamics).

RESULTS

Association of NEIL1 with RPA in vivo

We identified RPA, among the proteins present in the NEIL1 immunoprecipitate during our screen for replication-associated proteins in the NEIL1 IP, suggesting direct interaction of RPA with NEIL1. It has also been previously shown that RPA undergoes a complex scheme of hyperphosphorylation in response to oxidative stress causing a shift in function from DNA replication to repair (Oakley *et al.* 2001; Binz *et al.* 2004). We tested the effect of endogenous oxidative stress on the association of the RPA complex with NEIL1. The level of both RPA1 and RPA2 in the NEIL1-FLAG IP increased in response to Antimycin A treatment (Figure 5.1A). We were only able to detect the unmodified isoforms of RPA2 suggesting that modification of NEIL1 may be responsible for the increased association after stress. This is supported by the fact that the amount of PCNA and FEN1 in the NEIL1 IP is also increased after oxidative stress. In addition, we tested for a change in NEIL1 association with BRCA1 and RFC1 (Figure 5.1). However, we did not see a change in the level of either.

Because both RPA and NEIL1 have affinity for DNA, we considered the possibility that the observed interaction was mediated by independent binding of both proteins to DNA. Treatment of cell lysates with DNase I prior to co-immunoprecipitation did not affect the levels of RPA found in the NEIL1 IP (Figure 5.1B). From these observations, we concluded that the association between NEIL1 and RPA in human cells is not mediated via their interaction with DNA. In addition, the association was enhanced in response to oxidative stress along with that of PCNA and FEN1 (also 9-1-1, Chapter IV), suggesting increase in the formation of repair competent complexes under conditions of oxidative stress, presumably to efficiently repair the induced oxidative DNA damage.

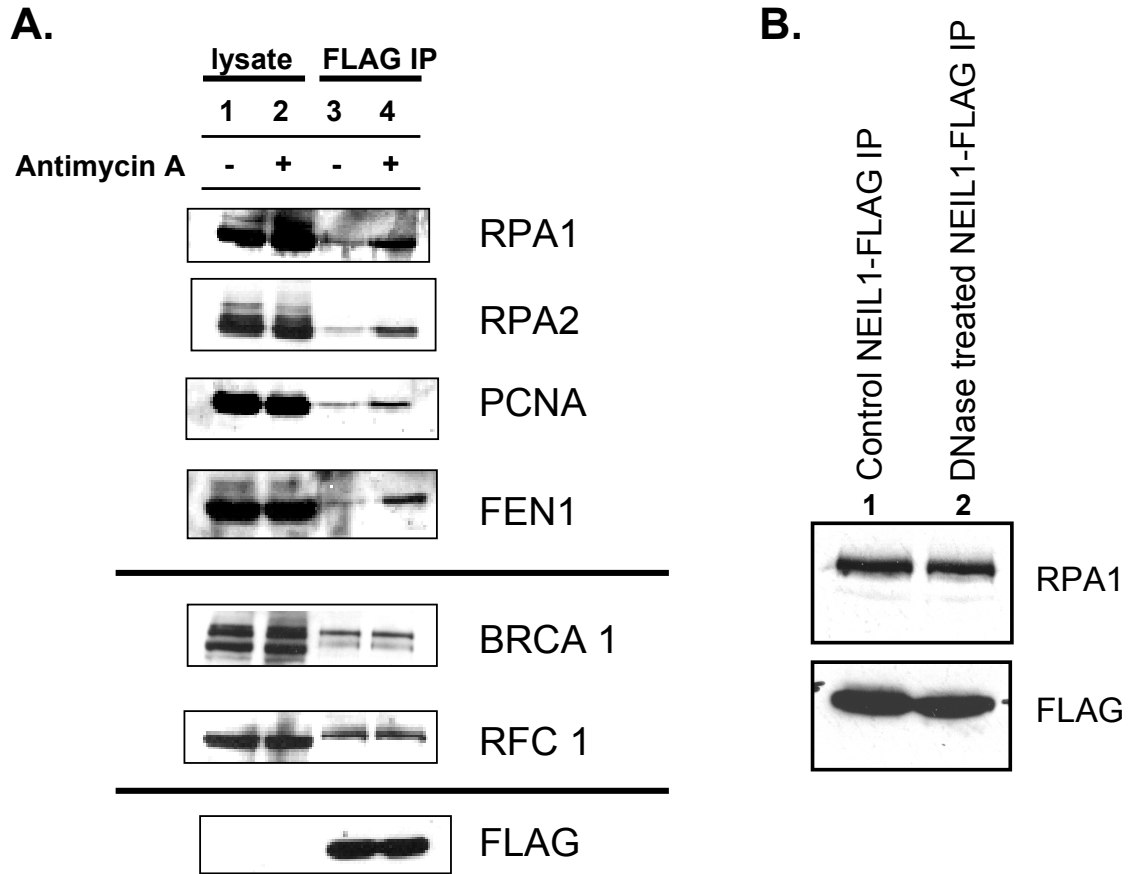


FIGURE 5.1: OXIDATIVE STRESS INCREASES THE LEVELS OF RPA, PCNA AND FEN1 FOUND IN THE NEIL1-FLAG IP. A. Western analysis of endogenous protein levels in the NEIL1-FLAG IP isolated from untreated cells (lane 3) or cells exposed to Antimycin A (lane 4) as described in Material and Methods. Equal levels of cell lysate from treated or non-treated cells were loaded in lanes 1 and 2. The specific primary antibody used for immunoblotting is listed to the right of each panel. B. Immunoblot analysis for the detection of RPA in untreated NEIL1-FLAG IP (lane 1) or IP pretreated with DNase I (500 units/mL) for removal of genomic DNA contamination. Lower panel was probed for FLAG levels in treated and untreated samples.

Mapping the RPA interaction to the NEIL1 C-terminus

RPA has been shown to interact with a large number of protein partners commensurate with its numerous roles in various DNA metabolic pathways. Most proteins interface primarily with RPA1 while few others with RPA2. We confirmed the binary interaction of NEIL1 and RPA in the absence of DNA using Far Western and co-elution analysis. NEIL1 interacted with the large 70 kDa subunit of RPA (RPA1) in a dose-dependent fashion, where as no interaction was observed with BSA (Figure 5.2A, left panel). In addition, we observed that the NEIL1 C Δ 40 mutant was capable of interacting with RPA although with apparently lower affinity than the WT protein (Figure 5.2A, right panel). A similar experiment showed no interaction with NEIL1 C Δ 101 mutant confirming that the same interaction domain near the C-terminus of NEIL1 is used for most of its partners (data not shown). We further refined the interaction interface of NEIL1 for RPA using GST-nested deletion mutants. In addition to WT and NEIL1 C Δ 40, we observed stable interaction of RPA with residues 289-389, 289-349 and 312-389 (Figure 5.2B). We concluded that the minimal interaction interface for RPA lies within NEIL1 residues 312-349 with possible involvement of additional residues at the extreme C-terminus as well.

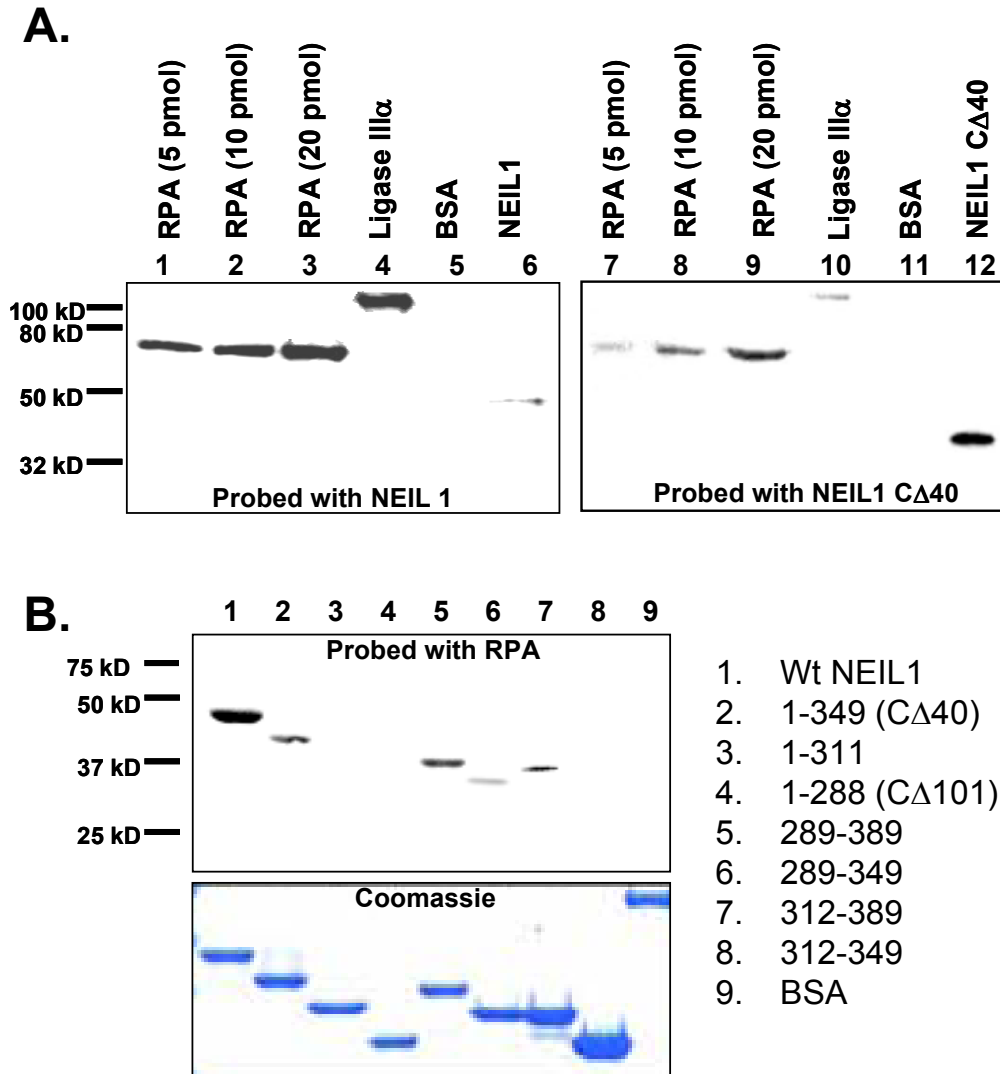


FIGURE 5.2: MAPPING THE RPA-INTERACTING INTERFACE ON NEIL1. A. Left panel: Membrane immobilized RPA (lanes 1-3), Ligase III α (lane 4) and BSA (lane 5) probed with WT NEIL1 (10 pmol/mL) followed by immunoblotting. RPA protein levels are as indicated, lanes 4 and 5 contain 20 pmol protein each and lane 6 contains 2 pmol WT NEIL1. Right panel: Far Western analysis using membrane immobilized proteins as in the right panel except for lane 12 which contains NEIL1 C Δ 40 (2 pmol). The membrane was probed for interaction using NEIL1 C Δ 40 (10 pmol/mL) followed by subsequent immunoblot analysis. B. Mapping the C-terminal interaction domain of NEIL1. Far Western analysis of RPA interaction with WT NEIL1 (lane 1), deletion mutants of NEIL1 (lanes 2-4) or GST-fused C-terminal domains of NEIL1 (lanes 5-8). Top panel: Far Western immunoblot with RPA, probed with RPA antibody. Bottom panel: Coomassie staining after SDS-PAGE.

We confirmed our Far Western results using both His- and GST-tag pull-down analyses. Co-elution of NEIL1 and NEIL1 C Δ 40 but not NEIL1 C Δ 101 with His-tagged RPA confirmed the location of the interaction interface within residues 289-349 of NEIL1 (Figure 5.3A, lanes 3-5)). WT NEIL1 in the absence of His-RPA was used as a control (Figure 5.3A, lane 2). Reciprocal co-elution of RPA with GST-fused C-terminal peptides of NEIL1 showed that residues 289-349 and 312-349 were sufficient for interaction independent of the whole protein (Figure 5.3B, lane 2, top panel). In contrast, very little PCNA co-eluted with residues 312-349 compared to residues 289-349 (Figure 5.3B, lane 2 versus 1, bottom panel). This supports previous work showing that the KA box motif, absent in the 312-349 fragment, is important for NEIL1-PCNA interaction and is found between residues 295-311 of the C-terminus of NEIL1. Thus, while the interaction interface of RPA and PCNA overlap there are residues outside the minimal interaction domain unique to each interacting partner that may function in coordinating a handoff between interacting protein partners.

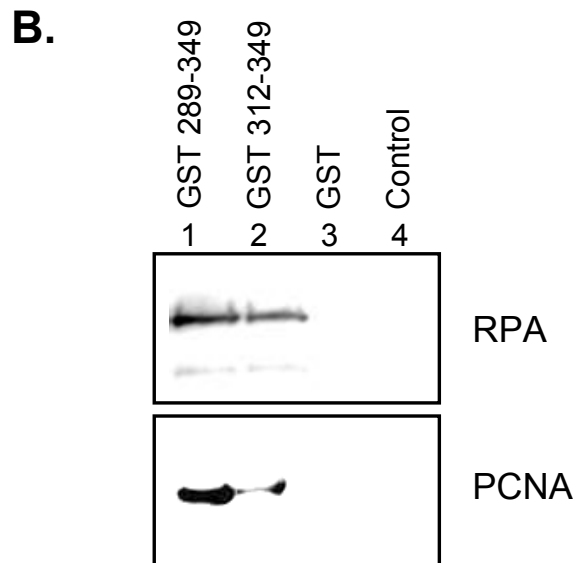
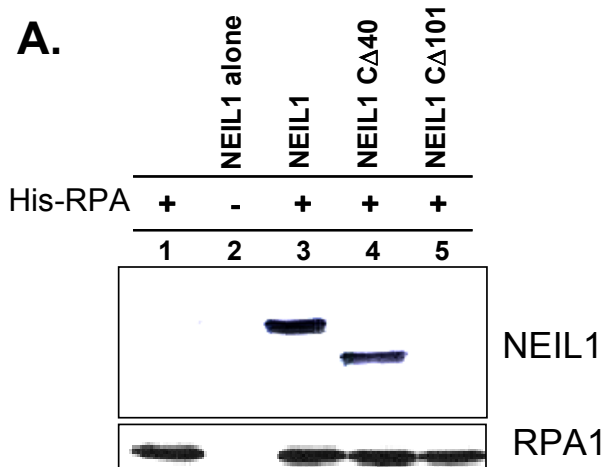


FIGURE 5.3: IN VITRO CO-ELUTION OF RPA AND NEIL1. A. His-tag pull-down of WT (lane 3) and deletion mutants (lanes 4 and 5) with His-tagged RPA coupled to His-select nickel-beads. His-RPA alone (lane 1) and WT NEIL1 alone (lane 2) serve as controls. Top panel, immunoblot against NEIL1; bottom panel immunoblot against RPA. B. Co-elution analysis of RPA (top panel) or PCNA (bottom panel) with GST-tagged C-terminal segments of NEIL1 (lanes 1 and 2) coupled to glutathione-Sepharose beads. GST alone (lane 3) and beads alone (lane 4) serve as controls for nonspecific binding. Immunoblot analysis was conducted using antibodies specified to the left of each panel.

Binding affinity analysis

We utilized the intrinsic fluorescence of RPA to measure the change of fluorescence intensity in the presence of the NEIL1 C-terminal peptide (residues 312-349). The fluorescence emission maximum of RPA decreased upon titration with the NEIL1 peptide suggesting that RPA may undergo a conformational change to a more compact form upon interaction with NEIL1 (Figure 5.4). The NEIL1 peptide lacking aromatic residues contributed negligibly to the fluorescence signal. An apparent dissociation constant (K_D) of approximately 20 nM was calculated for binding of RPA to the NEIL1 peptide residues 312-349 (Figure 5.4, lower panel). This peptide only contains the minimal interaction domain for RPA binding so other residues may have an effect on the binding constant. In any case, our results together indicate strong binary interaction between the NEIL1 C-terminal domain and the large subunit of RPA.

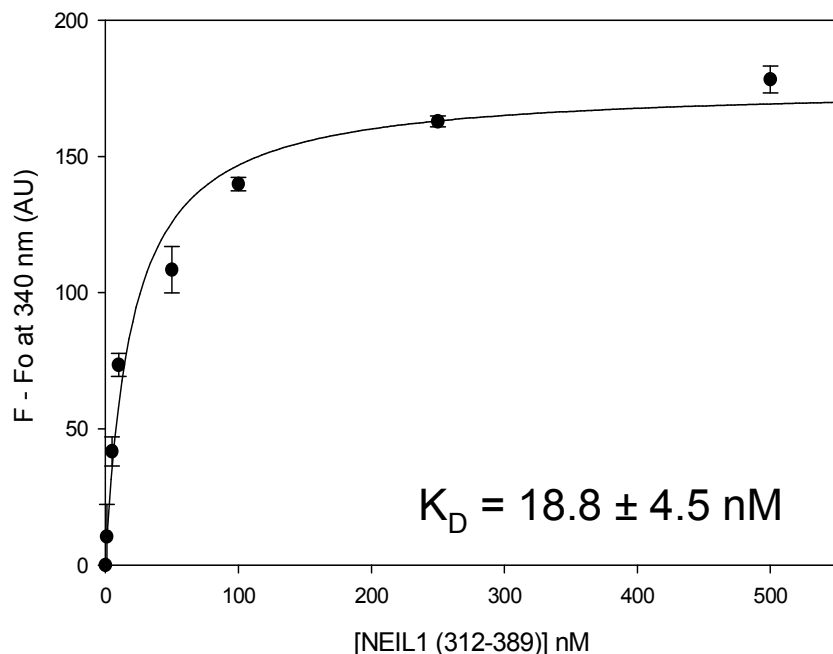
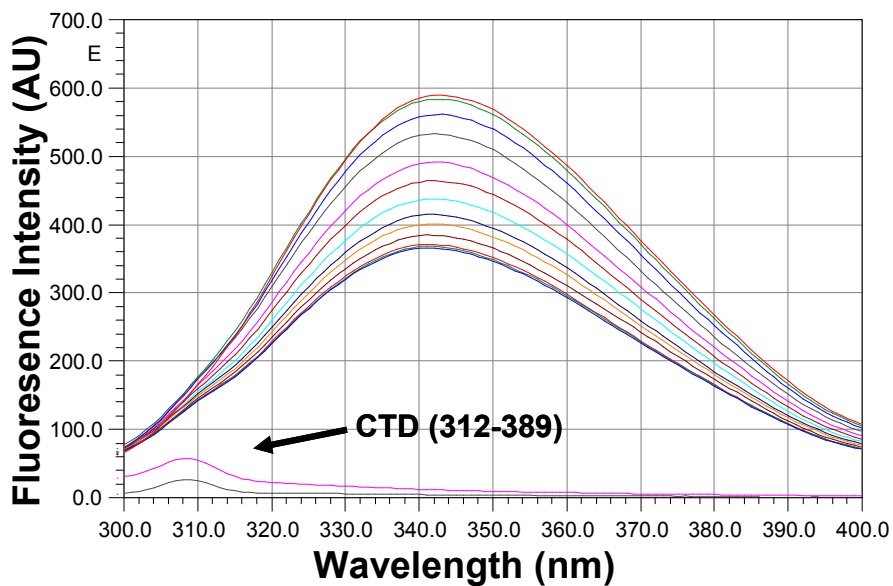


FIGURE 5.4: INTRINSIC FLUORESCENCE ANALYSIS OF RPA TITRATED WITH NEIL1 INTERACTION DOMAIN. Top Panel: Plot of the change in intrinsic tryptophan fluorescence of RPA alone or when titrated with NEIL1 C-terminal peptide containing residues 312-349. Intensity of fluorescence is graphed on the Y-axis versus wavelength. Repeated fluorescence spectra of the NEIL1 peptide alone are labeled on the bottom of the graph. Bottom Panel: Plot of change in RPA intrinsic fluorescence intensity caused by titration of the NEIL1 C-terminal peptide used in calculation of binding parameters.

RPA regulates NEIL1 activity with DNA structure specificity

We investigated NEIL1's cleavage activity with RPA-coated oligonucleotide substrates each containing a variable sized single-stranded region that mimicks various stages in chain elongation by the replicating DNA polymerase (Table 5.1). In these substrates, the damage (5-OHU) is considered to be present in the template strand. We compared the effect of an increasing molar ratio of RPA to substrate DNA and found significant inhibition of NEIL1 activity when the lesion was located in the single-stranded region or close to the primer-template junction of RPA-coated DNA (Figure 5.5). The level of inhibition correlated with two variables, the increase in RPA to DNA ratio as well as the distance of the lesion from the primer-template junction. On the other hand, RPA stimulated NEIL1 activity greater than 2-fold when the lesion was located in duplex DNA (Figure 5.6). We also examined the activity of the NEIL1 1-311 truncation mutant, which showed no interaction with RPA, with the same substrates (Figure 5.5). A nearly identical pattern of inhibition was seen when the lesion was in the single-stranded or primer-template junction regions. However, unlike WT NEIL1, we did not observe the stimulation of NEIL1 1-311 activity when the lesion was in the double-stranded region (Figure 5.7). RPA alone had no cleavage activity on any of these 5-OHU containing substrates, as expected (data not shown). Our results thus suggest that protein-protein interaction is not a requirement for inhibition of NEIL1 activity but is required for its stimulation.

ssDNA

3' - CCG TGC CAG ATG TGC CGT GTG CTC AXA TGT ACT ATG CTA AGG TTC GAT TCG - 5'

Rep 15

5' - GGC ACG GTC TAC ACG - 3'

3' - CCG TGC CAG ATG TGC CGT GTG CTC AXA TGT ACT ATG CTA AGG TTC GAT TCG - 5'

Rep 21

5' - GGC ACG GTC TAC ACG GCA CAC - 3'

3' - CCG TGC CAG ATG TGC CGT GTG CTC AXA TGT ACT ATG CTA AGG TTC GAT TCG - 5'

Rep 24

5' - GGC ACG GTC TAC ACG GCA CAC GAG - 3'

3' - CCG TGC CAG ATG TGC CGT GTG CTC AXA TGT ACT ATG CTA AGG TTC GAT TCG - 5'

Rep 29

5' - GGC ACG GTC TAC ACG GCA CAC GAG TGT AC - 3'

3' - CCG TGC CAG ATG TGC CGT GTG CTC AXA TGT ACT ATG CTA AGG TTC GAT TCG - 5'

dsDNA

3' - CCG TGC CAG ATG TGC CGT GTG CTC AXA TGT ACT ATG CTA AGG TTC GAT TCG - 5'

5' - GGC ACG GTC TAC ACG GCA CAC GAG TGT ACA TGA TAC GAT TCC AAG CTA AGC - 3'

Table 5.1: Sequences of 5-OHU containing oligodeoxynucleotide substrates. "X" represents 5-OHU. (ss – single-stranded; ds – double-stranded)

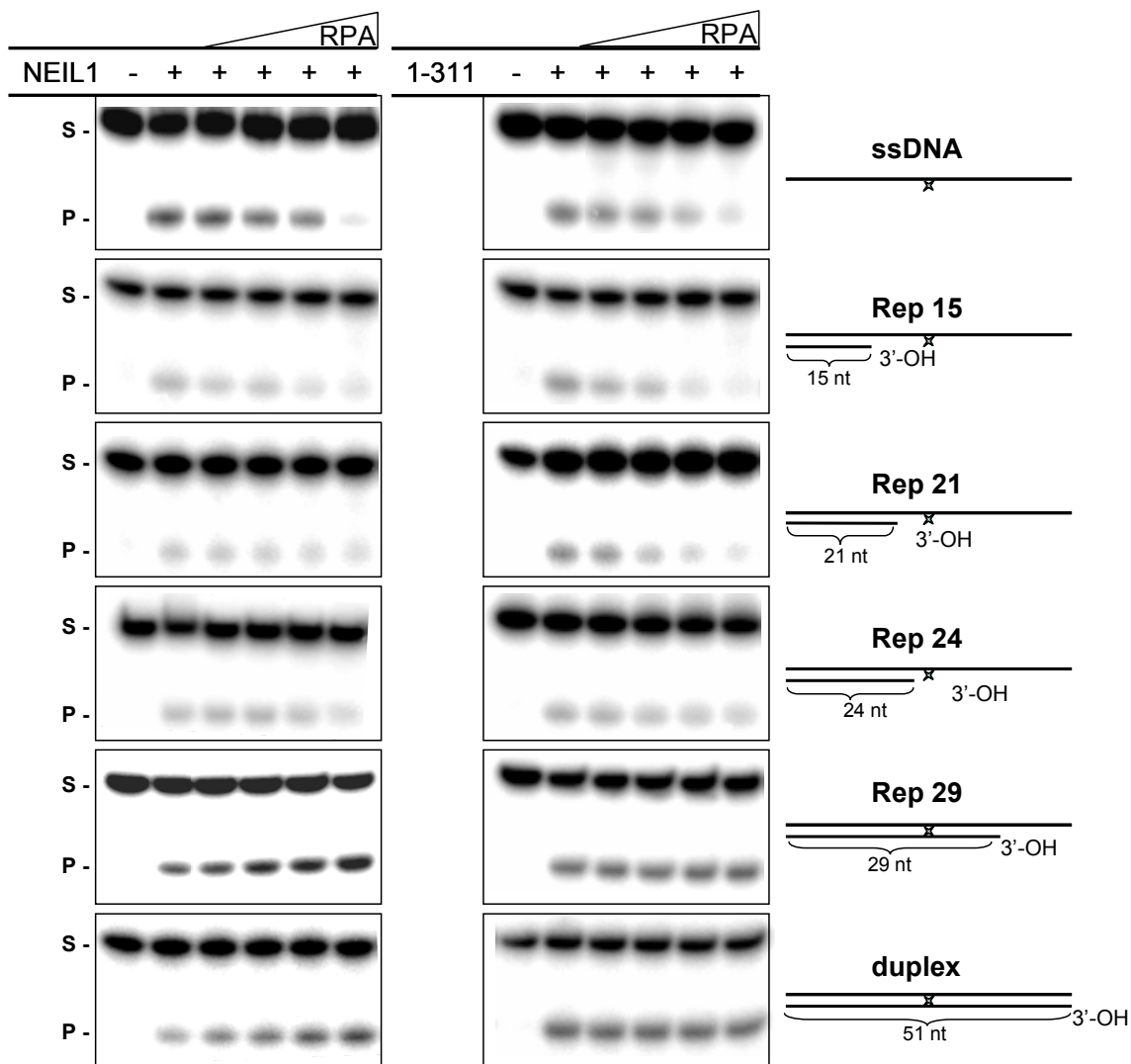


FIGURE 5.5: EFFECT OF RPA ON NEIL1 EXCISION OF 5-OHU FROM VARIOUS DNA STRUCTURES. A 51-mer 5-OHU-containing oligonucleotide (25nM) was used alone (single-stranded) or annealed with complementary strands to generate various structures (Table 5.1). NEIL1 (10 fmol) was added alone or after preincubation of the DNA with an increasing RPA:DNA molar ratio (1.25:1, 2.5:1, 5:1 or 10:1). S and P indicate uncleaved substrate and NEIL1 cleavage product, respectively.

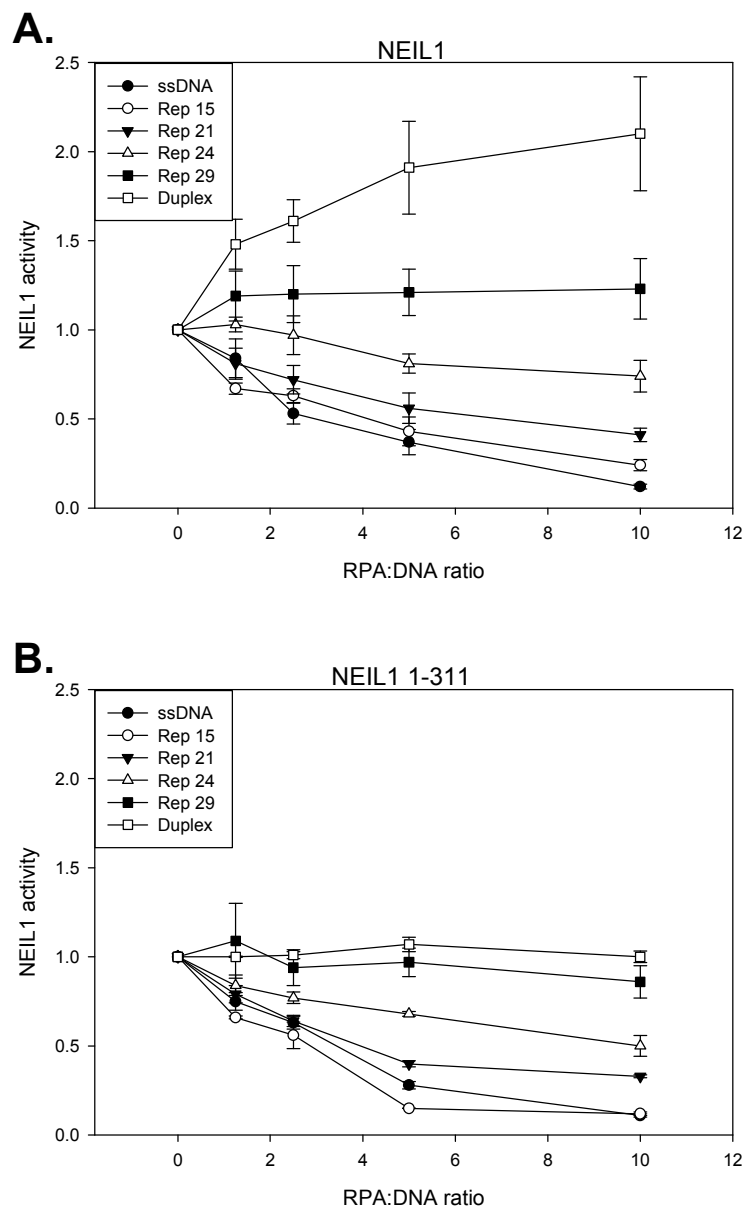


FIGURE 5.6: EFFECT OF RPA ON NEIL1 5-OHU CLEAVAGE ACTIVITY. A. RPA inhibition of NEIL1 single-stranded cleavage activity. The fold change in NEIL1 (10 fmol) activity ($\text{activity}_{\text{NEIL1-RPA}} - \text{activity}_{\text{NEIL1 alone}} / \text{activity}_{\text{NEIL1 alone}}$) with various DNA substrates (25 nM) is plotted as a function of RPA:DNA molar ratio. B. Physical interaction is not required for inhibition of NEIL1 single-stranded activity but is required for stimulation on duplex DNA. The fold change in NEIL1 1-311 (10 fmol) activity ($\text{activity}_{\text{NEIL1-RPA}} - \text{activity}_{\text{NEIL1 alone}} / \text{activity}_{\text{NEIL1 alone}}$) with various DNA substrates (25 nM) is plotted as a function of RPA:DNA molar ratio. Each point is the average of at least 3 experiments, error bars represent the standard deviation from the mean. Representative gels for both NEIL1 and NEIL1 1-311 shown in Figure 5.5.

RPA single-stranded DNA binding polarity effect on NEIL1 inhibition.

We then determined the level of RPA inhibition on NEIL1 activity using either a 3' primer-template or 5' primer-template substrate. These substrates are nearly identical except for the directionality of the primer, generating either a 3'-OH or a 5'-P terminus near the lesion. We observed inhibition of both NEIL1 and NEIL1 1-311 truncation mutant activity with both substrates. In fact, at the highest RPA:DNA ratio the level of inhibition was comparable between substrates (Figure 5.7). What was interesting, however, is that at lower concentrations of RPA, inhibition was significantly greater with the 5' primer-template relative to the 3' primer-template substrate (Figure 5.7). RPA has been shown to bind single-stranded DNA with a 5' → 3' molecular polarity as well as in a sequential multi-step manner (Iftode and Borowiec 2000; Kolpashchikov *et al.* 2001). Our results suggest that RPA's preference in binding polarity could affect its ability to regulate NEIL1 activity on lesions in single-stranded DNA near various primer-template junctions.

EMSA analysis of RPA binding

It was interesting that RPA was able to cause an identical dose-dependent inhibition of NEIL1 1-311 activity to that of WT NEIL1, even in the absence of the interaction interface. To gain further insight into this we examined RPA's substrate binding to oligos that contain lesions in single-stranded region DNA. NEIL1 activity was inhibited by RPA on each of these substrates (ssDNA, Rep15, Rep21 and Rep24). We identified multiple RPA-DNA complexes of different molecular size through gel shift analysis (Figure 5.8). The slower migrating complexes of larger size were more prominent at the highest concentration of RPA. The smaller faster migrating complexes were not present in these samples suggesting multiple RPA molecules bound to each oligo, thus slowing its migration. We also observed the lack of slower migrating complexes correlating with a decrease in the number of single-stranded nucleotides in the substrate when compared to the single-stranded 51-mer substrate (Figure 5.8). We concluded that the fastest migrating band represented a single RPA molecule bound to DNA, with the addition of another RPA molecule in each subsequent band of decreased mobility. The maximum number of RPA molecules per 51-mer oligonucleotide was four. This is in agreement with previous studies characterizing the different modes of RPA binding to DNA (Iftode and Borowiec 2000; Jiang *et al.* 2006; Cai *et al.* 2007). These results help explain the mechanism of dose-dependent inhibition of NEIL1 activity, without the need for physical interaction between NEIL1 and RPA, through steric hindrance of multiple RPA molecules binding a single substrate oligo.

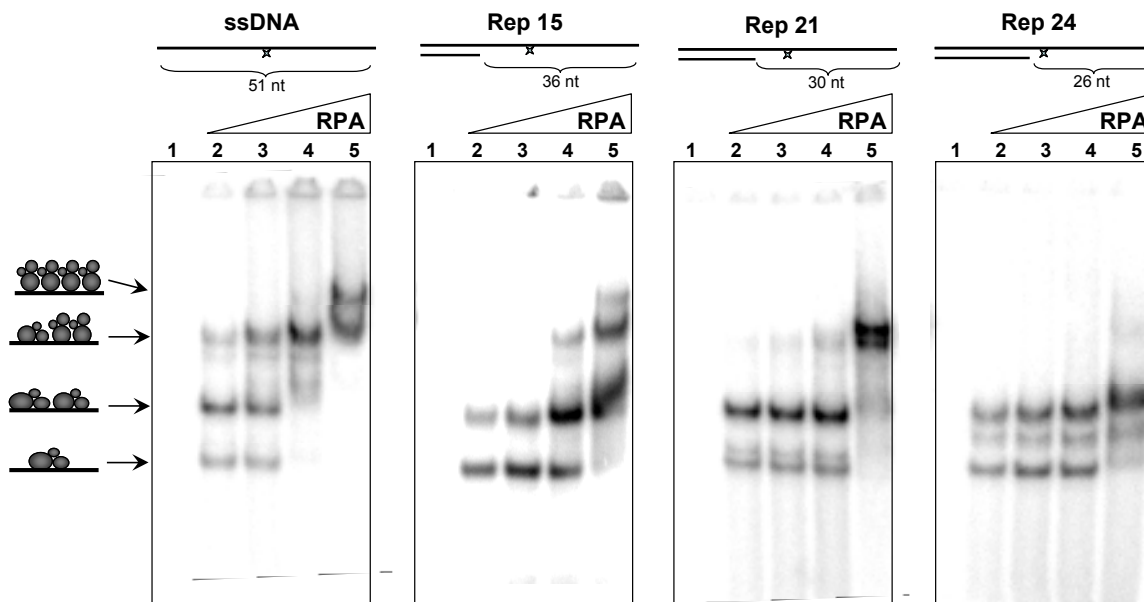


FIGURE 5.8: EFFECT OF SINGLE-STRANDED DNA LENGTH IN PRIMER-TEMPLATE SUBSTRATES ON RPA BINDING. EMSA of no enzyme (lane 1) or increasing ratio of RPA to DNA (1.25:1, 1:2.5, 1:5 or 1:10; lanes 2-5) using the indicated DNA oligonucleotide substrate (25 nM). RPA was incubated at 4°C for 30 min in a 20 μ L reaction prior to native gel electrophoresis at pH 8.3. The position of various RPA-DNA complexes is indicated.

NEIL1 forms a ternary complex with RPA-coated DNA

We tested by gel shift analysis whether NEIL1 could form a ternary complex with RPA-coated DNA. We previously showed that NEIL1 has intrinsic affinity for both duplex and single-stranded DNA even in the absence of any damage (Dou *et al.* 2003; Dou *et al.* 2008). These results were confirmed by the shift in single-stranded and duplex DNA mobility caused by increasing concentrations of NEIL1 (Figure 5.9; lanes 2-5). We then pre-incubated the DNA with RPA and observed a shift in mobility of the single-stranded oligo (Figure 5.8). The mobility of the RPA-DNA complex was super-shifted by an increase in NEIL1 concentration. It is important to stress that RPA did not complex with duplex DNA and appears to only slightly increase NEIL1 binding (Figure 5.9, right panel). This could explain the modest stimulatory effect RPA had on NEIL1 activity on duplex substrates. The RPA-DNA complex formation in Figure 5.9 is not identical to that in Figure 5.8, presumably because of the change in pH conditions (from 8.3 to 7.5) and the duration of electrophoresis. The change in pH to 7.5 was necessary for NEIL1 analysis and is not the optimal pH for RPA binding in gel shift analysis. Taken together, the additional shift in RPA-DNA complex mobility with the increase in NEIL1 suggests that a NEIL1-RPA-DNA ternary complex is formed, presumably through physical interaction of NEIL1 with RPA.

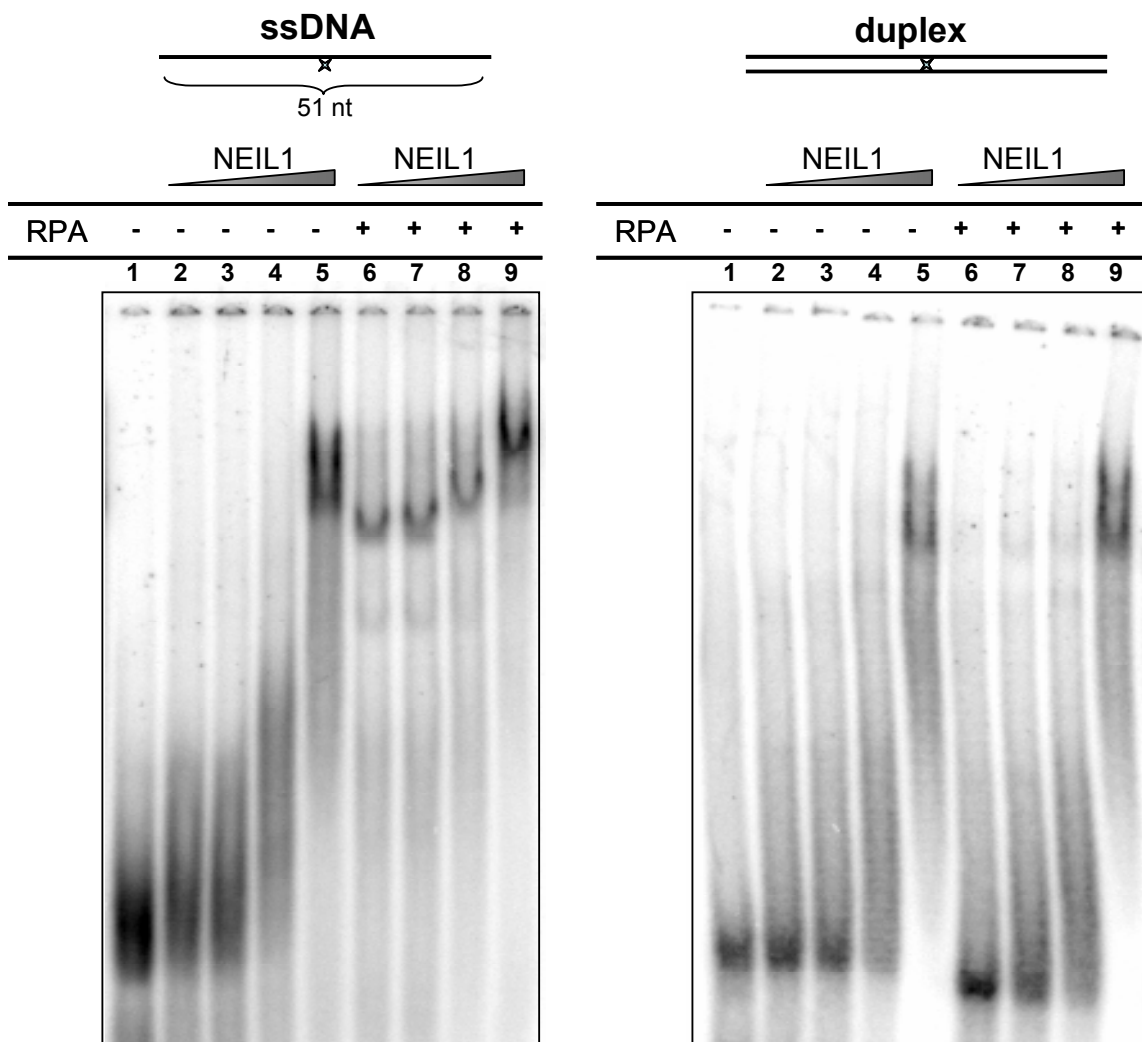


FIGURE 5.9: NEIL1 FORMS A TERNEIRY COMPLEX WITH RPA-COATED DNA. EMSA of no enzyme (lane 1), increasing amount of NEIL1 (50 – 400 nM; lanes 2-5) or increasing amount of NEIL1 (50 – 400 nM) with constant amount of RPA (100 nM; lanes 6-9) using the indicated DNA oligonucleotide substrate (25 nM). NEIL1 was incubated at 4°C for 15 min after preincubation of the DNA with RPA in a 20 μ L reaction prior to native gel electrophoresis at pH 7.5.

PCNA relieves RPA inhibition of NEIL1 activity

Our previous work with PCNA showed stimulation of NEIL1 on substrates containing uncoated single-stranded DNA, including bubble, fork and single-stranded structures. We examined PCNA's ability to stimulate NEIL1 on RPA-coated primer-template substrates containing single-stranded DNA. PCNA would be free to slide on and off the duplex region of the substrate and maintain equilibrium between bound and free PCNA. RPA inhibited NEIL1 in a dose-dependent manner as observed previously. Interestingly, NEIL1 activity was modestly stimulated when PCNA was added to the reaction and RPA was at a low molar ratio to DNA (Figure 5.10, lane 6). As the level of RPA increased, the stimulation of NEIL1 activity by PCNA reduced significantly. In fact, at the highest concentration, RPA was able to slightly inhibit NEIL1 activity in the presence of PCNA but not to the levels previously seen in the absence of PCNA. These data suggest that PCNA and RPA may work together and are responsible for regulating NEIL1 activity at the replication fork.

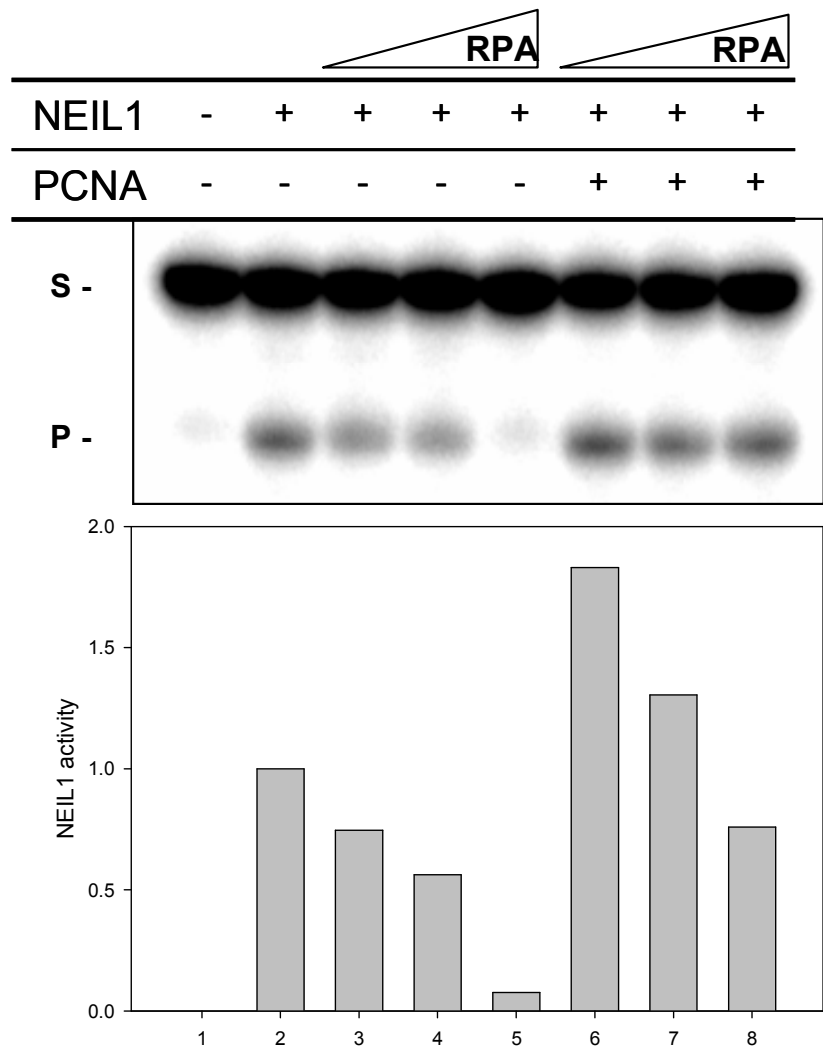


FIGURE 5.10: NEIL1 OVERCOMES RPA INHIBITION IN THE PRESENCE OF PCNA. NEIL1 activity on the 5-OHU-containing “Rep 21” substrate (25 nM) with no enzyme (lane 1), NEIL1 alone (lane 2), in the presence of increasing RPA:DNA molar ratio (1.25:1, 2.5:1 or 5:1; lanes 3-5) or in the presence of increasing RPA with PCNA (2 μ M; lanes 6-8). The DNA was allowed to pre-incubate with RPA at 4°C for 30 min prior to addition of other proteins. S and P represent uncleaved substrate and cleavage product, respectively.

DISCUSSION

We have shown the functionally relevant binary interaction of NEIL1 with RPA, an important component of DNA replication that binds to single-stranded template DNA. The NEIL1 immunocomplex isolated from human cells contain RPA1 and RPA2, an association that increases under oxidative stress along with PCNA and FEN1. We have also shown that NEIL1 and RPA directly interact *in vitro* using pull-down, fluorescence and Far Western analysis. NEIL1 uses the common interacting interface in the disordered C-terminal domain (mapped to residues 312-349) to specifically interact with the large 70 kDa subunit of RPA. The affinity of RPA to the C-terminal domain of NEIL1 was calculated to be ~20 nM.

RPA inhibits NEIL1 activity *in vitro* when the damage (5-OHU) is within the single-stranded region of a primer-template structure. The degree of inhibition decreases when the damage is closer to the primer-template junction. Interestingly, when the damaged base is located in the double-stranded region near the primer-template junction RPA stimulated WT NEIL1 but not NEIL1 1-311, which is largely missing the C-terminal interaction interface, suggesting interaction is critical for stimulation but not inhibition of activity. This implies that RPA out competes NEIL1 for binding to single-stranded DNA producing enough steric hindrance to prevent NEIL1 access to the lesion. Our EMSA results corroborate this scenario by showing an increase in the number of DNA-bound RPA molecules with increasing RPA concentration. This is further supported by the structural analyses conducted on RPA-DNA complexes demonstrating a sequential multi-step binding of RPA to single-stranded DNA and the occlusion of 8-10, 12-23 or ~ 30 nucleotides by a single RPA molecule (Bochkareva *et al.* 2002; Arunkumar *et al.* 2003; Jiang *et al.* 2006; Cai *et al.* 2007; Deng *et al.* 2007).

We also observed differential inhibition of NEIL1's activity with 3' vs. 5' primer-template substrates at low RPA concentration. EMSA demonstrated that only one or two RPA molecules are bound to a substrate molecule at such concentrations. Interestingly, NEIL1 forms a ternary complex with RPA-coated DNA as seen by a shift in our EMSA experiments suggesting that RPA interacts with NEIL1 even when bound to DNA. Another possibility is that NEIL1 binds to uncoated regions of DNA and not directly with RPA but our data suggest otherwise. It is also plausible that RPA functions as a damage sensor because of its direct association with DNA and recruits NEIL1 to the damage inhibiting NEIL1 cleavage activity until it can be safely repaired. However, it is intriguing to ponder the possibility of NEIL1 working with RPA to sense damage in the single-stranded DNA much like the XPA-RPA complex recognizes bulky adducts in NER (Wood 1999). While this has yet to be proven it proposes another method in which NEIL1 recognizes oxidative lesions (possibly among others) in the template DNA, temporarily stalling replication and initiating repair prior to DNA synthesis.

Finally, the inhibition of NEIL1's single-stranded activity by RPA is relieved in the presence of PCNA when the lesion is near the primer-template junction proposing a mechanism in which RPA inhibition may be overcome once it is safe to initiate repair. This also affirms PCNA's role as a scaffold/recruitment site for NEIL1 and stresses the importance of PCNA stimulation of NEIL1 activity. RPA's interaction with NEIL1 may serve many functions but the role in inhibiting NEIL1 cleavage of the single-stranded template DNA would be absolutely critical to the stability of the replication fork. Our results suggest that RPA, along with PCNA and possibly other proteins, work in collaboration to regulate a complex system that not only maintains efficient and proper replication but also repair of oxidative DNA to prevent mutagenesis and maintain genomic integrity.

CHAPTER VI

Summary and Conclusions

Oxidative damage to the mammalian genome, induced spontaneously or by radiation and other agents, represents the most pervasive genotoxic insult, and includes a plethora of often mutagenic oxidatively damaged bases and DNA strand breaks. Such damage has an etiological role in sporadic cancers, a variety of other pathological states and in the aging process. Oxidized lesions are primarily repaired through the DNA base excision repair pathway, initiated with recognition and removal of the damaged base via hydrolysis of the N-glycosylic bond by one of four DNA glycosylases, including NEIL1 and NEIL2. It was previously shown that NEILs initiate a unique APE1-independent short patch BER pathway mediated by PNK, Pol β , DNA Ligase III α , and XRCC1 (Wiederhold *et al.* 2004; Das *et al.* 2006). Both NEIL1 and NEIL2 form a complex *in vivo* with all of these proteins and directly interact with several of these downstream repair proteins of the BER pathway. This suggested that both NEIL1 and NEIL2 initiate a common BER pathway, similar to that of OGG1 and NTH1 except with the requirement for PNK, for global repair of oxidative base lesions and may also play a role in coordination of the subsequent steps in the pathway.

Both NEILs were shown to be distinct in their ability to excise base lesions from single-stranded, bubble or fork DNA generated during replication and transcription, unlike the previously characterized OGG1 and NTH1. However, the NEILs have distinct cell-cycle regulation suggesting a divergence in their specific initiated repair pathways. While NEIL2 expression is cell-cycle independent, we observed that NEIL1 expression is strongly dependent on the S-phase (Hazra *et al.* 2002a; Hazra *et al.* 2002b). Other studies

demonstrated that NEIL1-deficiency induces a mutator phenotype in hamster and human cells while radiosensitization in NEIL1-deficient mouse cells suggest a role in repairing radiation and ROS induced base damage. NEIL1 knockout mice display a unique phenotype consisting of obesity, dylipidemia, fatty liver disease, and hyperinsulinemia. In addition, inactivating mutations in the human NEIL1 gene have been epidemiologically linked with gastric cancer. These observations supported the role of NEIL1 in a preferential repair pathway for oxidative base damage specifically associated with the S-phase.

One unexplored issue thus far in BER is the need for preferential repair of the mutagenic, oxidized base lesions in functional regions of the genome. Most adult tissues contain nondividing, terminally differentiated cells in which DNA base lesions will not induce mutations. Furthermore, because only a small fraction of the mammalian genome contains transcription units, the repair of mutagenic lesions in nontranscribed sequences should not be as urgent as in the transcribed sequences. Additionally, the damage in the untranscribed strand may not affect transcription. However, repair of mutagenic oxidized bases in the untranscribed strands as well as nontranscribed regions of the genome of actively dividing cells, e.g., during development and in regenerative tissues, should be as critical as that of the transcribed strand. In such cases, mutations would be fixed due to damage in either strand. This is particularly important for oxidatively damaged bases which unlike bulky adducts do not usually block replication or transcription (Guschlbauer *et al.* 1991; Kathe *et al.* 2004; Tornaletti *et al.* 2004; Maga *et al.* 2007). We and others have postulated a model of replication-associated repair in which the repair enzyme scans the genome to repair damaged bases in the template strand before replication, in order to prevent mutations (Mitra *et al.* 1997; Krokan *et al.* 2000).

The emergence of the “cellular interactome” concept has led to a new paradigm in which collaboration of multiple proteins involving binary interactions in a coordinated fashion leads to enhanced efficiency of metabolic pathways. It is now evident that the cellular processes for repair of both endogenous and induced genomic damage are essential for maintaining genomic integrity and homeostasis, which involve dynamic and complex interactions among a multitude of proteins and with DNA in the repair interactome. In our model we propose the novel hypothesis that NEIL1 is preferentially involved in replication-associated repair of oxidative base damage through formation of a stable complex between NEIL1 and the replication machinery. Thus, NEIL1 would form a complex with at least PNK, Pol β , XRCC1, Ligase III α in G0/G1 cells to carry out basic short patch repair and another complex with essential proteins for replication during S-phase to carry out replication-associated repair. These proteins include PCNA, RPA, FEN1, Pol δ and Ligase I (in addition to 9-1-1) suggesting the replication-associated repair would follow the long patch BER pathway. A minimal common interaction interface identified for all of the interacting proteins partners is between residues 311-349 of the NEIL1 C-terminus (Figure 6.1). There are, however, contacts outside of this region that also play a part in the interaction such as the KA box motif for PCNA binding identified N-terminal of the common interface. It is interesting that so many proteins interface with the limited number of residues of the common interaction domain and that the disorder and flexibility of this region appears to explain this phenomenon.

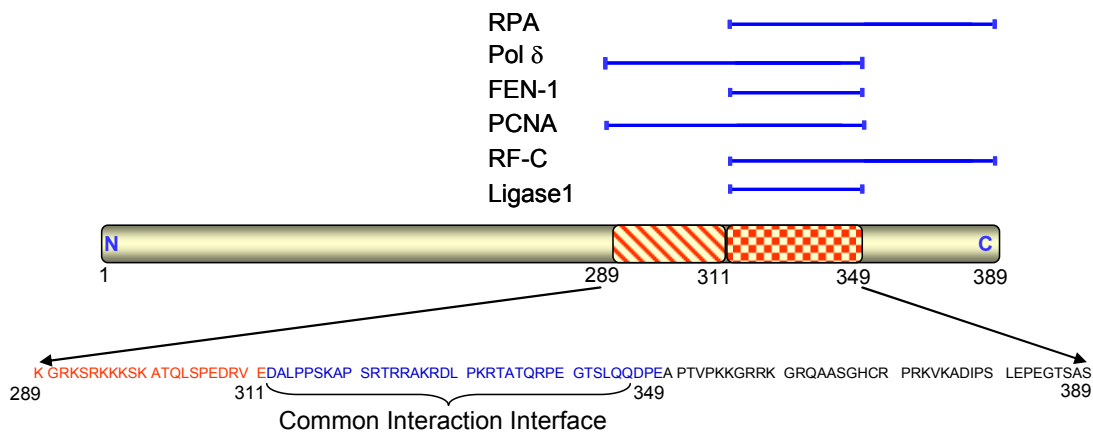


FIGURE 6.1: SCHEMATIC OF THE OVERLAPPING INTERACTION INTERFACE IN THE NEIL1 C-TERMINUS. The amino acid sequence of residues 289-389 are shown.

In eukaryotes, the two major pathways of BER are single-nucleotide short patch and 2-10 nucleotide long patch pathway, each requiring a different set of components with some common between both. The short patch BER pathway is the simpler of the two requiring a minimum number of proteins as previously described. Initial studies demonstrated that the NEIL1-dependent BER is of the short-patch type (Wiederhold *et al.* 2004). The 9-1-1 complex may also be a component of the short-patch BER such as the NEIL1-dependent pathway because of its direct interaction and stimulation of NEIL1. In fact, this may be enhanced under conditions of stress supported by the colocalization of NEIL1 and 9-1-1 after treatment with H₂O₂. However, the long patch BER pathway requires a glycosylase, APE1/PNK, RFC, FEN1, Pol δ/ϵ (or Pol β), PCNA, and Ligase I (Matsumoto *et al.* 1999; Pascucci *et al.* 1999). Because the 9-1-1 complex can interact with DNA ligase I (Smirnova *et al.* 2005), it has been suggested that it may be involved in the long-patch BER as well. Because the structure of the 9-1-1 complex resembles that of PCNA sliding clamp (Venclovas and Thelen 2000; Burtelow *et al.* 2001; Shiomi *et al.* 2002), it has been proposed that the 9-1-1 complex acts as a damage-specific substitute

for PCNA (Wang, W. *et al.* 2004; Friedrich-Heineken *et al.* 2005). The 9-1-1 complex may replace PCNA when active PCNA is depleted by p21 during cell cycle arrest in response to DNA damage (Waga *et al.* 1994). It would be interesting to investigate the mechanism by which NEIL1 switches its partners from PCNA to the 9-1-1 complex and further determine the role 9-1-1 has in BER.

Our observation of so many proteins in the NEIL1 IP raises the issue of stoichiometry of the complex formed *in vivo*. We propose a simple-minded scenario of NEIL1's role in repairing oxidized bases during DNA replication (Figure 6.2). In this model the replication complex contains NEIL1 which could either be recruited upon encountering an oxidized base lesion or could be an intrinsic component of the complex such as bound to PCNA or RPA. After unwinding of the template ahead of the growing chain, the single-stranded template is complexed with RPA, which protects the DNA from degradation. We propose that PCNA-bound or RPA-bound NEIL1 initiates repair of the oxidized base by recognizing the oxidative lesion site in either the leading or lagging strand template ahead of the polymerase. The strand interruption prevents further fork movement which then collapses to form a "chicken foot" structure (Heller and Marians 2006). Repair of the damage occurs in the reannealed duplex DNA and replication resumes after a helicase, e.g., Werner or Bloom protein resolves the collapsed fork (Sharma *et al.* 2004). In support of this scenario, we have recently shown that NEIL1 stably interacts with and is activated by the Werner protein (Das *et al.* 2007b). How the steps are coordinated in this process is still obscure. Nevertheless, it appears that the repair/replication complex is dynamic with the likelihood of coordinated handover among the interacting partners (Warbrick 2000). It is tempting to speculate that the weak interaction between PCNA and NEIL1 is needed for NEIL1's efficient release after completion of repair.

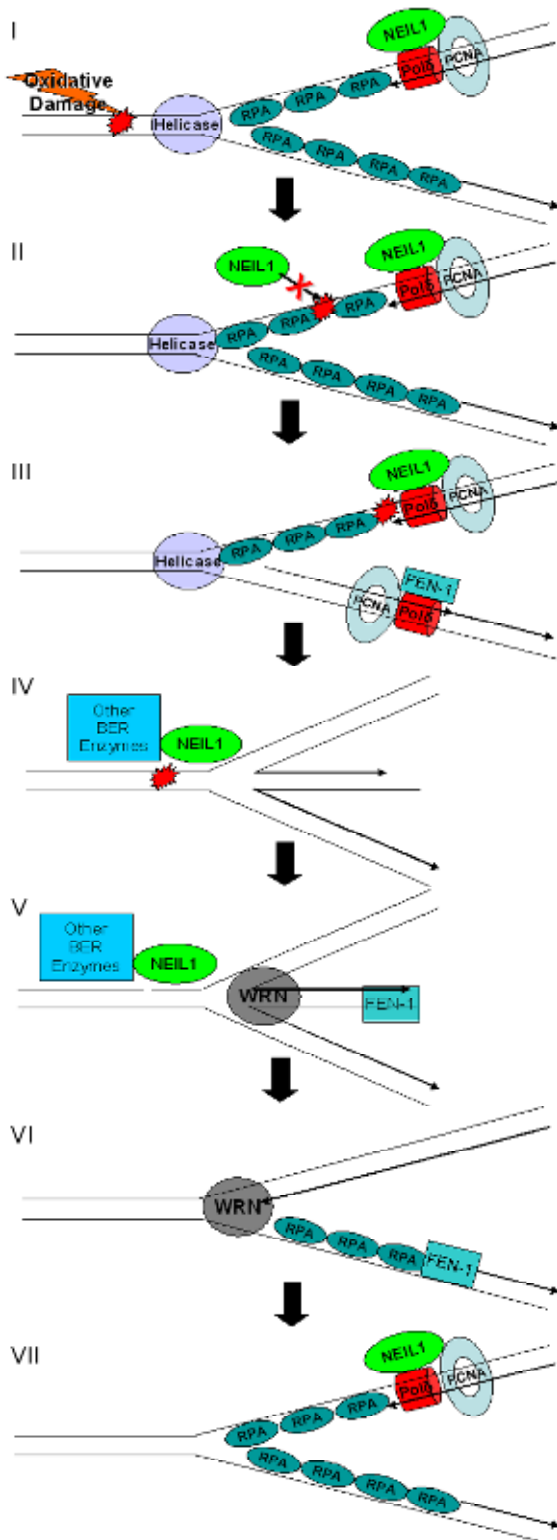


FIGURE 6.2: A MODEL FOR THE ROLE OF NEIL1 IN REPLICATION-ASSOCIATED REPAIR. The template DNA is unwound by the replicative helicase generating single-stranded template DNA that becomes complexed with RPA. For replication of the damage-containing leading strand template (shown above), the replication complex of Pol δ bound to PCNA also contains NEIL1 for damage surveillance (Step I). NEIL1 is inhibited by RPA from cleaving the DNA when the damage is in single-stranded DNA, preventing a double-strand break (Step II). Polymerase progression is stalled when NEIL1 recognizes a base lesion resulting in fork arrest (Step III) and its regression leading to a chicken foot structure, and reannealing of unreplicated duplex spanning the damage (Step IV). After NEIL1's recruitment of a BER complex, repair occurs followed by resolution of the chicken foot structure by WRN helicase (Step V) allowing FEN1 mediated degradation of the nascent lagging strand (Step VI) after which replication resume as normal with NEIL1 associated with the replication complex (Step VII).

PCNA has recently been shown to be monoubiquitylated in response to UV light which enhances its interaction with and activation of Pol η (Lehmann 2006). PCNA was shown earlier to interact with p300/CBP histone acetyltransferase and may be acetylated as well (Hasan *et al.* 2001; Naryzhny and Lee 2004). RPA has also been shown to be modified and have multiple phosphorylated isoforms depending on the condition of the cell (Brush *et al.* 2001; Binz *et al.* 2003; Oakley *et al.* 2003; Vassin *et al.* 2004). In addition, NEIL1 contains several residues, particularly in the C-terminus, that have been shown to be post-translationally modified in preliminary studies (i.e. acetylation and phosphorylation; C. Theriot and K. Bhakat, unpublished observations). Whether such covalent modifications of PCNA and RPA or NEIL1 modulate their interaction and overall repair efficiency remains to be established and would be a very interesting course of study.

The presence of multiple complexes of NEIL1 underscores the need for developing a comprehensive picture of the involvement of NEIL1 (and possibly other DNA glycosylases) in various subpathways of BER in response to both endogenous and induced oxidative damage in the genome, and of the linkage between BER, damage signaling and DNA metabolic pathways.

References

- Alani, E., R. Thresher, J. D. Griffith and R. D. Kolodner (1992). "Characterization of DNA-binding and strand-exchange stimulation properties of γ -RPA, a yeast single-strand-DNA-binding protein." J Mol Biol **227**(1): 54-71.
- Arunkumar, A. I., M. E. Stauffer, E. Bochkareva, A. Bochkarev and W. J. Chazin (2003). "Independent and coordinated functions of replication protein A tandem high affinity single-stranded DNA binding domains." J Biol Chem **278**(42): 41077-41082.
- Bandaru, V., S. Sunkara, S. S. Wallace and J. P. Bond (2002). "A novel human DNA glycosylase that removes oxidative DNA damage and is homologous to Escherichia coli endonuclease VIII." DNA Repair (Amst) **1**(7): 517-529.
- Bastin-Shanower, S. A. and S. J. Brill (2001). "Functional analysis of the four DNA binding domains of replication protein A. The role of RPA2 in ssDNA binding." J Biol Chem **276**(39): 36446-36453.
- Bellamy, S. R., K. Krusong and G. S. Baldwin (2007). "A rapid reaction analysis of uracil DNA glycosylase indicates an active mechanism of base flipping." Nucleic Acids Res **35**(5): 1478-1487.
- Binz, S. K., Y. Lao, D. F. Lowry and M. S. Wold (2003). "The phosphorylation domain of the 32-kDa subunit of replication protein A (RPA) modulates RPA-DNA interactions. Evidence for an intersubunit interaction." J Biol Chem **278**(37): 35584-35591.
- Binz, S. K., A. M. Sheehan and M. S. Wold (2004). "Replication protein A phosphorylation and the cellular response to DNA damage." DNA Repair (Amst) **3**(8-9): 1015-1024.
- Bjoras, M., E. Seeberg, L. Luna, L. H. Pearl and T. E. Barrett (2002). "Reciprocal "flipping" underlies substrate recognition and catalytic activation by the human 8-oxo-guanine DNA glycosylase." J Mol Biol **317**(2): 171-177.
- Bochkareva, E., S. Korolev, S. P. Lees-Miller and A. Bochkarev (2002). "Structure of the RPA trimerization core and its role in the multistep DNA-binding mechanism of RPA." Embo J **21**(7): 1855-1863.
- Boldogh, I., D. Milligan, M. S. Lee, H. Bassett, R. S. Lloyd and A. K. McCullough (2001). "hMYH cell cycle-dependent expression, subcellular localization and association with replication foci: evidence suggesting replication-coupled repair of adenine:8-oxoguanine mispairs." Nucleic Acids Res **29**(13): 2802-2809.
- Braun, K. A., Y. Lao, Z. He, C. J. Ingles and M. S. Wold (1997). "Role of protein-protein interactions in the function of replication protein A (RPA): RPA modulates the

- activity of DNA polymerase alpha by multiple mechanisms." Biochemistry **36**(28): 8443-8454.
- Brush, G. S., D. M. Clifford, S. M. Marinco and A. J. Bartrand (2001). "Replication protein A is sequentially phosphorylated during meiosis." Nucleic Acids Res **29**(23): 4808-4817.
- Burtelow, M. A., P. M. Roos-Mattjus, M. Rauen, J. R. Babendure and L. M. Karnitz (2001). "Reconstitution and molecular analysis of the hRad9-hHus1-hRad1 (9-1-1) DNA damage responsive checkpoint complex." J Biol Chem **276**(28): 25903-25909.
- Cai, L., M. Roginskaya, Y. Qu, Z. Yang, Y. Xu and Y. Zou (2007). "Structural characterization of human RPA sequential binding to single-stranded DNA using ssDNA as a molecular ruler." Biochemistry **46**(28): 8226-8233.
- Chang, D. J., P. J. Lupardus and K. A. Cimprich (2006). "Monoubiquitination of proliferating cell nuclear antigen induced by stalled replication requires uncoupling of DNA polymerase and mini-chromosome maintenance helicase activities." J Biol Chem **281**(43): 32081-32088.
- Das, A., I. Boldogh, J. W. Lee, J. A. Harrigan, M. L. Hegde, J. Piotrowski, N. de Souza-Pinto, W. Ramos, M. M. Greenberg, T. K. Hazra, S. Mitra and V. A. Bohr (2007a). "The human Werner syndrome protein stimulates repair of oxidative DNA base damage by the DNA glycosylase Neil1." J Biol Chem.
- Das, A., I. Boldogh, J. W. Lee, J. A. Harrigan, M. L. Hegde, J. Piotrowski, N. de Souza Pinto, W. Ramos, M. M. Greenberg, T. K. Hazra, S. Mitra and V. A. Bohr (2007b). "The human Werner syndrome protein stimulates repair of oxidative DNA base damage by the DNA glycosylase NEIL1." J Biol Chem **282**(36): 26591-26602.
- Das, A., L. Wiederhold, J. B. Leppard, P. Kedar, R. Prasad, H. Wang, I. Boldogh, F. Karimi-Busheri, M. Weinfeld, A. E. Tomkinson, S. H. Wilson, S. Mitra and T. K. Hazra (2006). "NEIL2-initiated, APE-independent repair of oxidized bases in DNA: Evidence for a repair complex in human cells." DNA Repair (Amst) **5**(12): 1439-1448.
- de Laat, W. L., E. Appeldoorn, K. Sugawara, E. Weterings, N. G. Jaspers and J. H. Hoeijmakers (1998). "DNA-binding polarity of human replication protein A positions nucleases in nucleotide excision repair." Genes Dev **12**(16): 2598-2609.
- Deng, X., J. E. Habel, V. Kabaleswaran, E. H. Snell, M. S. Wold and G. E. Borgstahl (2007). "Structure of the full-length human RPA14/32 complex gives insights into the mechanism of DNA binding and complex formation." J Mol Biol **374**(4): 865-876.
- Dhenaut, A., S. Boiteux and J. P. Radicella (2000). "Characterization of the hOGG1 promoter and its expression during the cell cycle." Mutat Res **461**(2): 109-118.

- Dianova, II, V. A. Bohr and G. L. Dianov (2001). "Interaction of human AP endonuclease 1 with flap endonuclease 1 and proliferating cell nuclear antigen involved in long-patch base excision repair." Biochemistry **40**(42): 12639-12644.
- Dou, H., S. Mitra and T. K. Hazra (2003). "Repair of oxidized bases in DNA bubble structures by human DNA glycosylases NEIL1 and NEIL2." J Biol Chem **278**(50): 49679-49684.
- Dou, H., C. A. Theriot, A. Das, M. L. Hegde, Y. Matsumoto, I. Boldogh, T. K. Hazra, K. K. Bhakat and S. Mitra (2008). "Interaction of the human DNA glycosylase NEIL1 with proliferating cell nuclear antigen. The potential for replication-associated repair of oxidized bases in mammalian genomes." J Biol Chem **283**(6): 3130-3140.
- Doublet, S., V. Bandaru, J. P. Bond and S. S. Wallace (2004). "The crystal structure of human endonuclease VIII-like 1 (NEIL1) reveals a zincless finger motif required for glycosylase activity." Proc Natl Acad Sci U S A **101**(28): 10284-10289.
- Duncan, B. K. and J. H. Miller (1980). "Mutagenic deamination of cytosine residues in DNA." Nature **287**(5782): 560-561.
- Ellison, V. and B. Stillman (2003). "Biochemical characterization of DNA damage checkpoint complexes: clamp loader and clamp complexes with specificity for 5' recessed DNA." PLoS Biol **1**(2): E33.
- Fan, J., Y. Matsumoto and D. M. Wilson, 3rd (2006). "Nucleotide sequence and DNA secondary structure, as well as replication protein A, modulate the single-stranded abasic endonuclease activity of APE1." J Biol Chem **281**(7): 3889-3898.
- Fortini, P. and E. Dogliotti (2007). "Base damage and single-strand break repair: mechanisms and functional significance of short- and long-patch repair subpathways." DNA Repair (Amst) **6**(4): 398-409.
- Fortini, P., B. Pascucci, E. Parlanti, R. W. Sobol, S. H. Wilson and E. Dogliotti (1998). "Different DNA polymerases are involved in the short- and long-patch base excision repair in mammalian cells." Biochemistry **37**(11): 3575-3580.
- Friedberg, E. C., A. R. Lehmann and R. P. Fuchs (2005). "Trading places: how do DNA polymerases switch during translesion DNA synthesis?" Mol Cell **18**(5): 499-505.
- Fromme, J. C. and G. L. Verdine (2004). "Base excision repair." Adv Protein Chem **69**: 1-41.
- Garg, P. and P. M. Burgers (2005). "DNA polymerases that propagate the eukaryotic DNA replication fork." Crit Rev Biochem Mol Biol **40**(2): 115-128.
- Grollman, A. P. and M. Moriya (1993). "Mutagenesis by 8-oxoguanine: an enemy within." Trends Genet **9**(7): 246-249.
- Guan, X., H. Bai, G. Shi, C. A. Theriot, T. K. Hazra, S. Mitra and A. L. Lu (2007). "The human checkpoint sensor Rad9-Rad1-Hus1 interacts with and stimulates NEIL1 glycosylase." Nucleic Acids Res **35**(8): 2463-2472.

- Guschlbauer, W., A. M. Duplaa, A. Guy, R. Teoule and G. V. Fazakerley (1991). "Structure and in vitro replication of DNA templates containing 7,8-dihydro-8-oxoadenine." Nucleic Acids Res **19**(8): 1753-1758.
- Harrigan, J. A., D. M. Wilson, 3rd, R. Prasad, P. L. Opresko, G. Beck, A. May, S. H. Wilson and V. A. Bohr (2006). "The Werner syndrome protein operates in base excision repair and cooperates with DNA polymerase beta." Nucleic Acids Res **34**(2): 745-754.
- Hasan, S., P. O. Hassa, R. Imhof and M. O. Hottiger (2001). "Transcription coactivator p300 binds PCNA and may have a role in DNA repair synthesis." Nature **410**(6826): 387-391.
- Hazra, T. K., A. Das, S. Das, S. Choudhury, Y. W. Kow and R. Roy (2007). "Oxidative DNA damage repair in mammalian cells: a new perspective." DNA Repair (Amst) **6**(4): 470-480.
- Hazra, T. K., T. Izumi, I. Boldogh, B. Imhoff, Y. W. Kow, P. Jaruga, M. Dizdaroglu and S. Mitra (2002a). "Identification and characterization of a human DNA glycosylase for repair of modified bases in oxidatively damaged DNA." Proc Natl Acad Sci U S A **99**(6): 3523-3528.
- Hazra, T. K., T. Izumi, L. Maitt, R. A. Floyd and S. Mitra (1998). "The presence of two distinct 8-oxoguanine repair enzymes in human cells: their potential complementary roles in preventing mutation." Nucleic Acids Res **26**(22): 5116-5122.
- Hazra, T. K., Y. W. Kow, Z. Hatahet, B. Imhoff, I. Boldogh, S. K. Mokkalapati, S. Mitra and T. Izumi (2002b). "Identification and characterization of a novel human DNA glycosylase for repair of cytosine-derived lesions." J Biol Chem **277**(34): 30417-30420.
- Hegde, M. L., C. A. Theriot, A. Das, P. M. Hegde, Z. Guo, R. K. Gary, T. K. Hazra, B. Shen and S. Mitra (2008). "Physical and functional interaction between human oxidized base-specific DNA glycosylase neil1 and flap endonuclease 1." J Biol Chem.
- Heller, R. C. and K. J. Marians (2006). "Replisome assembly and the direct restart of stalled replication forks." Nat Rev Mol Cell Biol **7**(12): 932-943.
- Helt, C. E., W. Wang, P. C. Keng and R. A. Bambara (2005). "Evidence that DNA damage detection machinery participates in DNA repair." Cell Cycle **4**(4): 529-532.
- Hitomi, K., S. Iwai and J. A. Tainer (2007). "The intricate structural chemistry of base excision repair machinery: implications for DNA damage recognition, removal, and repair." DNA Repair (Amst) **6**(4): 410-428.
- Iftode, C. and J. A. Borowiec (2000). "5' --> 3' molecular polarity of human replication protein A (hRPA) binding to pseudo-origin DNA substrates." Biochemistry **39**(39): 11970-11981.

- Iftode, C., Y. Daniely and J. A. Borowiec (1999). "Replication protein A (RPA): the eukaryotic SSB." Crit Rev Biochem Mol Biol **34**(3): 141-180.
- Ikeda, S., T. Biswas, R. Roy, T. Izumi, I. Boldogh, A. Kurosky, A. H. Sarker, S. Seki and S. Mitra (1998). "Purification and characterization of human NTH1, a homolog of Escherichia coli endonuclease III. Direct identification of Lys-212 as the active nucleophilic residue." J Biol Chem **273**(34): 21585-21593.
- Ishibashi, T., H. Hayakawa, R. Ito, M. Miyazawa, Y. Yamagata and M. Sekiguchi (2005). "Mammalian enzymes for preventing transcriptional errors caused by oxidative damage." Nucleic Acids Res **33**(12): 3779-3784.
- Izumi, T., L. R. Wiederhold, G. Roy, R. Roy, A. Jaiswal, K. K. Bhakat, S. Mitra and T. K. Hazra (2003). "Mammalian DNA base excision repair proteins: their interactions and role in repair of oxidative DNA damage." Toxicology **193**(1-2): 43-65.
- Jiang, X., V. Klimovich, A. I. Arunkumar, E. B. Hysinger, Y. Wang, R. D. Ott, G. D. Guler, B. Weiner, W. J. Chazin and E. Fanning (2006). "Structural mechanism of RPA loading on DNA during activation of a simple pre-replication complex." Embo J **25**(23): 5516-5526.
- Jiang, Y. L. and J. T. Stivers (2002). "Mutational analysis of the base-flipping mechanism of uracil DNA glycosylase." Biochemistry **41**(37): 11236-11247.
- Kathe, S. D., G. P. Shen and S. S. Wallace (2004). "Single-stranded breaks in DNA but not oxidative DNA base damages block transcriptional elongation by RNA polymerase II in HeLa cell nuclear extracts." J Biol Chem **279**(18): 18511-18520.
- Kim, K., S. Biade and Y. Matsumoto (1998). "Involvement of flap endonuclease 1 in base excision DNA repair." J Biol Chem **273**(15): 8842-8848.
- Klungland, A. and T. Lindahl (1997). "Second pathway for completion of human DNA base excision-repair: reconstitution with purified proteins and requirement for DNase IV (FEN1)." Embo J **16**(11): 3341-3348.
- Kolpashchikov, D. M., S. N. Khodyreva, D. Y. Khlimankov, M. S. Wold, A. Favre and O. I. Lavrik (2001). "Polarity of human replication protein A binding to DNA." Nucleic Acids Res **29**(2): 373-379.
- Krishna, T. S., X. P. Kong, S. Gary, P. M. Burgers and J. Kuriyan (1994). "Crystal structure of the eukaryotic DNA polymerase processivity factor PCNA." Cell **79**(7): 1233-1243.
- Krokan, H. E., H. Nilsen, F. Skorpen, M. Otterlei and G. Slupphaug (2000). "Base excision repair of DNA in mammalian cells." FEBS Lett **476**(1-2): 73-77.
- Krosky, D. J., F. P. Schwarz and J. T. Stivers (2004). "Linear free energy correlations for enzymatic base flipping: how do damaged base pairs facilitate specific recognition?" Biochemistry **43**(14): 4188-4195.

- Laroux, F. S., K. P. Pavlick, I. N. Hines, S. Kawachi, H. Harada, S. Bharwani, J. M. Hoffman and M. B. Grisham (2001). "Role of nitric oxide in inflammation." Acta Physiol Scand **173**(1): 113-118.
- Laval, J. (1996). "Role of DNA repair enzymes in the cellular resistance to oxidative stress." Pathol Biol (Paris) **44**(1): 14-24.
- Lavrovsky, Y., B. Chatterjee, R. A. Clark and A. K. Roy (2000). "Role of redox-regulated transcription factors in inflammation, aging and age-related diseases." Exp Gerontol **35**(5): 521-532.
- Lehmann, A. R. (2006). "Translesion synthesis in mammalian cells." Exp Cell Res **312**(14): 2673-2676.
- Lindahl, T. (1993). "Instability and decay of the primary structure of DNA." Nature **362**(6422): 709-715.
- Loeb, L. A. and B. D. Preston (1986). "Mutagenesis by apurinic/aprimidinic sites." Annu Rev Genet **20**: 201-230.
- Lu, A. L., H. Bai, G. Shi and D. Y. Chang (2006). "MutY and MutY homologs (MYH) in genome maintenance." Front Biosci **11**: 3062-3080.
- Lu, A. L. and W. P. Fawcett (1998). "Characterization of the recombinant MutY homolog, an adenine DNA glycosylase, from yeast *Schizosaccharomyces pombe*." J Biol Chem **273**(39): 25098-25105.
- Lu, A. L., J. J. Tsai-Wu and J. Cillo (1995). "DNA determinants and substrate specificities of *Escherichia coli* MutY." J Biol Chem **270**(40): 23582-23588.
- Luna, L., M. Bjoras, E. Hoff, T. Rognes and E. Seeberg (2000). "Cell-cycle regulation, intracellular sorting and induced overexpression of the human NTH1 DNA glycosylase involved in removal of formamidopyrimidine residues from DNA." Mutat Res **460**(2): 95-104.
- Lupardus, P. J. and K. A. Cimprich (2006). "Phosphorylation of *Xenopus* Rad1 and Hus1 defines a readout for ATR activation that is independent of Claspin and the Rad9 carboxy terminus." Mol Biol Cell **17**(4): 1559-1569.
- Maga, G., G. Villani, E. Crespan, U. Wimmer, E. Ferrari, B. Bertocci and U. Hubscher (2007). "8-oxo-guanine bypass by human DNA polymerases in the presence of auxiliary proteins." Nature.
- Maiti, A. K., I. Boldogh, H. Spratt, S. Mitra and T. K. Hazra (2008). "Mutator phenotype of mammalian cells due to deficiency of NEIL1 DNA glycosylase, an oxidized base-specific repair enzyme." DNA Repair (Amst) **7**(8): 1213-1220.
- Market, E. and F. N. Papavasiliou (2003). "V(D)J recombination and the evolution of the adaptive immune system." PLoS Biol **1**(1): E16.
- Matsumoto, Y. (2001). "Molecular mechanism of PCNA-dependent base excision repair." Prog Nucleic Acid Res Mol Biol **68**: 129-138.

- Matsumoto, Y., K. Kim, J. Hurwitz, R. Gary, D. S. Levin, A. E. Tomkinson and M. S. Park (1999). "Reconstitution of proliferating cell nuclear antigen-dependent repair of apurinic/aprimidinic sites with purified human proteins." J Biol Chem **274**(47): 33703-33708.
- Melendy, T. and B. Stillman (1993). "An interaction between replication protein A and SV40 T antigen appears essential for primosome assembly during SV40 DNA replication." J Biol Chem **268**(5): 3389-3395.
- Milam, S. B., G. Zardeneta and J. P. Schmitz (1998). "Oxidative stress and degenerative temporomandibular joint disease: a proposed hypothesis." J Oral Maxillofac Surg **56**(2): 214-223.
- Mitra, S., T. K. Hazra, R. Roy, S. Ikeda, T. Biswas, J. Lock, I. Boldogh and T. Izumi (1997). "Complexities of DNA base excision repair in mammalian cells." Mol Cells **7**(3): 305-312.
- Morland, I., V. Rolseth, L. Luna, T. Rognes, M. Bjoras and E. Seeberg (2002). "Human DNA glycosylases of the bacterial Fpg/MutM superfamily: an alternative pathway for the repair of 8-oxoguanine and other oxidation products in DNA." Nucleic Acids Res **30**(22): 4926-4936.
- Naryzhny, S. N. and H. Lee (2004). "The post-translational modifications of proliferating cell nuclear antigen: acetylation, not phosphorylation, plays an important role in the regulation of its function." J Biol Chem **279**(19): 20194-20199.
- Nelson, J. R., C. W. Lawrence and D. C. Hinkle (1996). "Deoxycytidyl transferase activity of yeast REV1 protein." Nature **382**(6593): 729-731.
- Nichols, A. F. and A. Sancar (1992). "Purification of PCNA as a nucleotide excision repair protein." Nucleic Acids Res **20**(13): 2441-2446.
- Nikolaishvili-Feinberg, N. and M. Cordeiro-Stone (2000). "Discrimination between translesion synthesis and template switching during bypass replication of thymine dimers in duplex DNA." J Biol Chem **275**(40): 30943-30950.
- Oakley, G. G., L. I. Loberg, J. Yao, M. A. Risinger, R. L. Yunker, M. Zernik-Kobak, K. K. Khanna, M. F. Lavin, M. P. Carty and K. Dixon (2001). "UV-induced hyperphosphorylation of replication protein a depends on DNA replication and expression of ATM protein." Mol Biol Cell **12**(5): 1199-1213.
- Oakley, G. G., S. M. Patrick, J. Yao, M. P. Carty, J. J. Turchi and K. Dixon (2003). "RPA phosphorylation in mitosis alters DNA binding and protein-protein interactions." Biochemistry **42**(11): 3255-3264.
- Otterlei, M., E. Warbrick, T. A. Nagelhus, T. Haug, G. Slupphaug, M. Akbari, P. A. Aas, K. Steinsbekk, O. Bakke and H. E. Krokan (1999). "Post-replicative base excision repair in replication foci." Embo J **18**(13): 3834-3844.
- Oyama, M., M. Wakasugi, T. Hama, H. Hashidume, Y. Iwakami, R. Imai, S. Hoshino, H. Morioka, Y. Ishigaki, O. Nikaido and T. Matsunaga (2004). "Human NTH1

- physically interacts with p53 and proliferating cell nuclear antigen." Biochem Biophys Res Commun **321**(1): 183-191.
- Parkins, C. S., M. F. Dennis, M. R. Stratford, S. A. Hill and D. J. Chaplin (1995). "Ischemia reperfusion injury in tumors: the role of oxygen radicals and nitric oxide." Cancer Res **55**(24): 6026-6029.
- Parlanti, E., G. Locatelli, G. Maga and E. Dogliotti (2007). "Human base excision repair complex is physically associated to DNA replication and cell cycle regulatory proteins." Nucleic Acids Res **35**(5): 1569-1577.
- Parsons, J. L., B. Kavli, G. Slupphaug and G. L. Dianov (2007). "NEIL1 is the major DNA glycosylase that processes 5-hydroxyuracil in the proximity of a DNA single-strand break." Biochemistry **46**(13): 4158-4163.
- Podlutzky, A. J., Dianova, II, V. N. Podust, V. A. Bohr and G. L. Dianov (2001). "Human DNA polymerase beta initiates DNA synthesis during long-patch repair of reduced AP sites in DNA." Embo J **20**(6): 1477-1482.
- Porello, S. L., A. E. Leyes and S. S. David (1998). "Single-turnover and pre-steady-state kinetics of the reaction of the adenine glycosylase MutY with mismatch-containing DNA substrates." Biochemistry **37**(42): 14756-14764.
- Roos-Mattjus, P., B. T. Vroman, M. A. Burtelow, M. Rauen, A. K. Eapen and L. M. Karnitz (2002). "Genotoxin-induced Rad9-Hus1-Rad1 (9-1-1) chromatin association is an early checkpoint signaling event." J Biol Chem **277**(46): 43809-43812.
- Sharma, S., M. Otterlei, J. A. Sommers, H. C. Driscoll, G. L. Dianov, H. I. Kao, R. A. Bambara and R. M. Brosh, Jr. (2004). "WRN helicase and FEN-1 form a complex upon replication arrest and together process branchmigrating DNA structures associated with the replication fork." Mol Biol Cell **15**(2): 734-750.
- Shimazaki, N., K. Yoshida, T. Kobayashi, S. Toji, K. Tamai and O. Koiwai (2002). "Over-expression of human DNA polymerase lambda in E. coli and characterization of the recombinant enzyme." Genes Cells **7**(7): 639-651.
- Shivji, K. K., M. K. Kenny and R. D. Wood (1992). "Proliferating cell nuclear antigen is required for DNA excision repair." Cell **69**(2): 367-374.
- Slupphaug, G., B. Kavli and H. E. Krokan (2003). "The interacting pathways for prevention and repair of oxidative DNA damage." Mutat Res **531**(1-2): 231-251.
- Smirnova, E., M. Toueille, E. Markkanen and U. Hubscher (2005). "The human checkpoint sensor and alternative DNA clamp Rad9-Rad1-Hus1 modulates the activity of DNA ligase I, a component of the long-patch base excision repair machinery." Biochem J **389**(Pt 1): 13-17.
- Sung, J. S. and B. Dimple (2006). "Roles of base excision repair subpathways in correcting oxidized abasic sites in DNA." Febs J **273**(8): 1620-1629.

- Takao, M., S. Kanno, K. Kobayashi, Q. M. Zhang, S. Yonei, G. T. van der Horst and A. Yasui (2002). "A back-up glycosylase in Nth1 knock-out mice is a functional Nei (endonuclease VIII) homologue." J Biol Chem **277**(44): 42205-42213.
- Thacker, J. and M. Z. Zdzienicka (2003). "The mammalian XRCC genes: their roles in DNA repair and genetic stability." DNA Repair (Amst) **2**(6): 655-672.
- Tomkinson, A. E., S. Vijayakumar, J. M. Pascal and T. Ellenberger (2006). "DNA ligases: structure, reaction mechanism, and function." Chem Rev **106**(2): 687-699.
- Tornaletti, S., L. S. Maeda, R. D. Kolodner and P. C. Hanawalt (2004). "Effect of 8-oxoguanine on transcription elongation by T7 RNA polymerase and mammalian RNA polymerase II." DNA Repair (Amst) **3**(5): 483-494.
- Vassin, V. M., M. S. Wold and J. A. Borowiec (2004). "Replication protein A (RPA) phosphorylation prevents RPA association with replication centers." Mol Cell Biol **24**(5): 1930-1943.
- Waga, S., G. J. Hannon, D. Beach and B. Stillman (1994). "The p21 inhibitor of cyclin-dependent kinases controls DNA replication by interaction with PCNA." Nature **369**(6481): 574-578.
- Warbrick, E. (2000). "The puzzle of PCNA's many partners." Bioessays **22**(11): 997-1006.
- Weber, S. (2005). "Light-driven enzymatic catalysis of DNA repair: a review of recent biophysical studies on photolyase." Biochim Biophys Acta **1707**(1): 1-23.
- Wiederhold, L., J. B. Leppard, P. Kedar, F. Karimi-Busheri, A. Rasouli-Nia, M. Weinfeld, A. E. Tomkinson, T. Izumi, R. Prasad, S. H. Wilson, S. Mitra and T. K. Hazra (2004). "AP endonuclease-independent DNA base excision repair in human cells." Mol Cell **15**(2): 209-220.
- Wilson, D. M., 3rd, M. Takeshita, A. P. Grollman and B. Demple (1995). "Incision activity of human apurinic endonuclease (Ape) at abasic site analogs in DNA." J Biol Chem **270**(27): 16002-16007.
- Wilson, S. H. and T. A. Kunkel (2000). "Passing the baton in base excision repair." Nat Struct Biol **7**(3): 176-178.
- Wold, M. S. (1997). "Replication protein A: a heterotrimeric, single-stranded DNA-binding protein required for eukaryotic DNA metabolism." Annu Rev Biochem **66**: 61-92.
- Wood, R. D. (1999). "DNA damage recognition during nucleotide excision repair in mammalian cells." Biochimie **81**(1-2): 39-44.
- Wu, X., S. M. Shell and Y. Zou (2005). "Interaction and colocalization of Rad9/Rad1/Hus1 checkpoint complex with replication protein A in human cells." Oncogene **24**(29): 4728-4735.

- Wyka, I. M., K. Dhar, S. K. Binz and M. S. Wold (2003). "Replication protein A interactions with DNA: differential binding of the core domains and analysis of the DNA interaction surface." Biochemistry **42**(44): 12909-12918.
- Yuan, F., Y. Zhang, D. K. Rajpal, X. Wu, D. Guo, M. Wang, J. S. Taylor and Z. Wang (2000). "Specificity of DNA lesion bypass by the yeast DNA polymerase eta." J Biol Chem **275**(11): 8233-8239.
- Zhang, P., Y. Sun, H. Hsu, L. Zhang, Y. Zhang and M. Y. Lee (1998). "The interdomain connector loop of human PCNA is involved in a direct interaction with human polymerase delta." J Biol Chem **273**(2): 713-719.
- Zhang, S. J., X. R. Zeng, P. Zhang, N. L. Toomey, R. Y. Chuang, L. S. Chang and M. Y. Lee (1995). "A conserved region in the amino terminus of DNA polymerase delta is involved in proliferating cell nuclear antigen binding." J Biol Chem **270**(14): 7988-7992.
- Zharkov, D. O., G. Shoham and A. P. Grollman (2003). "Structural characterization of the Fpg family of DNA glycosylases." DNA Repair (Amst) **2**(8): 839-862.
- Zhou, B. B. and S. J. Elledge (2000). "The DNA damage response: putting checkpoints in perspective." Nature **408**(6811): 433-439.
- Zou, L. and S. J. Elledge (2003). "Sensing DNA damage through ATRIP recognition of RPA-ssDNA complexes." Science **300**(5625): 1542-1548.
- Zou, Y., Y. Liu, X. Wu and S. M. Shell (2006). "Functions of human replication protein A (RPA): from DNA replication to DNA damage and stress responses." J Cell Physiol **208**(2): 267-273.

Vita

Corey Allen Theriot, the son of Debbie and Thomas Theriot, was born July 9th, 1979 in Lake Charles, Louisiana. He grew up in Southwest Louisiana where he attended elementary and high school in Grand Lake, Louisiana. He graduated magna cum laude from McNeese State University with a B.S. in Biological Sciences and a minor in Chemistry in 2002. He continued graduate studies at McNeese State University for a year, focusing his studies on Biochemistry and Environmental Toxicology, before matriculating to graduate school at the University of Texas Medical Branch in 2003. He began studies in the basic biomedical science curriculum and joined the Ph.D. program in Biochemistry and Molecular Biology in 2004. He has since worked in the laboratory of Dr. Sankar Mitra at UTMB studying the repair of oxidative stress induced DNA damage, specifically characterizing the role of the mammalian NEIL1 DNA glycosylase in initiation of a novel replication-associated base excision repair pathway.

He has accepted a scientist position as NASA Johnson Space Center in Houston, TX. to study the effects of radiation exposure in space and develop effective human countermeasures for mitigating the effects of space radiation on astronauts.

Permanent address: 109 Theriot Rd., Bell City, LA. 70630

Publications

Theriot, C.A., Hegde, M., Hazra, T. K., Mitra. S.; RPA Physically Interacts with the Human DNA Glycosylase NEIL1 and Regulates Excision of Oxidative DNA Damage in Primer-template Structures. In: *Journal of Biological Chemistry* (Submitted)

Hegde, M., Theriot, C. A., Das, A., Hegde, P., Guo, Z., Gary, R., Hazra, T. K., Shen, B., and Mitra, S.; Physical and Functional interaction between Human Oxidized Base-Specific DNA Glycosylase NEIL1 and Flap Endonuclease 1 (FEN-1). *Journal of Biological Chemistry*. 2008 Oct 3; 283 (40): 27028-37.

Dou, H. *, Theriot, C. A. *, Das, A., Hegde, M. L., Matsumoto, Y., Boldogh, I., Hazra, T., Bhakat K. and Mitra, S.; Interaction of the Human DNA Glycosylase NEIL1 with Proliferating Cell Nuclear Antigen: The Potential for Replication-associated Repair of Oxidized Bases in Mammalian Genomes. *Journal of Biological Chemistry*. 2008 Feb 8; 283 (6): 3130-40. *Both authors contributed equally to this work.

Guan, X., Bai, H., Shi, G., Theriot, C.A., Hazra, T.K., Mitra, S., Lu, A.L.; The Human Checkpoint Sensor Rad9-Rad1-Hus1 Interacts with and Stimulates NEIL1 Glycosylase. *Nucleic Acids Research*. 2007 Mar 29; 35 (8):2463-72.

Jackson, E. B., Theriot, C. A., Chattopadhyay, R., Mitra, S., Izumi, T.; Analysis of Nuclear Transport Signals in the Human Apurinic/apyrimidinic Endonuclease (APE1/Ref1). *Nucleic Acids Research*. 2005 Jun 7; 33 (10):3303-12.

Papaconstantinou, J., et. al.; Training Students for Changing Demands in Research: Student Perspectives on Meeting this Challenge at the University of Texas Medical Branch. Copyright 2005.

This dissertation was typed by Corey A. Theriot.